Renewable and Sustainable Energy Reviews 81 (2018) 3186–3214

Contents lists available at ScienceDirect

Renewable and Sustainable Energy Reviews

journal homepage: www.elsevier.com/locate/rser

Review of hydrogen production using chemical-looping technology

Ming Luo[a,*], Yang Yi[a], Shuzhong Wang[b], Zhuliang Wang[a], Min Du[a], Jianfeng Pan[a], Qian Wang[a]

[a] School of Energy and Power Engineering, Jiangsu University, Zhenjiang 212013, China
[b] Key Laboratory of Thermo-Fluid Science and Engineering of MOE, School of Energy and Power Engineering, Xi'an Jiaotong University, Xi'an 710049, China

ARTICLE INFO

Keywords:
Hydrogen
Chemical-looping
CO_2 capture
Oxygen carrier

ABSTRACT

Hydrogen is an attractive energy carrier due to its potentially high energy efficiency and low generation of pollutants, which can be used for transportation and stationary power generation. However, hydrogen is not readily available in sufficient quantities and the production cost is still high. Steam methane reforming (SMR) process is now the most widely used technology for H_2 production, but this process is complex and cannot get thorough carbon capture. Hydrogen production using chemical looping technology has received a great deal of attention in recent years because it can produce hydrogen with higher process efficiency and can capture carbon dioxide. Many researchers have carried out intensive research work on the hydrogen production processes using chemical looping technology. Based on the previous studies stated in the literature, the authors try to give an overview on the recent advances of two categories, chemical looping reforming (CLR) and chemical looping hydrogen production (CLH) processes. Besides, the characteristics of the processes are pointed out based on the comparison with the conventional SMR process. The existing technical problems and the aspects of future research of each approach are also summarized.

1. Introduction

With an increasing expansion of the vehicle population, the reduction of carbon dioxide and the pollutants emission during the combustion process has become the focus of attention around the world. In 2014, transport was the second-largest sector to emit carbon dioxide, which represented 23% of global CO_2 emissions [1]. Meanwhile, the pollutant emissions from the vehicles have become the main resource in the urban areas, especially for China [2,3]. It is found that the contribution rate of mobile sources are greater than 80% and 40% respectively for the total emissions of CO and NO_x in Beijing [3]. Global demand for transport appears unlikely to decrease in the foreseeable future. The WEO 2010 projects that transport fuel demand will grow more than 20% by 2035 [4]. Therefore, to decrease the emissions in the transport sector is one of the urgent problems.

For vehicle pollutants reduction, this can be achieved by tightening the vehicle emission standards and improving the quality of fuel for vehicle. For the carbon reduction, each transport sector only releases a relatively small amount of CO_2, thus it is not feasible to capture CO_2 from each vehicle and hence, to reduce emissions from the transport sector a change to electricity or renewable fuels is necessary.

Hydrogen appears to be one of the most promising energy carriers as it is considered to be environmentally friendly. It emits only water vapor during the combustion process, which can reduce the emission of pollutants and greenhouse gases. The amount of energy produced during hydrogen combustion is higher than that of any other fuel on a mass basis, such as methane, gasoline or coal, respectively. Therefore, the research activities on H_2 production increase rapidly in many countries. However, for hydrogen to become a major energy source, it must be produced in an efficient and sustainable manner.

There are a few different approaches for hydrogen transportation and storage, but steam methane reforming (SMR) is now the most widely used technology for H_2 production in the industrial scale [5]. However, due to the superior characteristics of system simplification and/or carbon capture inherently compared to the SMR method, hydrogen production using chemical-looping technology has attracted great attention and has been widely investigated recently. Although there have been some reviews related, those published literature only contain part of this technology [6–10], or even only focus on the oxygen carrier materials [11–14]. The aim of this present paper is to introduce the recent findings published and give an extensive review of this technology. The SMR technology is firstly described only for comparison, and then the development of hydrogen production using chemical looping technology is discussed. The principles, characteristics, the development of oxygen carrier materials, the progress in reactor equipment and the system simulation are all summarized and analyzed in this paper.

* Corresponding author.

http://dx.doi.org/10.1016/j.rser.2017.07.007
Received 5 April 2017; Received in revised form 4 June 2017; Accepted 4 July 2017
Available online 09 July 2017
1364-0321/

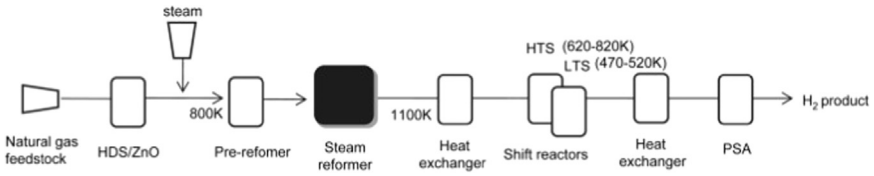

Fig. 1. Simplified flow diagram of conventional SMR process [24].

2. Steam methane reforming process

The SMR process consists of feed stock purification, steam reforming, a high-temperature shift reactor, a low-temperature shift reactor followed by a pressure swing adsorption apparatus for purification of the produced hydrogen. The schematic diagram of the SMR process is shown in Fig. 1.

The methane needs to be firstly desulfurized since small amounts of sulfur are enough to poison the catalyst. Desulfurized methane is then catalytically reformed at the temperature range of 970–1100 K to produce synthetic gas (syngas) with a mixture of CO and H_2 [15]:

$$CH_4+H_2O = CO+3H_2\text{-}206{\cdot}3\ kJ/mol \quad (1)$$

Syngas is cooled and then shifted in the water-gas shift (WGS) reactors, where the WGS reaction happens to increase the H_2 yield and to decrease the CO concentration [16–18].

$$CO+H_2O = CO_2+H_2+41{\cdot}0\ kJ/mol \quad (2)$$

As a final stage, the gases including CO_2, water, methane, and CO need to be removed from the flue gas, and the total reaction of SMR process is as follows:

$$CH_4+2H_2O = CO_2+4H_2\text{-}165{\cdot}3\ kJ/mol \quad (3)$$

The SMR reaction (Eq. (1)) is highly endothermic and usually runs at high temperature above 1073 K. In order to sustain this endothermic reaction, heat is supplied to the reforming reactor by burning part of the natural gas or the purge gas from the pressure-swing adsorption (PSA) in a furnace. Therefore, this process also gives off carbon monoxide and carbon dioxide. Nickel is usually used as the major metallic component of the SMR reaction catalysts. However, the catalyst loaded into the tubes of the reformer is poorly utilized as the heat transfer coefficient of the internal tube wall being the rate-limiting parameter [19]. SMR process also involves the risk of carbon formation with Ni particles as catalyst. Generally, the methane decomposition (Eq. (4)) and the Boudouard reaction (Eq. (5)) may occur during the process [20,21]. Carbon formation may lead to degradation of catalysts and other severe operational trouble, which must be eliminated.

$$CH_4 = C+2H_2 \quad (4)$$

$$2CO = C+CO_2 \quad (5)$$

The WGS reaction (Eq. (2)) involved a complex system. This is traditionally carried out in two fixed bed adiabatic reactors, connected in series with a cooler between them [16]. The first reactor operates at higher temperatures and employs a Fe/Cr catalyst. The second reactor with a Cu/Zn/Al catalyst operates at lower temperatures in order to increase the possible equilibrium conversion of CO as the WGS reaction is exothermic.

PSA and amine absorption technology can be used to capture CO_2 and purify H_2 produced in the SMR process. In older plants, CO_2 is subsequently removed by means of a chemical absorption unit. Modern hydrogen plants apply PSA to separate hydrogen from the other components, which produces higher quality hydrogen (99.999% against 95–98% for scrubbing systems) at feedstock pressure (circa 25 bar) [22]. However, these processes increase the total investment costs and decrease the thermal efficiency of the SMR process. It is estimated that the cost of hydrogen generation will increase by more than 22% if carbon capture and storage (CCS) system is added [23].

Therefore, although it is wildly used in hydrogen generation, SMR process is a complex process that involves many complex catalytic steps. Additional energy and equipment is needed to separate CO_2 from the exhaust gas, and this process cannot achieve a 100% CO_2 capture rate. In addition, the heat transfer coefficient of the internal tube in reformer is the rate-limiting parameter, which needs to be increased.

3. Hydrogen production using chemical looping technology

Chemical looping technology has received great attention in recent years. A typical process is chemical looping combustion (CLC). This process is different from conventional combustion process, which is accomplished by using two reactors and a circulating metal oxide, see Fig. 2. The oxygen carrier constantly circulates between the fuel reactor (FR) and air reactor (AR). In the FR, the particles are reduced by the fuels, and the fuels are oxidized to CO_2 and H_2O through reaction 6. In the AR, they are oxidized to its initial state with O_2 through reaction 7. Due to the fact that the fuel and air are separated in CLC, the combustion products of CO_2 and H_2O are not diluted with nitrogen. This means that by condensing the H_2O, it is possible to obtain almost pure CO_2 without expending any extra energy needed for separation. Other benefits include a large elimination of NO_x emission [25–29] and high thermal efficiency [27].

$$(2n + m)M_xO_y+C_nH_{2\ m} = (2n + m)M_xO_{y\text{-}1} + mH_2O+nCO_2 \quad (6)$$

$$M_xO_{y\text{-}1} + 1/2O_2 = M_xO_y \quad (7)$$

Chemical looping combustion is used in heat and power generation process. Hydrogen production using chemical looping technology utilize the same general principles as CLC. The difference is that the wanted products are not heat but H_2 or/and syngas (H_2 and CO). Hydrogen production using chemical looping technology can be summarized into two categories, chemical looping reforming (CLR) and chemical looping hydrogen production (CLH). Other new processes coupled the chemical looping to produce H_2, such as methane cracking thermally coupled with a CLC process [31], or the methane direct thermocatalytic decomposition by using an activated carbon as a catalyst [32] have also been proposed and investigated, but they are not contained in this paper and can be found elsewhere.

3.1. Chemical looping reforming

The concept of CLR was originally proposed by Mattisson and Lyngfelt et al. [33] in 2001. Based on the principle and characteristics,

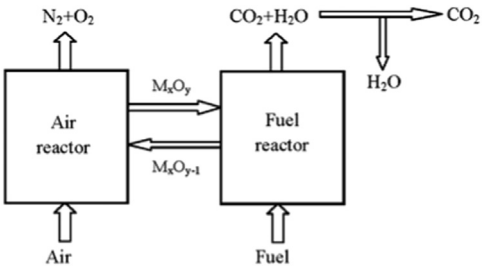

Fig. 2. The schematic diagram of chemical-looping combustion process [30].

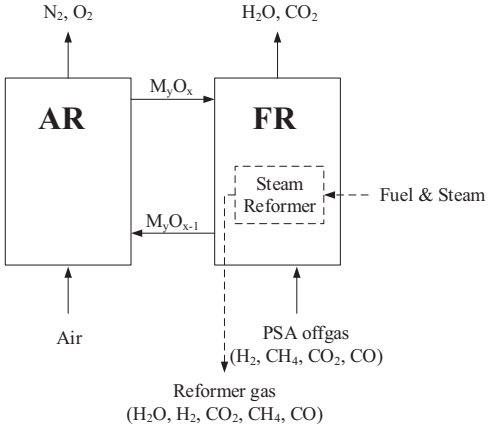

Fig. 3. Schematic description of CLR(s).

it can be classified into three approaches: i) Steam reforming using chemical looping combustion, CLR(s), which is also called "Steam reforming integrated with chemical looping combustion (SR-CLC)" in many literatures, ii) Autothermal chemical looping reforming, CLR(a), and iii) Chemical looping reforming of methane, CLRM, which is also called "Chemical looping steam methane reforming (CL-SMR)" or "Two-step steam methane reforming".

3.1.1. Chemical looping reforming processes

3.1.1.1. CLR(s). The schematic description of CLR(s) is shown in Fig. 3. In this process, the steam reforming part does not differ from the conventional steam reforming process in the way that the reactions take place inside tubes using suitable catalysts and working at elevated pressure. However, the steam reforming tubes are placed inside the FR or a fluidized bed heat exchanger in a CLC unit. Hence, the reformer tubes are heated by the oxygen carrier particles from the AR but not by direct firing outside of the tubes. The offgas from the steam reforming which is a gas mixture of CH_4, CO_2, CO and H_2 is used as the feed gas to the FR. The flue gas from the AR is depleted air, and the output gas from the FR is the mixture of CO_2 and H_2O. Pure CO_2 can be easily obtained and captured by condensing H_2O.

Compared with the SMR process, CLR(s) has some advantages [34]: i) Almost 100% CO_2 can be captured during the process only by a separation of H_2O in the flue gas of FR without expending any extra energy needed for separation because the offgas from the PSA unit is used as fuel in the FR; ii) Higher heat-transfer coefficient can be obtained for the outside of a tube in a fluidized bed than in a furnace due to the hot fluidized particles, so it should be relatively easy to obtain and maintain desired reformer temperature; iii) No thermal NO_x will be formed due to the relatively low-temperature level in the AR, which is similar with that of CLC process; iv) The power consumption for compression of produced H_2 will be reduced as steam reform takes place at elevated pressure.

As shown in Fig. 4. the reformer tubes can be located either in the FR [34] or in the AR [35,36], but the erosion of the reformer tubes inside the reactors may become a serious problem due to the high temperature of reformer and the harsh environment in the fluidized bed reactor. In addition, this process also needs conventional WGS and PSA units, which also increase the investment costs and decrease the efficiency of the system.

3.1.1.2. CLR(a). CLR(a) utilizes the same basic principles as CLC. The difference is that the aim products are not heat but H_2 and CO. Therefore, the air to fuel ratio is kept low to prevent the fuel from being fully oxidized to CO_2 and H_2O. The gas mixture produced from the FR consists of mainly CO and H_2 in addition to small amounts of CO_2 and H_2O. To achieve a pure hydrogen stream, this reformer-gas should be converted in a WGS reactor to maximize hydrogen production and finally CO_2 and H_2 could be separated with pressure swing adsorption or absorption with suitable amine solvent. The basic principles of CLR(a) are illustrated in Fig. 5.

If the fuel is methane and NiO is selected as an oxygen carrier, the main reactions in the FR are:

Direct partial oxidation with metal oxide:

$$CH_4+NiO = CO+2H_2+Ni-211{\cdot}9\ kJ/mol \quad (8)$$

Heterogeneously catalyzed steam reforming and CO shift reaction:

$$CH_4+H_2O = CO+3H_2-\ 225{\cdot}5\ kJ/mol \quad (9)$$

$$CO+H_2O = CO_2+H_2+33{\cdot}6\ kJ/mol \quad (10)$$

Internal combustion:

$$CO+NiO = CO_2+Ni+47{\cdot}2\ kJ/mol \quad (11)$$

$$H_2+NiO = H_2O+Ni+13{\cdot}6\ kJ/mol \quad (12)$$

$$CH_4+4NiO = CO_2+2H_2O+4Ni-137{\cdot}7\ kJ/mol \quad (13)$$

In the AR the metal oxide will be oxidized by air according to:

$$Ni+1/2O_2 = NiO+469{\cdot}9\ kJ/mol \quad (14)$$

The total reaction of the CLR(a) process is:

$$CH_4+H_2O+1/2O_2=CO_2+H_2 \quad (15)$$

CLR(a) in its most basic form could be described as a combination process of the partial oxidation and steam reforming of hydrocarbon fuels. The partial oxidation process is exothermic, but the steam reforming process is highly endothermic. To keep the total process maintaining at exothermic status, the ratio of the reforming process to the partial oxidation process should be kept at a low value. Ortiz et al. [37] conducted the mass and heat balances to determine the auto-thermal operating conditions that maximize H_2 production in a CLR(a) system when using Ni-based oxygen carriers. It was found that to reach auto-thermal conditions the oxygen-to-methane molar ratio should be higher than 1.20, which means that the maximum H_2 yield is about 2.75 mol H_2/mol CH_4.

As can be seen, the main advantages of CLR(a) compared to SMR technology are [38,39]: i) No external combustion is required to provide heat to the reforming process; ii) No CO_2 emissions arise from external combustion as all carbon involved is available in the synthesis gas; iii) Less steam is required and less catalyst are required per unit fuel feed; iv) No limitation of the reaction rate by heat transfer as the heat transfer is very high in the fluidized bed; v) Less concern with respect to sulfur contaminants [40], and no thermal NO_x will be formed [27,28]. Besides the advantageous mentioned above, CLR(a) is also an interesting alternative for production of synthesis gas for methanol production and for Fischer-Tropsch synthesis, which are important industrial processes where synthesis gas with a (H_2/CO) ratio of 2 is wanted. Such synthesis gas cannot be produced directly by steam reforming of CH_4.

3.1.1.3. CLRM. CLRM is a technology which could generate pure hydrogen and syngas separately and simultaneously. Similar with CLR(a), methane is partially oxidized by the lattice oxygen of the oxygen carrier in the FR to produce syngas, but the reduced oxygen carrier is not oxidized by air in AR but by steam to recover lattice oxygen and simultaneously produce hydrogen in the steam reactor (SR). Usually, an AR is added to recover the lattice oxygen completely (Fig. 6**. (b)**). The reactions of CLRM process can be illustrated as follows:

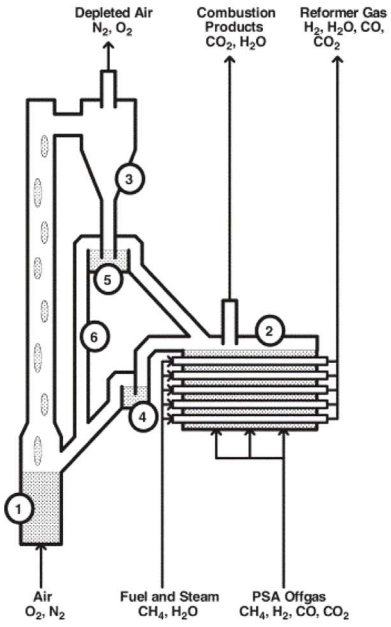

(a) The reformer in the FR [31].

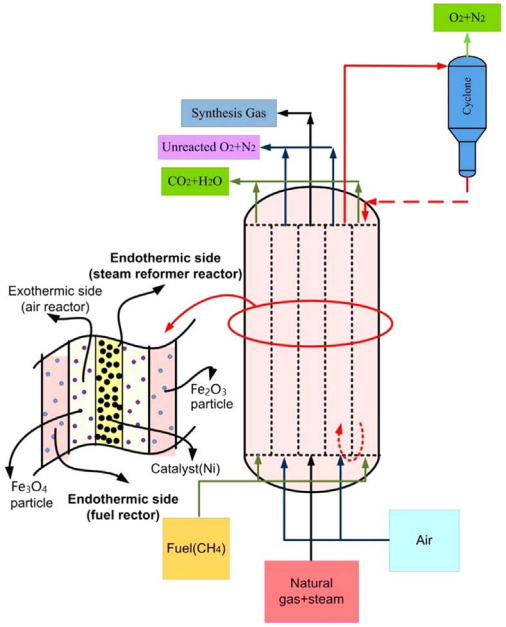

(b) The reformer in the AR [35].

Fig. 4. Schematic diagram of the CLR(s) system.

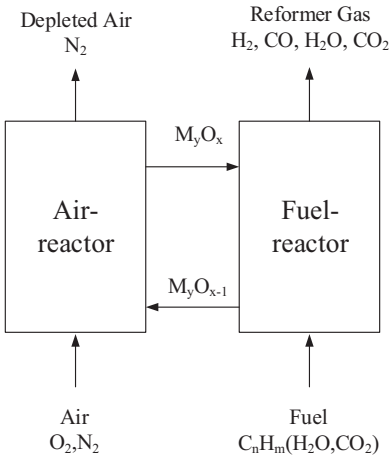

Fig. 5. The schematic diagram of CLR(a).

Methane Reduction: $M_yO_x + \delta_2 CH_4 = M_yO_{x-\delta1-\delta2} + \delta_2(2H_2+CO)$ (16)

Steam Oxidation: $M_yO_{x-\delta1-\delta2} + \delta_2 H_2O = M_yO_{x-\delta1} + \delta_2 H_2$ (17)

Air Oxidation: $M_yO_{x-\delta1} + \delta_1/2O_2 = M_yO_x$ (18)

where M_yO_x is an oxygen carrier, $M_yO_{x-\delta1}$ and $M_yO_{x-\delta1-\delta2}$ are the corresponding reduced oxygen carrier with different reduction degree.

The CLRM process is attractive because it can produce syngas and hydrogen simultaneously. Pure hydrogen can be obtained from the SR exit by simply cooling and condensing the steam, without any additional gas treatments required. However, the studies of CLRM process is mainly focused on oxygen carrier screening and performance optimization. A proper material needs to have sufficiently high reactivity with methane to produce syngas, good performance for water splitting to produce hydrogen, and high stability during redox cycles. As the carbon deposited particles produced in FR will react with steam in SR and contaminate the H_2 generated, therefore, the oxygen carriers also need to have the ability of carbon deposition resistance. A serious of metal oxides such as Fe_3O_4 [24,41], WO_3 [42,43], SnO_2 [44], Ni-ferrites [45], (Zn, Mn)-ferrites [46], Cu-ferrites [47–49], and Ce-based oxides [50–55] have been considered as possible oxygen carriers for this process.

3.1.2. Development of oxygen carriers

A key issue for the CLR development is the selection of an oxygen carrier with suitable properties. The oxygen carriers with different active metals, inert supports and prepared by different preparation methods have been screened and selected. Table 1 shows a summary of different kinds of oxygen carriers used in the literature.

3.1.2.1. Ni-based oxygen carriers. Metallic Ni is used in most commercial steam reforming catalysts, and nickel-based oxides have been demonstrated as one of the most promising oxygen carriers in CLR processes due to the high reactivity and selectivity. Zafar et al. [73] compared the reactivity between different active metal oxides (NiO, CuO, Fe_2O_3 and Mn_2O_3) supported on SiO_2 and methane in a laboratory fluidized bed reactor. In general, the reactivity of active oxides with methane was in the order NiO > CuO > Mn_2O_3 > Fe_2O_3. Moreover, only NiO/SiO_2 showed high selectivity toward H_2 during the later stages of reduction, while large amounts of unreacted CH_4 existed at the exit of the reactor when use other metal oxides. The high reactivity in combination with high selectivity to H_2 for NiO/SiO_2 makes it an interesting candidate as an oxygen carrier for CLR(a).

Different inert support and the preparation method also have an effect on the properties of the Ni-based oxygen carriers. Johansson et al. [81] compared the reactivity of two different oxygen carriers, NiO/$NiAl_2O_4$ and NiO/$MgAl_2O_4$ in CLR(a) process. There were higher methane conversion, higher selectivity to reforming and lower tendency for carbon formation when NiO/$MgAl_2O_4$ was used at elevated temperatures. de Diego et al. [56] found that the support (different types of alumina) had an important effect on the reactivity of the oxygen carriers, on the gas product distribution, and on the carbon deposition. The reduction reactivity of the carrier of NiO on α-Al_2O_3 was higher than that on γ-Al_2O_3 due to the limited solid state reaction between NiO and α-Al_2O_3. The kinetics of reduction and oxidation reactions [67] and the catalytic activity [65] during CLR(a) process when using those two materials can be found elsewhere. Antzara et al.

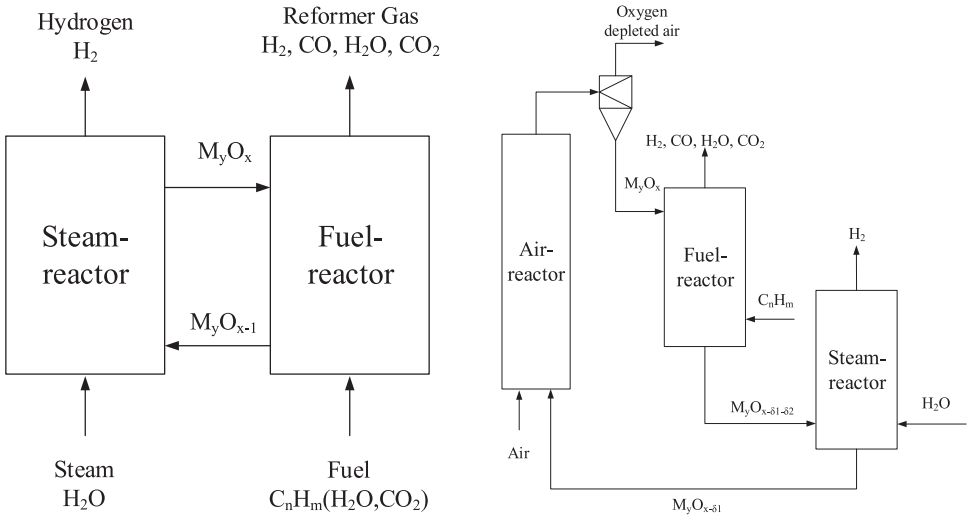

Fig. 6. CLRM for syngas and hydrogen production.

[83] also evaluated the performance of NiO-based oxygen carriers supported on ZrO_2, TiO_2, SiO_2, Al_2O_3 and $NiAl_2O_4$ in CLRM process. It was found that the NiO/ZrO_2 exhibited the best performance on CH_4 conversion and stability in 20 redox cycles. In addition, it was observed that the oxygen carriers prepared by a deposition-precipitation method had higher tendency to increase the carbon deposition than the oxygen carriers prepared by dry impregnation [56].

Despite the superior activity and the selectivity, the selectivity to synthesis gas of the nickel-based oxides need to be further improved [39,63]. Mattisson et al. [163] found that almost complete conversion of CH_4 into CO_2 and H_2O could be achieved even with a very small amount of NiO. Therefore, the syngas yield largely depends on the oxidation degree of the oxygen carrier. CO_2 and H_2O can be easily formed by highly oxidized Ni-based oxides and CO and H_2 generated by reduced particles [65,75]. Nakayama et al. [70,126] proposed the reactivity of $NiO–Cr_2O_3–MgO$ complex oxide as an oxidant to produce nitrogen-free synthesis gas or hydrogen by the partial oxidation of methane. It was found that the lattice oxygen was effectively transferred to CH_4 to give H_2 and CO in the ratio of 2–3:1 at 700 °C. The oxygen carrier exhibited high and constant catalytic activities for repeated reduction with CH_4 and oxidation with air cycles without significant carbon deposition. The addition of Cr_2O_3 weakened the Ni–O bond in NiO–MgO complex oxide, and decreased the temperature of the reaction of CH_4 with NiO [70].

One of the major issues in the CLR processes of hydrocarbons using the nickel-based materials is the deactivation caused by carbon deposition on the surface of the matierial. One possible way to serve this problem is to add small amount of alkali metals, which could effectively reduce carbon deposition on the material surface in the high temperature reforming process [164,165]. Another method is to add small amount of steam to the reactor to reduce or even eliminated the carbon deposition [39,75]. However, the successfully operation of a140 kW dual circulating fluidized bed pilot plant has been implemented using $NiO/NiAl_2O_4$ with or without small MgO added as oxygen carriers and natural gas as fuel [38]. Results showed that even though no steam was added to the natural gas, no carbon formation was found for global excess air ratios larger than 0.4. Thus, the carbon deposition was not a problem in a real process. Furthermore, other characteristics, such as the toxicity and the cost of nickel-based oxygen carriers may limit their application.

Other than CH_4, Ni-based oxygen carriers also have promising properties in converting liquid and solid fuels to syngas, which will be reviewed in Section 3.1.3.

3.1.2.2. Ce-based oxygen carriers. The feasibility of the CeO_2 on the partial oxidation of methane into synthesis gas has been confirmed by Otsuka et al. [51,166] and Wei et al. [89]. Direct conversion of methane into synthesis gas with the H_2/CO ratio of 2 has been demonstrated using CeO_2 as an oxidant at temperatures higher than 600 °C. However, methane cracking and the decrease of reactivity was also observed when CeO_2 was used during redox cycles [53]. Different materials have been added as promoters to increase the selectivity of the Ce-based oxygen carriers.

The mixed-metal oxides by combining another material to CeO_2 could be a way to increase the reactivity, stability, and selectivity. Many kinds of Ce-based oxides, such as Ce–Zr [94,95,101], Ce–Fe [52,86,92,96–98], Ce–Al_2O_3 [87,89], Ce–MgO [99], Ce–Cu, Ce–Mn [85], Ce–Nd [93] and so on were investigated. In general, Ce–Fe mixed oxides exhibited good activity and stability among all the oxides. But their selectivity for syngas generation was strongly affected by the specific surface area of oxygen carriers. Moreover, the doping ratio of Fe to Ce should be carefully settled because the high content of Fe failed to increase the CH_4 conversion and inclined to decrease the CO selectivity [98].

The addition of Pt [50,51,88] and Rh [88] remarkably accelerated the formation rates of H_2 and CO and decreased the activation energy of synthesis gas production. The promoters not only drastically enhanced the conversion of methane, but also lowered the temperature necessary to reduce the cerium oxide, while the promoters may also lead to some carbon formation [88]. The reduced oxide can be fully regenerated and the carbon deposited can be completely removed by oxygen. He et al. [85] investigated the effect of additions Fe, Cu, and Mn on the reactivity of CeO_2. It was revealed that the addition of transition-metal oxides into cerium oxide could improve the reactivity of the Ce-based oxygen carrier, and the three kinds of mixed oxides showed high CO and H_2 selectivity at the temperatures above 800 °C. Among the three kinds of oxygen carriers, Ce–Fe–O presented the best performance, and methane was converted to synthesis gas at a H_2/CO molar ratio close to 2:1 at a temperature of 800–900 °C. Wei et al.[91] also explored the reactivity of Ce–Fe–O mixed oxide (Ce/Fe=7:3) in direct partial oxidation of methane to syngas process. Approximately 99.4% H_2 selectivity, 98.8% CO selectivity and 94.9% CH_4 conversion were achieved at 900 °C in fixed bed experiments. The Ce–Fe–O mixed oxide as the oxygen carrier showed good methane selectivity into syngas by the lattice oxygen and cycle performance in redox cycles.

Note that, the feasibility of the Ce-based materials is confirmed

Table 1
Summary of the oxygen-carriers tested in different CLR units.

Oxygen carrier			Fuel in reduction process	Reactor type[b]	References
Metal oxide	Support material	Preparation method[a]			
(i) 11 wt% NiO (ii) 16 wt% NiO (iii) 21 wt% NiO (iv) 26 wt% NiO (v) 28 wt% NiO	(i) α-Al_2O_3 (ii) θ-Al_2O_3 (iii) γ-Al_2O_3 (iv) α-Al_2O_3 (v) γ-Al_2O_3	(i)–(iii) DP (iv)–(v) DIMP	n.g.	TGA, bFB	[56]
17–18.5 wt% NiO	$CaAl_2O_4$	PUR	CH_4+H_2, CH_4	PB	[57]
18 wt% NiO	α-Al_2O_3	PUR	Glycerol	FxB	[58]
18 wt% NiO	α-Al_2O_3	PUR	Waste cooking vegetable oil	PB	[59,60]
18 wt% NiO	α-Al_2O_3	PUR	Pyrolysis oil	PB	[61]
18 wt% NiO	α-Al_2O_3	PUR	Acetic acid	PB	[62]
(i) 18 wt% NiO (ii) 20 wt% NiO (iii) 21 wt% NiO	(i) α-Al_2O_3 (ii) $MgAl_2O_4$ (iii) γ-Al_2O_3	(i) IMP (ii) FG (iii) IMP	n.g.	cFB	[63]
(i) 18 wt% NiO (ii) 21 wt% NiO	(i) α-Al_2O_3 (ii) γ-Al_2O_3	WIMP	CH_4	TGA, cFB	[64]
(i) 18 wt% NiO (ii) 21 wt% NiO	(i) α-Al_2O_3 (ii) γ-Al_2O_3	IMP	CH_4+H_2, H_2	FxB	[65]
(i) 18 wt% NiO (ii) 21 wt% NiO	(i) α-Al_2O_3 (ii) γ-Al_2O_3	WIMP	CH_4	pFB	[66]
(i) 18 wt% NiO (ii) 21 wt% NiO	(i) α-Al_2O_3 (ii) γ-Al_2O_3	IMP	CH_4, H_2, CO	TGA	[67]
(i) 18 wt% NiO (ii) 21 wt% NiO	(i) α-Al_2O_3 (ii) γ-Al_2O_3	(i) WIMP (ii) HWIMP	Bioethanol	cFB	[68]
(i) 18 wt% NiO (ii) 25 wt% NiO	(i)α-Al_2O_3 (ii)γ-Al_2O_3	PUR	Ethanol/bio-oil aqueous fraction mixture	PB	[69]
(i)–(vii) 20 mol% NiO (viii) NiO–Cr_2O_3 (ix) NiO–MgO (x) NiO–M–MgO(M=Al_2O_3, CaO, Cr_2O_3, Fe_2O_3, Co_3O_4), Ni/additive/Mg = 16:4:25 as a molar ratio	(i) MgO (ii) Al_2O_3 (iii) SiO_2 (iv) TiO_2 (v) Y_2O_3 (vi) La_2O_3 (vii) CeO_2 (viii) MgO (ix)–(x) None	(i)–(vii) IMP (viii)–(x) EM	CH_4	FxB	[70]
20 wt% NiO	$CaAl_2O_4$	PUR	H_2, CO, CH_4	TG, FxB	[71]
25 wt% NiO	Al_2O_3	COP	Glycerol	FxB	[72]
(i) 35 wt% NiO (ii) 39 wt% Fe_2O_3 (iii) 41 wt% CuO (iv) 47 wt% Mn_2O_3	(i)–(iv) SiO_2	DIMP	CH_4	bFB	[73]
40 wt% NiO	(i) α-Al_2O_3 (ii) α-Al_2O_3–MgO	SD	n.g.	cFB	[74]
40 wt% NiO	Mg–stabilized ZrO_2	FG	n.g.	cFB	[75]
40 wt%NiO	(i) Al_2O_3 (ii) ZrO_2	WIMP	CH_4	TGA, FxB	[76]
40 wt% NiO	α-Al_2O_3	SD	Raw gas from biomass gasifier	cFB	[77]
40 wt% NiO	(i) $NiAl_2O_4$ (ii) 42 wt% $NiAl_2O_4$+18 wt% $MgAl_2O_4$	SD	n.g.	cFB	[38]
40 wt% NiO	(i) α-Al_2O_3 (ii) α-Al_2O_3+MgO	SD	n.g.	cFB	[74]
40 wt% NiO	MgO–ZrO_2	FG	Kerosene	cFB	[78]
(i) 40 wt% NiO (ii) 40 wt% Mn_3O_4 (iii) 60 wt% NiO (iv) ilmenite ores	(i) $NiAl_2O_4$ (ii) Mg–ZrO_2 (i) $MgAl_2O_4$ (iv) None	(i)–(iii)FG (iv)–	Toluene	TGA, FxB	[79]
(i) 40 wt% NiO (ii) 40 wt% Mn_3O_4 (iii) 60 wt% NiO (iv) ilmenite ore	(i) $NiAl_2O_4$ (ii) Mg–ZrO_2 (i) $MgAl_2O_4$(iv) None	(i)–(iii)FG (iv)–	CH_4, CO, CH_4+H_2O, CH_4+C_7H_8+H_2O, CO+H_2, CH_4+C_7H_8+H_2O+CO+H_2, CH_4+C_7H_8+H_2O+CO+H_2+CO_2	TGA, FxB	[80]
(i) 40 wt% NiO (ii) 60 wt% NiO	(i) $NiAl_2O_4$ (ii) $MgAl_2O_4$	FG	CH_4	bFB	[81]
42.1 wt% NiO	$NiAl_2O_4$	COP	Glycerol	MB	[82]
42.1 wt% NiO	$NiAl_2O_4$	COP	Glycerol	FxB	[72]
60 wt% NiO	$MgAl_2O_4$	FG	n.g.	cFB	[39]
(i) 100 wt% NiO (ii)–(vi) 40 wt% NiO	(ii) ZrO_2 (iii)TiO_2 (iv)SiO_2 (v)Al_2O_3 (vi)$NiAl_2O_4$	WIMP	CH_4	FxB	[83]
(i) 100 wt% NiO (ii) xNi (x = 10 , 20, 30 wt%)	(i)– (ii)Montmorillonite	Ultrasound assisted cation exchange	Ethanol	TGA, FxB	[84]

(continued on next page)

Table 1 *(continued)*

Oxygen carrier			Fuel in reduction process	Reactor type[b]	References
Metal oxide	Support material	Preparation method[a]			
(iii) 20 wt% Ni	(iii)Al_2O_3	impregnation method			
CeO_2	–	PUR	CH_4	FxB	[51]
CeO_2	–	P	CH_4	FxB	[53]
(i) CeO_2 (ii) Ce–ZrO_2(Ce:Zr ratio of 7:3)	–	COP	CH_4	FxB	[54]
(i) CeO_2 (ii) Ce–Fe–O (Ce/Fe=5:5 as mass ratio) (iii) Ce–Cu–O (Ce/Cu=5:5 as mass ratio) (iv) Ce–Mn–O (Ce/Mn=5:5 as mass ratio) (iv) Ce–Fe–O (Ce/Fe=7:3 as mass ratio)	–	COP	CH_4	TGA, FxB	[85]
(i) CeO_2 (ii) CeO_2–Fe_2O_3(Ce/(Ce + Fe)=1, 0.75, 0.5, 0.25, 0) (iii) 1 wt% Au/CeO_2–Fe_2O_3(Ce/(Ce + Fe) =1, 0.75, 0.5, 0.25, 0) (iv) 3 wt% Au/CeO_2–Fe_2O_3(Ce/(Ce + Fe)= 0.25) (v) 1 wt% Au/CeO_2–Fe_2O_3(Ce/(Ce + Fe)= 0.25)	–	DP	Methanol	FxB	[86]
(i) 20 wt% CeO_2 (ii) 0.5 wt% Pt/20 wt% CeO_2 (iii) 0.5 wt% Rh/20 wt% CeO_2	γ-Al_2O_3	WIMP	CH_4	TR	[87]
(i) 20 wt% CeO_2 (ii) 0.5 wt% Pt/20 wt% CeO_2 (iii) 0.5 wt% Rh/20 wt% CeO_2	γ-Al_2O_3	WIMP	H_2	FxB	[88]
xCeO_2 (x = 5, 10, 20, 30, 40 wt%)	γ-Al_2O_3	WIMP	CH_4	FxB	[89]
xCeO_2 (x = 5, 10, 20 wt%)	$LaFeO_3$	GB	CH_4	FxB	[90]
xCeO_2 (x = 10, 30, 50 wt%)	ZrO_2	P	CH_4	TPR, TR	[55]
CeO_2–Fe_2O_3 (Ce/Fe=7:3 as mass ratio)	–	COP	CH_4	FxB	[52]
Ce–Fe–O (Ce/Fe=7:3 as mass ratio)	–	COP	CH_4	TGA, FxB	[91]
Ce–Fe–O (Ce/Fe=7:3 as mass ratio)	–	COP	H_2	TGA	[92]
$CeNbO_{4+\delta}$	–	SSM	H_2, CH_4	FxB	[93]
$Ce_{0.8}Zr_{0.2}O_2$	–	COP, CCTM	CH_4	FxB	[94]
$Ce_xZr_{1-x}O_2$ (x = 0, 0.3, 0.5, 0.7, 1)	–	COP	CH_4	FxB	[95]
$Ce_{1-x}Fe_xO_{2-\delta}$ (x = 0, 0.1, 0.2, 0.3, 0.4, 0.5, 0.6, 1)	–	CP	CH_4	FxB	[96]
$Ce_{1-x}Fe_xO_{2-\delta}$ (x = 0, 0.1, 0.2, 0.3, 0.4, 0.5, 1)	–	COP	H_2, CH_4	FxB	[97]
$Ce_{1-x}Fe_xO_{2-\delta}$ (x = 0, 0.1, 0.2, 0.3, 0.4, 0.5, 0.6, 1)	–	CP	H_2, CH_4	FxB	[98]
(x)Ce–Fe–Zr–O (x = 10, 15, 20, 25, 30 wt%, n_{Ce}: n_{Fe}: n_{Zr}=7:3:0.5)	MgO	COP	CH_4	TR	[99]
40 wt% Fe–CeO_2 40 wt% $Ni_{0.02}Fe_{0.98}$–CeO_2 40 wt% $Ni_{0.12}Fe_{0.88}$–CeO_2 40 wt% $Ni_{0.33}Fe_{0.67}$–CeO_2 40 wt% Ni–CeO_2	–	WIMP	CH_4	FxB	[100]
(i) 0.5% Pt/$Ce_{1-x}Zr_xO_2$, (x = 0, 0.2, and 0.5) (ii) 0.5% Ru/$Ce_{1-x}Zr_xO_2$, (x = 0, 0.2, and 0.5)	–	CAM	CH_4	TR	[101]
WO_3 modified with CeO_2–ZrO_2 (n_W/(n_{Ce} +n_{Zr}+n_W) = 100, 90, 80, 69, 65%, n_{Ce}: n_{Zr}=1;1)	–	UH	H_2	FxB	[43]
$AFeO_3$ (A =La, Nd, Eu)	–	SG	CH_4	FxB	[102]
$LaFeO_3$	–	CCTM, SC	H_2, CH_4	FxB	[103]
$LaFeO_3$	–	SC	CH_4	FxB	[104]
$LaFeO_3$	–	SG	CH_4	FxB	[105]
$LaFeO_3$	–	SFEP	CH_4	TPR, TGA, FxB	[106]
$LaFe_{1-x}Co_xO_3$ (x = 0.1, 0.3,0.5, 0.7, 1.0)	–	SC	H_2, CH_4	FxB	[107]
$LaFe_{1-x}Ni_xO_3$ (x = 0.1, 0.15, 0.2, 0.3)	–	SC	H_2, CH_4	FxB	[108]
$La_{1-x}Sr_xMO_3$ (M=Mn, Ni; x = 0–0.4) $La_{1-x}MnO_{3-\alpha}Fe_\beta$ (β/(3-α)=0.1)	–	SC	CH_4	TPR, FxB	[109]
$La_{1-x}Sr_xFeO_3$ (x = 0, 0.1, 0.2, 0.5)	–	SC	H_2, CH_4	TPR, FxB	[110]
$La_{1-x}Sr_xFeO_3$ (x = 0.1, 0.3, 0.5, 0.9)	–	SC	H_2, CH_4	TPR, TGA, FxB	[111]
$La_{1-x}Sr_xFeO_{3-\delta}$ (x = 1/3, 1/2, 2/3, 1,)	–	SC	CH_4	XRD	[112]
$La_{1-x}Sr_xFeO_3$ (x = 0, 0.3, 0.5, 0.9)	–	SC	H_2, CH_4	TPR, TGA, FxB	[113]
$La_xSr_{1-x}FeO_{3-\delta}$ (x = 0.5, 0.8, 1)	–	GNP, SD	CH_4	TPR, FxB	[114]
(i) 10 wt% $La_{0.8}Sr_{0.2}FeO_3$ (ii) 10 wt% $La_{0.8}Sr_{0.2}FeO_3$ (iii) 10 wt% $LaFeO_3$	(i) ZNANO(Unimpregnated monoclinic ZrO_2 manufactured from)	WIMP	Benzene, ethylene	bFB	[115]

(continued on next page)

Table 1 *(continued)*

Oxygen carrier			Fuel in reduction process	Reactor type[b]	References
Metal oxide	Support material	Preparation method[a]			
(iv) 0.668 wt% La (v) 0.106 wt%Sr (vi) 1.011 wt%Fe	(ii)–(vi)ZTECH(Unimpregnated plasma–processed monoclinic ZrO_2)				
Fe_2O_3	–	PUR	CH_4	TGA, FB	[24]
(i) Fe_2O_3 (ii) 30 wt% Fe_2O_3–70 wt% $Ce_{0.5}Zr_{0.5}O_2$ (iii) $Ce_{0.5}Zr_{0.5}O_2$	–	UH	H_2	TR	[116]
(i) Fe_2O_3 (ii) $ZnFe_2O_4$ (iii) $MnFe_2O_4$ (Jacobsite) (iv) $MnFe_2O_4$ (Iwakiite)	–	SSM	CH_4	TGA	[46]
(i) Fe_3O_4 (ii) $CuFe_2O_4$	–	(i) PUR (ii) COP	CH_4	TGA, FxB	[47]
AFe_2O_4 (A = Fe, Co, Ni)	–	COP	Ethanol	IR	[117]
AFe_2O_4 (A = Ni or Fe)	–	COP	Ethanol	FxB	[118]
$CoFe_2O_4$	–	COP	Ethanol	FxB	[119,120]
Fe_3O_4	–	COP	Ethanol	TPR	[121]
(i) 40 wt% Fe_2O_3 (ii) 36.36 wt%Fe_2O_3–54.54 wt%CaO	Al_2O_3	MM	Coal	bFB	[122]
40 wt% Fe_2O_3	Al_2O_3	SD	CH_4	bFB	[123]
(i)–(v) 50 wt% Fe_2O_3 (vi) 50 wt% Co_3O_4 (vii) 50 wt% Mn_2O_3	(i) $LaFeO_3$ (ii) $La_{0.8}Sr_{0.2}FeO_3$ (iii) $La_{0.7}Sr_{0.}3FeO3$ (iv) $La_{0.5}Sr0.5FeO_3$ (v) $SrFeO_3$ (vi) $La_{0.8}Sr_{0.}2FeO3$ (vii) $La_{0.8}Sr_{0.}2FeO3$	PEC	CH_4	TGA, TR	[124]
(i)–(iv) 60 wt% Fe_2O_3 (v) 50 wt% Fe_2O_3	(i)$MgAl_2O_4$ (ii)Al_2O_3 (iii)YSZ (iv)–(v)$La_xSr_{1-}xFeO3$	(i)–(iv) SSM (v) PEC	H_2, CH_4	DB	[125]
(i) 10 mol% Fe_2O_3–M (M= MgO, Al_2O_3, TiO_2, Y_2O_3, La_2O_3, CeO_2, None) (ii) xFe_2O_3/Y_2O_3 (x = 5, 10, 20, 50, 90 mmol/1 g Y_2O_3) (iii) Fe_2O_3–M/Y_2O_3 (M=Rh_2O_3, PtO, PdO, IrO_2, RuO_2) (20 mmol-additive 0.5 mmol/1 g of Y_2O_3) (iv) Fe_2O_3–M (M=NiO, Co_3O_4, Cr_2O_3), n_{Fe2O3}/n_M=2:1) Fe_2O_3–N–Cr_2O_3 (N=MgO, CaO, SrO), $n_{Fe2O3}/n_N/n_{Cr2O3}$=3:1:2 (v) NiO–MgO, NiO–M–MgO(M= Al_2O_3, CaO, Cr_2O_3, Fe_2O_3, Co_3O_4, $n_{NiO}/n_M/n_{MgO}$=16:4:25) (vi) NiO–Cr_2O_3–MgO (n_{NiO}=0–80 mol%, n_{Cr}:n_{Mg}=4:25)	–	IMP	CH_4	FxB	[126]
(i) 75 wt% Fe_3O_4–25 wt% $La_{0.8}Sr_{0.2}FeO_{3-\delta}$ (ii) 60 wt% Fe_3O_4–40 wt% $La_{0.8}Sr_{0.2}FeO_{3-\delta}$ (iii) $La_{0.8}Sr_{0.2}FeO_{3-\delta}$	–	SSM	CH_4	FxB	[127]
60 wt% Fe_3O_4–40 wt% $La_{0.8}Sr_{0.2}FeO_{3-\delta}$	–	SSM	CH_4	FxB, bFB	[128]
(i) yFe, y = 10, 15, 20, 30, 40 wt% (ii) yFe, y = 10, 15, 20, 30, 40 wt% (iii) 15 Fe–xCa, x = 5, 10 wt% (iv) 15 wt% Fe/5 wt% Ca, x = 5, 10 wt%	(i)–(iv) γ-Al_2O_3	(i) IMP (ii) COP (iii) COP (iv) SIMP	CH_4	FxB	[129]
(i) 15 wt% Fe–xMg (x = 0, 5, 10 wt%) (ii) 15 wt% Fe–5 wt% Mg	(i)–(ii) Al_2O_3	(i) CI (ii) SIMP	CH_4	FxB	[130]
15 wt% Fe–xM(x = 0, 5, 10 wt%, M = Ca or Ce)	Al_2O_3	WIMP	CH_4	FxB	[131]
22 wt% Fe_2O_3	(i) Al_2O_3 (ii) $MgAl_2O_4$	(i) IMP (ii) SIMP	CH_4	FxB	[132]
60 wt% Fe_2O_3	Al_2O_3	MM	Charcoal	MB	[133]
(i) 70 wt% Fe_2O_3 (ii) Ni–modified (i) (mass ratio of Ni was 0.43 wt%, 1.04 wt%, 1.72 wt%)	Al_2O_3	(i) MM (ii) MM+IMP	H_2, CH_4	TGA, FxB	[134]
20 wt% $CuFe_2O_4$	(i) ZrO_2 (ii) CeO_2	AOM	CH_4	TGA, FxB	[49]
(i) $BaFe_2O_4$ (ii) $CaFe_2O_4$	–	COP	Coal	TGA, FxB	[135]
(i) $Cu_xFe_{3-x}O_4$(x = 0, 0.3, 0.5, 0.7, 1, 1.5) (ii) $Cu_{0.7}Fe_{2.3}O_4$	(i) ZrO_2 (ii) Ce–ZrO_2 (n_{Ce} : n_{Zr} = 1/1, 2/1, 3/1)	COP	CH_4	FxB	[48]
(i) 60 wt% $Ni_xCu_{0.5-x}Fe_{2.5}O_4$(x = 0, 0.1,	(i) ZrO_2	COP	CH_4	FxB	[136]

(continued on next page)

Table 1 *(continued)*

Oxygen carrier			Fuel in reduction process	Reactor type[b]	References
Metal oxide	Support material	Preparation method[a]			
0.2, 0.3, 0.4, 0.5) (ii) 60 wt% Cu–Fe–O(Cu/Fe ratio was set at 0.7/2.3, Ce/Zr ratio was varied at 1/1, 2/1, and 3/1)	(ii) Ce–ZrO_2				
(i) $M_{0.39}Fe_{2.61}O_4$(M = Ni , Co or Zn) (ii) 33.3 wt%$Ni_{0.39}Fe_{2.61}O_4$	(i) None (ii) ZrO_2	(i) COP (ii) AOM	CH_4	FxB	[45]
Fe–Ni–O (Fe_2O_3/Al_2O_3/NiO = 7/3/0.53 as mass raion)	Al_2O_3	WIMP	Biomass	cFB	[137]
40 wt% M (M = Fe, Cu, Co, Mn)	(i) Al_2O_3 (ii) TiO_2	P	CH_4	FxB	[138]
40 wt% M (M = Fe, Cu, Co, Mn)	Al_2O_3	COP	CH_4	FxB	[139]
(i) Fe_2O_3@$La_{0.8}Sr_{0.2}FeO_{2.85}$(LSF) ($n_{Fe2O3}$: n_{LSF} =1:1) (ii) Fe_2O_3:LSF(n_{Fe2O3}: n_{LSF} =1:1)	–	(i) PEC (ii) SG	CH_4	TGA, TR	[140]
Bauxite residual	–	FG	Coal char	bFB	[141]
Hematite	–	–	Biomass	cFB	[142]
Ilmenite ore	–	–	Raw gas from biomass gasifier	cFB	[143]
(i) Ilmenite (ii) 40 wt% NiO	(i) None (ii) α-Al_2O_3	(i) – (ii) SD	Raw gas from the gasifier	cFB	[144]
Natural hematite	–	–	Biomass	bFB	[145–147]
Natural hematite	–	–	Biomass	bFB, cFB	[148]
Natural olivine	–	–	H_2	TGA	[149]
Iron ore	–	–	CH_4	TGA	[150]
Iron ore	–	–	Biomass	cFB	[151]
xNiO–iron ore(x=1.285, 6.034, 11.387 wt %)	–	IMP	Biomass Char	TGA, FxB	[152]
$BaCoO_3$, $BaFeO_3$, $SrCo_{0.8}Fe_{0.2}O_3$, $Ba_{0.5}Sr_{0.5}Co_{0.8}Fe_{0.2}O_3$	–	SG	Coal	FxB	[153]
CuO	PURALOX, bauxite, γ-Al_2O_3, mullite	IMP	Biomass gasification gas	bFB	[154]
xCuO (x = 10, 15, 20, 25, 30 wt%)	(i) yZrO_2–Al_2O_3(y = 10, 20, 30 wt%) (ii)Al_2O_3	IMP	CH_4	FxB	[155]
(i) 40 wt% CuO (ii) 10 wt% $La_{0.8}Sr_{0.}$2FeO3	(i) $MgAl_2O_4$ (ii) γ-Al_2O_3	(i) SD (ii) IMP	C_2H_4, C_6H_6, C_7H_8	bFB	[156]
40 wt% Mn_3O_4	$MgZrO_3$	FG	Raw gas from biomass gasifier	cFB	[157]
(i) 100 wt% $CaMn_{0.775}Mg_{0.10}Ti_{0.125}O_{3-\delta}$ (ii) 40 wt% CuO (iii) 40 wt% CuO (iv) 60 wt% Fe_2O_3 (v) 60 wt% Fe_2O_3 (vi) 100 wt% $La_{0.8}Sr_{0.2}FeO_3$ (vii) 10 wt% $La_{0.8}Sr_{0.2}FeO_3$ (viii) 37 wt% Mn_3O_4 (ix) 65.4 wt% NiO (x) quartz sand (xi) bauxite (xii) ilmenite (xiii) LD stone	(i) None (ii) $MgAl_2O_4$ (iii) ZrO_2 (iv) α-Al_2O_3 (v) $MgAl_2O_4$ (vi) None (vii) γ-Al_2O_3 (viii) ZrO_2 (ix) α-Al_2O_3 (x)–(xiii) None	(i)–(ii), (vi), (ix) SD (iii)–(v) FG (vii) IMP	Synthetic gasification gas	bFB	[158]
$CaSO_4$	–	PUR	Coal	TR	[159]
$CaSO_4$	–	PUR	Coal	TGA	[160]
Phosphogypsum	–	–	Coal	TGA	[161]
$Pr_{1-x}Zr_xO_{2-\delta}$ (x = 0, 0.1, 0.3, 0.5, 0.7, 0.9)	–	P	CH_4	FxB	[162]
(i) SnO_2 (ii) In_2O_3 (iii) ZnO (iv) WO_3 (v) MoO_3 (vi) MoO_2 (vii) Fe_3O_4 (viii)– (x) 50 wt% WO_3	(i)–(vii) None (viii) SiO_2 (ix) Al_2O_3 (x) ZrO_2	(i)–(v) TD (vi) H_2–reduction (vii) COP (viii)–(x) IMP	CH_4	FxB	[42]

n.a.: not available.

[a] Key for preparation method: ALD: atomic layer deposition, AOM: aerial oxidation method, CAM: citric acid method, CCTM: colloidal crystal template method, CCM: citric acid method, CI: co-impregnation, COP: coprecipitation, CP: chemical precipitation, DIMP: dry impregnation, DIS: dissolution, DP: deposition-precipitation, EM: evaporation method, FG: freeze granulation, GB: gas-bubble-assisted method, GNP: glycine-nitrate process, HIMP: hot impregnation, HS: hydrothermal synthesis, IMP: impregnation, SIMP: Sequential impregnation, SFEP: soap free emulsion polymerization, HWIMP: hot incipient wet impregnation MM: mechanical mixing, P: precipitation, PE: pelletizing by extrusion, PEC: pechini, PUR: purchase, SC: solution combustion, SD: spray drying, SF: spin flash, SG: sol-gel, SP: spray pyrolysis, SSM: solid state reaction method, TD: thermal decomposition, WG: wet granulation, WIMP: wetness impregnation, UH: urea hydrolysis method.

[b] Key for reactor type: bFB: batch fluidized bed, cFB: continuous fluidized bed, DB: differential bed reactor, ETB: electronics thermobalance, FxB: fixed bed, MB: moving bed reactor, MR: microreactor, PB: packed bed, pFxB: pressurized fixed bed, TGA: thermogravimetric analyzer, TEOM: tapered element oscillating microbalance, TPR: temperature programmed reduction apparatus, TPO: temperature programmed oxidation, TR: tube reactor.

almost in a fixed bed reactor or a pulse apparatus. As the most likely setup is circulating fluidized bed, the performance of these Ce-based materials needs further investigation.

3.1.2.3. Perovskite-type oxygen carriers. Perovskite-type oxides (ABO_3, where A and B are usually rare earth and transition metal cations, respectively) represent an alternative class of reducible oxides with potential as partial oxidation catalysts. The transition metals serve as both lattice oxygen carriers and catalysts for activating hydrocarbons. They usually exhibit excellent redox properties, high oxygen mobility, and thermal stability, good oxygen suppliers, and the high selectivity to synthesis gas instead to CO_2 and H_2O, therefore, they are quite effective for catalytic oxidation reactions including hydrogenation, CO oxidation, and catalytic combustion [167]. The perovskite-type particles are interesting for many applications, such as oxygen permeable membranes [13]. Moreover, they are also found suitable for the CLR processes.

Due to the relatively high capacity of reversible oxygen storage, high activity, high structural stability and high selectivity to synthesis gas, $LaFeO_3$ was attractive as a catalyst and oxygen carrier for methane partial oxidation [104–106]. Dai et al.[102] investigated the selective reactivity of a series of perovskite $AFeO_3$ oxides (A =La, Nd, Eu) in the methane partial oxidation to synthesis gas in a fixed-bed reactor. The results showed that methane could be converted selectively to synthesis gas, and the $LaFeO_3$ sample exhibited the best performance for synthesis gas production. The $LaFeO_3$ oxide maintained high catalytic activity and structural stability in redox atmospheres, and carbon deposits did not occur in sequential redox cycles. Recently, the synergistic effect between the CeO_2 and $LaFeO_3$ materials has been observed by Zheng et al [90]. They found that the coexistence of the Ce^{3+} and Fe^{2+} irons induces higher oxygen vacancies in the CeO_2/$LaFeO_3$, and the material shows higher oxygen storage capacity and reactivity for methane oxidation.

To find an oxygen carrier with a better reactivity, selectivity, stability, and a good resistance to carbon deposition, a series of defect perovskite oxides, such as $La_{1-x}Sr_xMO_3$ (M=Mn, Ni; x=0–0.4) and $La_{1-x}Sr_xFeO_3$ [109–111], $La_{0.3}Sr_{0.7}Fe_{0.8}M_{0.2}O_{3-\delta}$ (M= Ga, Al) and $La_xSr_{1-x}FeO_{3-\delta}$ perovskites [114], $LaFe_{1-x}Ni_xO_3$ [108] and $LaFe_{1-x}Co_xO_3$ [107] were also be confirmed well suited for syngas generation due to the high selectivity towards CO/H_2.

He and Li [127,128] reported a perovskite $La_{0.8}Sr_{0.2}FeO_{3-\delta}$ promoted Fe_3O_4 as a redox catalyst for partial oxidation of methane and water-splitting reaction. Using the Fe_3O_4–LSF oxygen carrier coupled with a layered reverse-flow reactor, up to 77% steam to hydrogen conversion was achieved at 930 °C, which exceeds the thermodynamic limit for the FeO_x–H_2O–H_2 ternary system by 15% [127]. Neal et al. [124,125,140] investigated the feasibility of core-shell oxygen carriers (MeO_x @ $La_ySr_{1-y}FeO_3$) that combines a transition metal oxide core with a mixed ionic-electronic conductive perovskite shell for CLRM of methane. The results indicated that core-shell catalyst Fe_2O_3@LSF is more active, stable and selective than that of Fe_2O_3 : LSF composite catalyst [140]. Compared to Mn or Co oxide cores, Fe_2O_3 @ $La_ySr_{1-y}FeO_3$ were found to be more effective for CLR applications [124]. They proposed that the iron oxide core serves as the primary source of lattice oxygen, whereas the LSF shell provides an active surface and facilitates O^{2-} and electron conductions (Fig. 7).

In general, the perovskites-type oxygen carriers can be used in the CLR process. However, the reduction rate of perovskites for synthesis production needs to be increased because reduction rate is much lower than that of oxidation rate [104]. In addition, the carbonaceous deposits was reported in some literature [105,113]. Moreover, the oxygen storage capacity of perovskites-type oxygen carriers tend to be low, limiting their practical application in a real operation process, and long-term tests in a fluidized bed reactor are also needs to be conducted to confirm the feasibility in a real industrial process.

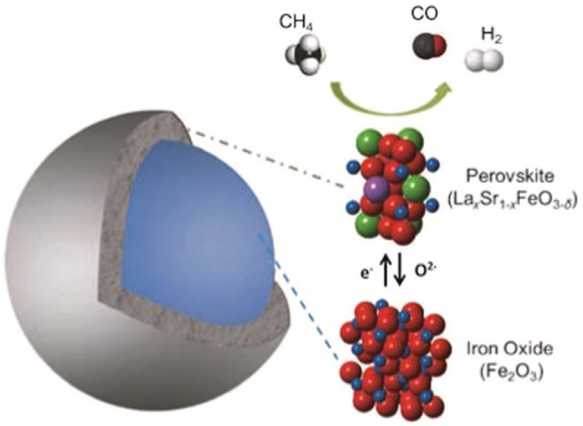

Fig. 7. Schematic of the core-shell redox oxygen carrier [125].

3.1.2.4. Other oxygen carriers. Except for the oxygen carriers mentioned above, other kinds of oxygen carriers, such as Fe-based, Cu-based [154–156], Mn-based [157] Pr-based [162] and even Ca-based [159–161] matierials were also prepared and investigated. Among those materials, iron oxide is an attractive oxygen carrier for the application of CLR of methane because of its abundance, high melting point and low price. Forutan et al. [139] used iron, copper, magnesium and cobalt metal oxides supported on alumina in CLR(a) process. The iron-based material had the highest resistance against sintering and the highest capacity for oxygen adsorption among the four carriers. The reactivity of iron supported on Al_2O_3 was better than that on TiO_2 [138]. However, the iron-based oxygen carriers often restricted for the lower reactivity rate, low oxygen transport capacity, and low selective to syngas. The materials of with the addition of promoters, such as Fe_2O_3–Rh_2O_3/Y_2O_3, Fe_2O_3–Cr_2O_3–MgO [126] and Fe_2O_3–CuO [136], were proved to be selective to syngas. Hafizi and the co-operators added Mg [130], Ca [129,131] or Ce [131] as promoters in the iron-based oxygen carrier in the CLR(a) process of methane. High H_2 production capacity and stability in redox cycles was confirmed with those materials. The methane conversion reached to 100% and the hydrogen production yield reached to 83% at 700 °C when using 15 wt% Fe–5 wt%Ca/γ-Al_2O_3 as an oxygen carrier [129]. Different Ca-based sorbents including industrial CaO, synthesized CaO and CaO–CeO_2 (Ce/Ca = 0.2) were also added in the CLR(a) process [132]. The addition of sorbents not only can produce high purity hydrogen, but also can enhance the reaction of partial oxidation of methane. The H_2/CO molar ratio of 16.7 was obtained when using $Fe_2O_3/MgAl_2O_4$ oxygen carrier and synthesized Ce/Ca = 0.2 sorbent at 600 °C. Moreover, the low cost materials, such as the red mud prepared from Bauxite residual was used as the oxygen carrier in CLR(a) of coal char for syngas production. It was found that, the material showed a strong catalytic function for char gasification and syngas reforming [141]. The natural hematite has also been used for CLR(a) process of biomass in a 25 kW_{th} interconnected fluidized bed reactor [142,148].

3.1.3. Chemical looping reforming using solid and liquid fuels

Higher hydrocarbons than CH_4, such as the liquid fuels and even the solid fuels have also been explored in the CLR processes to produce H_2 and CO.

Moldenhauer et al. [78] investigated the feasibility of liquid fuel in CLR(a) process in a 300 W chemical looping reactor with continuous particle circulating for 20 h. Kerosene was used as a liquid fuel and NiO/MgO–ZrO_2 as an oxygen carrier. The experimental results showed that nearly all hydrocarbon could be reformed into synthesis gas with concentrations of hydrocarbons as low as 0.01%, which indicated that

the liquid fuel can have the similar performance with that of gaseous fuels in a continuous CLR(a) process. Ortiz et al. [168] investigated the reaction conditions at for a high Syngas-H_2 production in the CLR(a) system with ethanol as fuel based on the thermodynamic equilibrium state. The feasibility of CLR(a) using bioethanol was demonstrated in a 1 kWth circulated fluidized bed reactor during more than 50 h [68]. A syngas composed of ≈ 61 vol% H_2, ≈ 32 vol% CO, ≈ 5 vol% CO_2 and ≈ 2 vol% CH_4 was obtained.

Mendiara et al. [79,80] selected toluene (C_7H_8) as model compound of biomass tar and evaluated the feasibility of CLR(a) process as a technology for biomass tar cleaning. The performance of four oxygen carriers (60% NiO/$MgAl_2O_4$ (Ni60), 40% NiO/$NiAl_2O_4$ (Ni40), 40% Mn_3O_4/Mg–ZrO_2 (Mn40) and $FeTiO_3$ (Fe)) were tested under alternating redox cycles and the conditions to minimize the carbon deposition have also been investigated. It was found that Ni40 and Mn40 showed stable reactivity to C_7H_8 after a few cycles. Ni40 showed a high tendency to carbon deposition, but this could be completely avoided by adding water with a H_2O/C_7H_8 molar ratio of 26.4. However, the deposition could not be completely avoided in spite of the high H_2O/C_xH_y molar when CH_4 and C_7H_8 were mixed when using Ni40 as oxygen carrier [80]. Lea-Langton et al. [61] studied the feasibility of pine oil and palm empty fruit bunches (EFB) oil with Ni/Al_2O_3 as a catalyst and an oxygen transfer in a packed bed at 600 °C. The results were remarkable with the maximum averaged fuel conversions of pine oil and EFB oil ~ 97% and 89% when the steam/carbon ratios of 2.3 and 2.6 respectively during the reduction process. The yield efficiency of H_2 produced were approximately 60% and 80% with little CH_4 as by-product. However, the H_2 yield and the rate of reduction decreased during redox cycles.

The researchers in university of Leeds have investigated the CLR(a) processes using different liquid materials, such as acetic acid [62], sunflower oil [169], glycerol [58] and waste vegetable cooking oil [59,60] to determine the suitability of liquid fuels to maintain steam reforming activity under chemical looping reforming conditions. It is worth noting that when waste cooking oil was used, high purity hydrogen (> 95%) was produced at 600 °C and 1 atm with the molar steam to carbon ratio of 4. The fuel and steam conversion were higher when the sorbent material was added.

In CLRM process, the modified ferrospinels MFe_2O_4 (M = Fe, Co or Ni) were employed as oxygen carrier materials, and they showed promising features for hydrogen production using ethanol or methanol as the reducing agent [117–121]. The chemical looping process for ethanol reforming over the modified ferrospinels is shown in Fig. 8. The sintering of magnetite and carbon deposition during redox cycles [121], the reaction routes and the related reaction mechanism [117] together with the reactivity of the mixed ferrospinels [118] during the processes of ethanol anaerobic decomposition and oxidation were also studied. According to the obtained results it can be concluded that, compared with magnetite, the Ni ferrite showed a higher activity in ethanol anaerobic oxidation and decomposition [118]. For Co-ferrite, a complete re-oxidation of $CoFe_2O_4$ to its original oxidation state was not possible using only water as the oxidant; therefore, an extra oxidation of the material with air was needed [119]. The reaction routes of the anaerobic oxidation of ethanol followed over each material were investigated by using in situ DRIFTS-MS method [117]. Results showed that the first step in ethanol transformation appeared to be

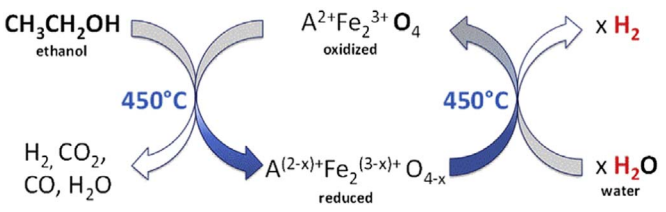

Fig. 8. The CLRM of ethanol over modified ferrospinels. A= Fe, Co, Ni or Cu [118].

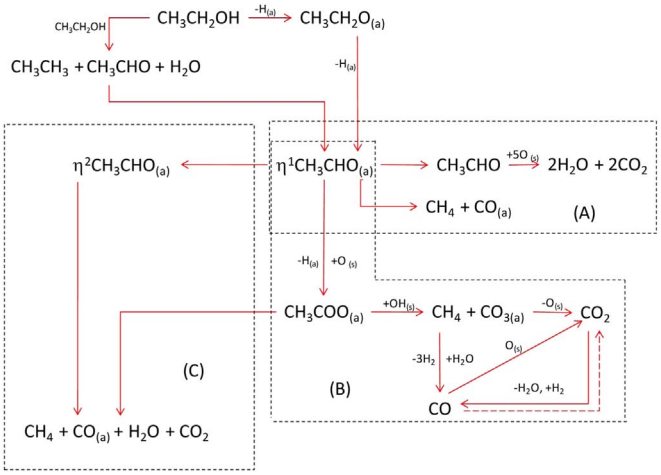

Fig. 9. Ethanol adsorption and transformation over $CoFe_2O_4$ (A), $NiFe_2O_4$ (B), and Fe_3O_4 (C) [117].

common to all spinels and corresponds to a dehydrogenation to acetaldehyde. However, the following pathways depended on the spinel. Acetaldehyde could be either oxidized to acetates ($NiFe_2O_4$), mainly decomposed to CO and methane ($CoFe_2O_4$), or completely oxidized (Fe_3O_4) (see Fig. 9).

Jiang and the co-operators [84] in Dalian University of Technology investigated the reactivity of synthesized NiO supported on montmorillonite using ethanol as fuel in a fixed-bed reactor. It was found that 20Ni–MMT exhibited high H_2 selectivity (above 70%) and ethanol conversion. The ethanol conversion maintained almost 80% even after 20 cycles. They also investigated the CLR(a) process of glycerol using Ni-based oxygen carriers supported on $NiAl_2O_4$ [72,82] and Al_2O_3-Montmorillonite with or without Ce promoter [170] as oxygen carriers. The authors found that the CeNi/Al–M–41 displayed the superior reactivity and excellent stability due to the strengthened anti-sintering and coke capability [170]. The H_2 concentration of 90% of the equilibrium value was achieved at 600 °C, and glycerol conversion was up to 99% [72]. When CaO was added as a sorbent to remove the CO_2, high-purity H_2 of 94.6% is obtained when steam to carbon (S/C) was 3 at the initial temperature of 600 °C [82].

CLR technology can also be used for tar elimination (cleaning) in biomass-derived gasification gas [143]. In the FR, the oxygen carriers not only acts as an oxygen carrier, but also acts as a catalyst for tar reforming. The reforming of tars has been tested with the natural ore ilmenite [115,143,157,158], synthetic Mn_3O_4 supported on ZrO_2 [157] and NiO supported on α-Al_2O_3 [77,144] as oxygen carriers. Ni-based materials showed the best catalytic performance with the overall tar conversion more than 95% at 880 °C [77,144], while the corresponding value for ilmenite catalyst was 60% at 850 °C [144]. Even though the superior reactivity to convert hydrocarbons, Ni-based materials suffer from the characteristics of toxic and high price. The alternative materials such as supported Cu-based materials and perovskite $La_{0.8}Sr_{0.2}FeO_3$ were identified as promising bed materials for CLR with C_2H_4 as a tar surrogate [158]. However, it was found that Cu-based materials unable to convert aromatics and C_2H_4 with the presence of monoaromatic compounds, while $La_{0.8}Sr_{0.2}FeO_3$ perovskite supported on γ-Al_2O_3 achieved high conversion of all tar surrogates investigated [156].

Different from CLC, the target products in FR of CLR processes are syngas, therefore, it would be recommended if the oxygen carrier can react with the solid fuels but not further with the synthesis gas produced to produce CO_2 and water, therefore, it is hard to control the reaction selectivity to produce syngas. Only few investigations reported in the literature about the CLR processes using coal as fuel to produce syngas [122,153,159,160]. Liu et al. [159] investigated coal

gasification using calcium sulfate ($CaSO_4$) in a fixed-bed reactor. It was found that the $CaSO_4$/C molar ratio should be higher than 0.2 to reach auto-thermal balance and the corresponding syngas yield is about 1.2 moles per mole carbon, respectively. They also observed that the total syngas yield decreased with the present of oxygen carrier due to the reaction of syngas generated with $CaSO_4$. They also found that CO_2 can promote the reaction between coal and $CaSO_4$ [160]. Guo et al. [122] assessed the reactivity of Ca-decorated iron based oxygen carriers with coal in a batch fluidized-bed reactor for synthesis gas generation. They found that when Fe_2O_3 was used as the oxygen carrier, the volume concentration of the synthesis gas was lower than that without the oxygen carrier since iron oxide reacts with the synthesis gas produced by coal-steam gasification. However, the H_2 volume concentration and carbon conversion increased when CaO was added due to the catalytic effects of CaO. Recently, Siriwardane et al. [135] confirmed that $BaFe_2O_4$ and $CaFe_2O_4$ were excellent for CLR(a) of coal as those two materials had high reactivity with coal but low reactivity with synthesis gas. The synergetic effect between steam and the oxygen carriers was observed. The investigations of hydrogen-enriched gas production from steam gasification using CaO-based materials as a catalyst and oxygen carrier transfer in the chemical looping gasification process has been reviewed by Udomsirichakorn et al [171].

Considering the biomass, Wang et al. [172] conducted the thermodynamic analysis of syngas generation from biomass based on the method of Gibbs free energy minimization with Mn_2O_3 as an oxygen carrier, and the results showed that the total dry concentration of CO and H_2 could reach to 98.8%. García-Díez et al. [173] also conducted the mass and heat balances to determine the auto-thermal conditions that maximize H_2 production using three different types of bioethanol as fuel. Results showed that when diluted ethanol (~52 vol%) was used, 4.62 mol of H_2 per mol of ethanol was obtained and the system could reach the auto thermal state. The CLR(a) process of biomass has been demonstrated in TGA [149,152], small batch fixed-bed reactor [152], tube reactor [159], or fluidized-bed reactor [145–147]. It was found that the iron oxide not only act as a catalyst for biomass tar cracking [149] but also as an oxygen carrier to transfer oxygen. Nevertheless, the reactivity of lattice oxygen in hematite particles is slightly lower than that of steam [145]. Steam introduction can promote the reforming reactions [147]. A 25 kW_{th} prototype in Southeast University was constructed to investigate the performance of biomass direct CLR(a) using hematite as an oxygen carrier [142]. The maximum syngas yield reached to 0.74 $Nm^3\ kg^{-1}$ when the gasification temperature was set to be 860 °C. Ge et al. [148] carried out the CLR(a) of biomass in a 25 kW_{th} continuous reactor using natural hematite as an oxygen carrier. The syngas yield in the continuous reactor reached the maximum value of 0.64 $Nm^3\ kg^{-1}$ at 850 °C.

3.1.4. Continuous operation experience of the circulating reactors

To investigate the industrial operation of CLR, the different research groups of Sweden, Spain Australia, and China have investigated the process in different continuous reactors. Chemical-looping processes could be designed in several ways but circulating fluidized beds are likely to have an advantage over other alternatives since this design provides good contact between gas and solids and allows a smooth flow of oxygen-carrier particles between the reactors. The CLR processes have been demonstrated at atmospheric pressure not only at a laboratory scale, but also in continuous units up to 140 kWth pilot plant. The summary of CLR circulating reactors are listed in Table 2, and the corresponding CLR facilities are shown in Fig. 10.

Rydén et al. [39] described the continuous chemical-looping reforming of natural gas in a laboratory reactor. The reactor consisted of two interconnected fluidized beds, which is shown in Fig. 10**(a).** NiO-based oxygen carriers supported on $NiO/MgAl_2O_4$ [39], Al_2O_3(α-Al_2O_3 or γ-Al_2O_3) [63] NiO/Mg–ZrO_2 [75] were used as oxygen carriers. Complete conversion of natural gas was achieved in the FR and the selectivity towards H_2 and CO was high and the mole ratio of the H_2 to CO equaled to about 2:1. The carbon formation was reduced or eliminated by adding 25–30 vol% steam to the natural gas. Except the common gaseous fuels, a liquid fuel, sulfur-free kerosene, has been used for H_2 production in this continuous unit with NiO/(MgO–ZrO_2) as an oxygen carrier [78]. During the experiments lasted for 20 h, nearly all hydrocarbon could be reformed into a synthesis gas. In the best case, only 0.01% of the fuel carbon remained as hydrocarbon.

de Diego et al. and the co-operators in Institute of Carboquímica presented the experimental results obtained in a circulating fluidized bed reactor using methane [64] and bioethanol [68] as fuel. The schematic diagram of the facility is shown in Fig. 10**(b)**. NiO21–γ-Al_2O_3 and NiO18–α-Al_2O_3 were used during more than 50 h of operation respectively. It was found that in all operating conditions almost full conversion of CH_4 or the bioethanol was achieved, and carbon formation was easily avoided. The auto-thermal conditions could be obtained by adjust in the NiO to fuel molar ratio. When using bioethanol as fuel, a syngas composed of ≈ 61 vol% H_2, ≈ 32 vol% CO, ≈ 5 vol% CO_2 and ≈ 2 vol% CH_4 was reached at auto-thermal conditions for both materials [68]. A pilot plant up to 140 kW (see Fig. 10**(c)**) has been successfully constructed and operated in Vienna University of Technology for the CLR(a) of natural gas [38]. Two nickel-based oxygen carriers, NiO/$NiAl_2O_4$ with or without small MgO added were used as bed materials. Results showed that the FR exhaust gas approached thermodynamic equilibrium. Even though no steam was added to the natural gas feed no carbon formation was found for global excess air ratios larger than 0.4.

As mentioned in Section 3.1.3, CLR technology has also been proposed for tar elimination (cleaning) in biomass-derived gasification gas. The researchers in Chalmers University of Technology tested the reforming of tars in a circulated continuous unit (see Fig. 10**(d)**) with the natural ore ilmenite [143], synthetic Mn_3O_4 supported on ZrO_2 [157] and NiO supported on α-Al_2O_3 [77,144] as bed materials. It was found that the tar removal efficiency is high than 95% when using Ni-based materials, and the matierials maintained the oxygen transfer and catalystic properties during the test [77,157].

Solid fuels such as biomass has been investigated in different circulated units. Ge et al. [142,148] investigated the performance of syngas production process using natural hematite as an oxygen carrier and biomass as fuel in a 25 kW_{th} interconnected fluidized bed reactor (Fig. 10**(e)**). It was found that when the hematite mass percentages was higher than 40 wt%, the system could reach auto thermal station. The experimental results also showed that 860 °C was the optimal gasification temperature corresponding to higher carbon conversion efficiency and maximal syngas yield (0.74 $Nm^3\ kg^{-1}$). The CLR(a) of biomass was also performed in a 10 kW_{th} interconnected fluidized bed rector (see Fig. 10**(f)**) with Fe–Ni bimetallic oxygen carrier in Guangzhou Institute of Energy Conversion [137]. The composition of CO and H_2 as well as the gasification efficiency of biomass increased when using Fe–Ni bimetallic oxygen carrier than that using the Fe_2O_3/Al_2O_3 oxygen carrier. The optimal value of the gasification efficiency reached to 70.48% when the biomass feeding rate was 1.6 kg/h. Recently, Zeng et al. [151] proposed and investigated a novel chemical looping gasification process to generate syngas with high H_2/CO ratio. As shown in Fig. 10**(g)**, H_2 is generated by steam-iron process in the SR, and CO is produced by biomass gasification process in the FR, therefore, the ratio of can be adjusted. When sawdust was used as fuel and iron ore as an oxygen carrier, the cold gas efficiency of 77.21% and the H_2 yield of 0.279 $Nm^3\ kg^{-1}$ were obtained at the optimized conditions.

3.1.5. System integration and economic analysis

The economic analysis of CLR(a) process has been conducted at atmospheric and pressurized conditions [174–176]. The calculation results showed that pressurized CLR(a) potentially has very high efficiency. The efficiency could be at least 4% higher than that for the conventional steam reforming with CO_2 capture by amine scrubbing.

Table 2
Summary of CLR circulating reactors.

Location	Unite size (kW)	Configuration	Fuel	Oxygen careers	Operation time (h)	References
Chalmers University of Technology, Chalmers, Sweden	0.1–0.3	AR-fluidized bed FR-fluidized bed	n.g.	$NiO/MgAl_2O_4$	41	[39]
				$NiO/Mg–ZrO_2$	24	[75]
				$NiO/MgAl_2O_4$, NiO/α-Al_2O_3, NiO/γ-Al_2O_3	160	[63]
			kerosene	$NiO/(MgO–ZrO_2)$	20	[78]
Institute of Carboquímica, ICB–CSIC, Spain	0.9–1	AR-bubbling fluidized bed FR-bubbling fluidized bed	CH_4	NiO/γ-Al_2O_3,	> 50	[64]
			Bioethanol	NiO/α-Al_2O_3	> 50	[68]
Vienna University of Technology, Vienna, Austria	120–140	AR-fast fluidized bed FR-turbulent fluidized bed	n.g.	NiO/α-Al_2O_3, $NiO/(\alpha$-Al_2O_3–MgO)	> 90	[38,74]
Chalmers University of Technology, Chalmers, Sweden	n.a.	AR-circulating fluidized bed FR-bubbling fluidized bed	Raw gas from biomass gasifier	Ilmenite ore	n.a.	[143]
				$Mn_3O_4/MgZrO_3$	n.a.	[157]
				NiO/α-Al_2O_3	7	[77]
				Ilmenite, NiO/α-Al_2O_3	8	[144]
Southeast University, Nanjing, China	25	AR-high velocity fluidized bed FR-bubbling fluidized bed	Rice husk	Natural hematite	n.a.	[142,148]
Guangzhou Institute of Energy Conversion, Chinese Academy of Sciences(CAS), Guangzhou, China	10	AR-fast fluidized bed FR- bubbling fluidized bed	Sawdust of pine	Fe–Ni bimetallic (Fe_2O_3/Al_2O_3/NiO = 7/3/0.53 as mass raion)	n.a.	[137]
Southeast University, Nanjing, China	n.a.	FR-fast fluidized bed SR- bubbling fluidized bed	Pine sawdust	Iron ore	n.a.	[151]

n.a.: not available.

The reformer efficiency above 81% is possible if the oxygen carrier particles have high stability at the temperature as high as 1200 °C. The reactivity of two Ni-based oxygen carriers under pressurized conditions during the CLR(a) process was confirmed by Ortiz et al [66]. It was found that at all operating pressures the CH_4 conversion was very high (> 98%) and no carbon formation was detected.

Note that the CLR(a) under pressure conditions also face some problems before this can be realized. Firstly, the fuel conversion is thermodynamically hampered by pressure so the FR temperatures of 1000 °C or higher will be required to obtain sufficient conversion of the fuel [174]. Integration with a gas turbine is indispensable in order to obtain high efficiency. Otherwise there would be a large efficiency penalty for air compression. Secondly, the pressurized circulating fluidized beds are not conventional technology. Hence the pressurized CLR(a) technology needs further development to be used in industrial process.

da Silva et al. [177] analyzed the performance of a PEMFC (proton exchange membrane fuel cell) system integrated with a biogas CLR(a) processor. Compared with conventional process, the results showed that CLR(a) process can achieve high advantages when integrated with a PEMFC system. CLR(a) can be seen as an advantageous reforming technology, not only because it allows that the global process can be operated under auto-thermal conditions but also due to that it allows the PEMFC stack to achieve values of voltage and power closer to those obtained when SR fuel processors are used. The global efficiency obtained for fuel processors based on CLR(a) technology is close to those achieved by conventional fuel processors. At low loads, efficiency is around 45%, whereas, at higher power demands, efficiencies around 25% are calculated for all the fuel processors.

Spallina et al. [178] proposed a membrane assisted chemical looping reforming (MA-CLR) system for pure H_2 production. In this system, the natural gas is converted in the FR by reaction with steam and an oxygen carrier, and the produced H_2 permeates through the membranes for separation. Techno-economic assessment of the concept showed promising results. The H_2 production efficiency of the MA–CLR system was above 90%, which was 30% higher than that of the conventional fired tubular reforming (FTR) with CO_2 capture technology (MDEA absorption method). The cost of H_2 production also reduced from 0.28 €/Nm^3_{H2} to 0.19 €/Nm^3_{H2}.

He et al. [128,179] proposed a hybrid solar-redox scheme (Fig. 11). Both the liquid fuel and hydrogen are produced from methane and integrated solar energy in two redox steps based on CLRM process. In the Reducer, methane is partial oxidized by the material (Fe_3O_4–LSF) into CO and H_2, which is then converted into naphtha and diesel in the Fischer–Tropsch (F–T) reactors. In the Oxidizer, steam oxidizes the reduced material from the previous step, producing concentrated H_2. The overall process efficiency is estimated to be 67.5% (HHV), which is 7.7% (HHV) more efficient than SMR based co-production processes. The methane to fuel efficiency from the hybrid solar-redox process is estimated to be 99.4% on an HHV basis [179].

There are few investigations about the CLR(s) process. Pans et al. [36] conducted the evaluation of the two configurations using iron-based oxygen carriers based on the mass and enthalpy balances. The results showed that a H_2 yield value of 2.45 mol H_2 per mol of CH_4 can be obtained with the reformer tubes located inside the AR. This corresponds to a CH_4 to H_2 conversion of 74.2%, which is similar to state-of-the-art H_2 production technologies, but with inherent CO_2 capture in this process. Rydén et al. [175,176] evaluated the economy of CLR(s) process. It was found that CLR(s) process also seems well suited for large scale production of high purity H_2 with CO_2 capture. This concept utilizes conventional technology and moderate temperature and pressure, and may be easier to put into practice than CLR(a). An overall efficiency in the order of 80% seems possible.

3.2. Chemical looping hydrogen production

Fuel cell technology can convert chemical energy into electrical energy with high efficient without emissions of environmental pollutants, which makes fuel cells one of the most promising sources for future power generation. The carbon monoxide level in the gas has to be reduced to a level below 20 ppm in order to avoid poisoning of the catalyst at the fuel cell electrodes [180–182]. Therefore, high-purity

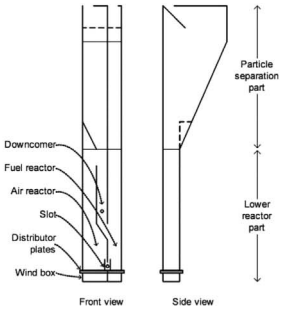

(a) 100W CLR for natural gas, Chalmers University of Technology, Sweden [39].

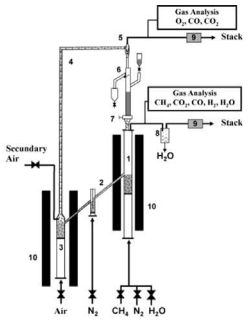

(b) 900W CLR for CH_4, Institute of Carboquímica, Spain [64].

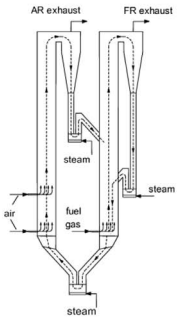

(c) 140kW CLR for natural gas, Vienna University of Technology, Austria [38].

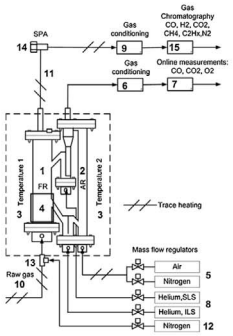

(d) CLR for raw gas from biomass gasifier, Chalmers University of Technology, Sweden [157].

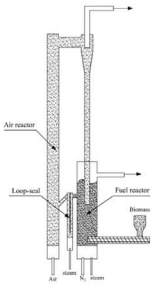

(e) 25kW CLR for biomass, Southeast University, China [142].

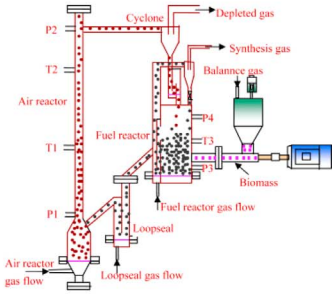

(f) 10kWth CLR for biomass, Southeast University, China [137].

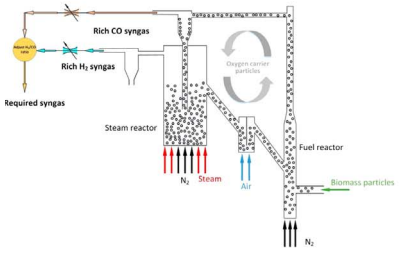

(g) CLR for biomass, Southeast University, China [151].

Fig. 10. CLR facilities of different fuels in interconnected fluidized beds.

hydrogen is required in the fuel cells, such as polymer electrolyte fuel cells (PEFCs). At present, more attention is paid to the steam-iron process because it can produce hydrogen with high purity [183–186]. The high purity hydrogen with the concentration of CO lower than 5 ppm can be produced using CLH process [186].

Iron has long been known to produce H_2 when reacted with steam. In 1910, Messerschmitt [187] patented the steam-iron process for producing hydrogen using the Fe_3O_4 to $Fe_{0.947}O$ transition. In recent years, the steam-iron process again gets attention because of the potential to produce H_2 with inherent CO_2 separation.

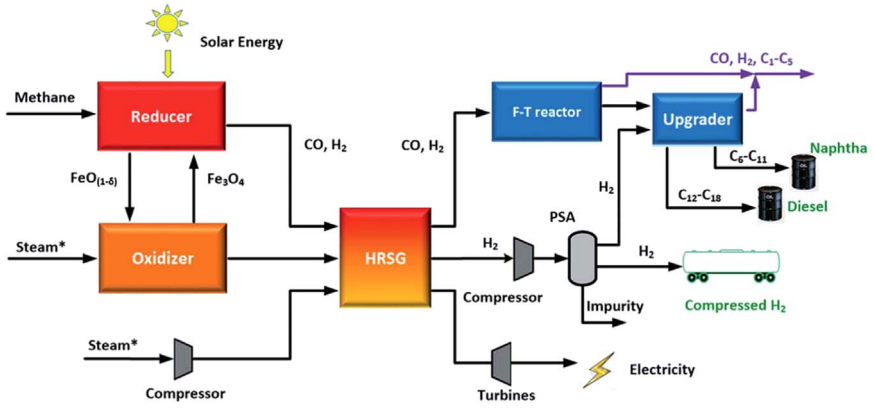

Fig. 11. Simplified schematic of the hybrid solar-redox process [128].

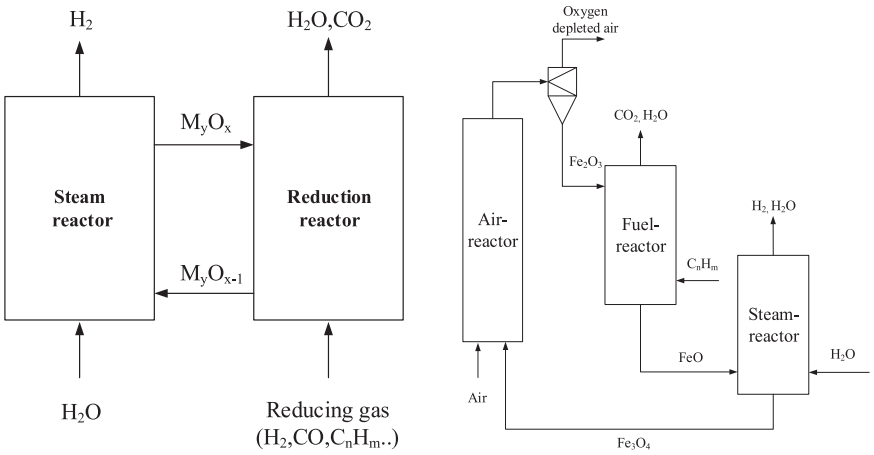

(a) Two-reactor system (b) Three-reactor system [188]

Fig. 12. The schematic diagram of the chemical looping hydrogen production.

The schematic of CLH process is shown in Fig. 12. In the FR, the reducing gases reduce the metal oxide (MO) to the metal form (M) according to reaction 19, releasing water vapor and carbon dioxide:

$$MO + CO/H_2 = M + CO_2/H_2O \quad (19)$$

The reduced metal particles are transported to the steam oxidation reactor and react with steam according to reaction 20, producing hydrogen and metal oxide particles. The regenerated metal oxide can be used in another redox cycle.

$$M + H_2O = MO + H_2 \quad (20)$$

If the fuel can be fully converted, the flue gas from the FR will be CO_2 and H_2O. The exhaust gas form the steam oxidation reactor is only the mixture of H_2 and water vapor. Almost pure CO_2 and H_2 can be obtained from the outlet of the FR and the SR only with water condensed. In general, the advantages of the CLH process can be classified as follows:

1) No water gas shift reactor and CO_2 separation process are needed;
2) Only one kind of oxygen carrier is required compared to the complex solid catalysts in SMR process;
3) No further hydrogen purification process is needed due to the highly concentrated of hydrogen.

CLH process is also called “Chemical Looping Steam Reforming (CLSR)”, “Chemical looping water splitting (CLWS) process” or “Chemical storage of hydrogen process” in some literature.

The traditional steam-iron process mainly focused on hydrogen production and could only partially convert the reducing gas [189]. The low conversions for both reducing gas and steam are limited by the thermodynamic property of the FeO and Fe_3O_4 phases. The two-reactor steam-iron arrangement can be modified by adding an AR [188,190]. The schematic diagram of the three-reactor CLH system is shown in Fig. 12**(b)**. In the third reactor AR, Fe_3O_4 is subsequently regenerated to Fe_2O_3 by oxidizing oxygen in air. Final oxidation in air has the potential to oxidize any contaminants, e.g. carbon or sulfur, deposited on the particles, and the produced Fe_2O_3 can increase the conversion of reducing fuels.

The possible reactions in the three reactors when coupling the gasification process are listed as follows [186]:

Under the CO_2 conditions, the coal gasification occurs as

$$C+CO_2 = 2CO\text{-}172{\cdot}4\ kJ/mol \quad (21)$$

The reductions of Fe_2O_3 with CO, a major component in syngas, occur by

$$3Fe_2O_3+CO = 2Fe_3O_4+CO_2+43{\cdot}2\ kJ/mol \quad (22)$$

$$0{\cdot}947Fe_3O_4+0{\cdot}788CO = 3Fe_{0{\cdot}947}O+0{\cdot}788CO_2\text{-}37{\cdot}3\ kJ/mol \quad (23)$$

$$Fe_{0{\cdot}947}O+CO = 0{\cdot}947Fe+CO_2+16{\cdot}7\ kJ/mol \quad (24)$$

The produced Fe or $Fe_{0.947}O$ can be oxidized by steam to generate hydrogen

$$0{\cdot}947Fe+H_2O = Fe_{0{\cdot}947}O+H_2+23{\cdot}8\ kJ/mol \quad (25)$$

$$3Fe_{0{\cdot}947}O+0{\cdot}788H_2O=0{\cdot}947Fe_3O_4+0{\cdot}788H_2+69{\cdot}2\ kJ/mol \quad (26)$$

In the air reactor, Fe_3O_4 can be reoxidized to Fe_2O3

$$2Fe_3O_4+1/2O_2 = 3Fe_2O_3+239{\cdot}7\ kJ/mol \quad (27)$$

The total process is

$$C+1{\cdot}25H_2O+0{\cdot}375O_2 = CO_2+1{\cdot}25H_2 +90{\cdot}6\ kJ/mol \quad (28)$$

CLH process can be described as a combination process of the partial oxidation and steam gasification of solid fuels, and the total process is exothermic. In the FR, reduction to Fe would be advantageous, since the capacity for producing hydrogen over the Fe_3O_4 to Fe transition is approximately four times greater than that for the Fe_3O_4 to $Fe_{0.947}O$ transition, but the production of H_2 declines less sharply during the redox processes. After ten cycles, H_2 production at all three temperatures is unsatisfactorily low [186]. Also, Fe acts as a catalyst for the reverse Boudard reaction, which can promote the carbon deposition process [191], decreasing the purity of the hydrogen. Therefore, to prevent the decomposition of methane, the reduction of iron oxide should be limited to $Fe_{0.947}O$ [192].

3.2.1. Development of oxygen carriers

The oxygen carriers that can be utilized in the CLH process requires a number of characteristics in order to make the process feasible [191]: (i) High reactivity with syngas and favorable thermodynamics regarding the fuel conversion to CO_2 and H_2O; (ii) High stability during redox cycles and maintained for a number of redox cycles for favorable economics; (iii) Good regenerable of the reduced form of the metal oxide and high steam-to-hydrogen conversion; (iv) High resistance to agglomeration and sintering.

Many researchers have evaluated the hydrogen production property of many metal oxides. It was found that Fe_2O_3 provided the best conversion of syngas to combustion products CO_2 and H_2O along with a high conversion of steam to hydrogen [191,194,195]. Solunke et al. [196] compared the thermodynamic reactivity combined with cost and toxicity of the metal oxides in the process and found that iron oxides is most suitable for CLH process. Li et al. [193] screened the properties of different metal oxide particles considering overall properties including oxygen carrying capacity, thermodynamic properties, reaction kinetics, physical strength, melting points, and environmental effects. The comparisons of the key properties of different metal oxide candidates is shown in Table 3. It was found that iron oxide is determined to be a desired oxygen carrier for hydrogen production.

Iron-based oxygen carriers have been found to be the best candidates for hydrogen production. The reactivity and the stability during the redox have been investigated in different reactor type. Table 4 shows a summary of the iron containing particles investigated by different authors and the testing conditions to evaluate their feasibility for use as oxygen carriers in a CLH system published after 2000.

3.2.1.1. Supported iron-based oxygen carriers. As mentioned above, iron oxide are the best active metal oxide, but the pure iron oxide without inert or additives deactivated quickly for the redox reaction due to sintering [185,193,204,207,242,251], so the properly maintenance and stability of the materials during multi-cycles are the key factors of the industrial process.

Inert supports are always used to increase the reactivity and the stability of the oxygen carriers. Kang et al. [195] found that $MgAl_2O_4$ and ZrO_2 were favorable support from thermal stability, chemical stability and specific heat capacity aspects. The reactivity and the stability of Fe-based oxygen carriers when supported with Al_2O_3 [193,204,215,219,223] and TiO_2 [223] were also investigated experimentally. It was found that the oxygen carriers supported with Al_2O_3 had superior reactivity than that with TiO_2, and the Fe_2O_3 with 60 wt% Al_2O_3 as support showed the highest hydrogen yield, the best reactivity, and no deterioration over the multi-cycle experiments at 900 °C in a fluidized bed during the multiple cycles [223]. The high maintenance of

Table 3
Comparisons of the key properties of different metal oxide candidates [193].

	Fe_2O_3	NiO	CuO	Mn_3O_4	CoO
Cost	+[a]	–	≈	–	–
Oxygen capacity (wt%)[b]	30	21	20	20	21
thermodynamics: syngas conversion[c]	Fe_2O_3/ Fe_3O_4 /FeO	NiO /Ni	CuO/ Cu_2O	Mn_3O_4/ MnO	CoO/Co
	100/83.2/ 42.5	99.3	100/ 100	100/0	96.3
Thermodynamics: steam conversion[d]	Fe/FeO/ Fe_3O_4	–	–	–	Co
	55.9/15.8/ 0.05				3.5
Reduction kinetics/ reactivity[e]	≈	+	+	≈	–
Melting points[f]	1275	1452	1026	1260	1480
Strength	+	–	–	≈	≈
Environmental and health impacts	≈	–	≈	–	–

[a] +, positive; -, negative; ≈, neutral.
[b] Maximum possible oxygen carrying capacity by weight percent, pure basis; achievable using excess fuel (actual).
[c] Maximum theoretical conversion of a syngas (66.6% CO and 33.3% H_2) to CO_2 and H_2O with the presence of the given metal oxide at 850 °C (calculated by Aspen Plus).
[d] Maximum theoretical conversion of steam with the presence of the given metal oxide at different oxidation states at 850 °C (calculated by Aspen Plus).
[e] Reactivity refers to the rates of the reactions between metal oxides and syngas (CO and H_2).
[f] Lowest melting points of the metal/metal oxides under various oxidation states (°C); Co_3O_4 and Co_2O_3 are not considered in this case since they are difficult to be oxidized.

reactivity of Fe_2O_3/Al_2O_3 was also confirmed by Li et al. [193] for more than 100 reduction-oxidation (redox) cycles in a TGA. Kierzkowska et al. [204] also confirmed the stable yields of H_2 over 40 cycles when using 60 wt% Fe_2O_3/40 wt% Al_2O_3 as an oxygen carrier produced by sol-gel method in a packed bed reactor. Iron oxide supported on Al_2O_3 can also be used at the elevated system pressures. Voitic et al. [227,228] found the hydrogen production was not influenced by the elevated system pressure using 90 wt% Fe_2O_3/10 wt% Al_2O_3 as an oxygen carrier. The hydrogen produced with the reformer steam iron process was obtained at a very high purity off 99.93% with only CO_2 as impurity [227]. They [230] also investigated the effect of elevated system pressure on the hydrogen production property and carbon contamination using $Fe_2O_3/Al_2O_3/CeO_2$ as an oxygen carrier with synthesis gas as fuel at the range of 36.0–49.8 bar. The hydrogen purity was within the range of 99.958–99.999% with CO as the main impurity. The amount of contaminations due to the oxidation of the carbon deposition is not influenced by the elevated system pressure.

Dueso et al. [207] embedded the iron oxide within a stable matrix $La_{0.7}Sr_{0.3}FeO_{3-\delta}$, and a synergetic effect was observed between the iron oxide and the lanthanum strontium ferrite (LSF) as the composite oxygen carrier with 30 wt% iron oxide showed high stability during 25 redox cycles. Galinsky et al. [220] also prepared the oxygen carrier containing 60 wt% iron oxide supported on LSF($La_{0.8}Sr_{0.2}FeO_3$) as the inert support. Reactivity tests performed in a TGA showed that the support LSF enhanced the reactivity of the oxygen carrier by 5–70 times compared than that with conventional TiO_2-, Al_2O_3- or YSZ support.

3.2.1.2. Modified iron-based oxygen carriers. Small amount of additives or promoters added in the iron-based oxygen carriers may have a synergetic effect on the stability and reactivity. Bohn et al. [237] investigated the addition of Al, Cr, Mg and Si on the stability of iron oxide in the CLH process. Results showed that stable H_2 yields over 10 cycles were achieved for the sample with 30 mol%Cr. Otsuka et al. [184] found that the additives such as Al, Cr, Zr, Ga and V were the effective elements for iron oxide, because they can promote the

Table 4
Summary of the oxygen-carriers tested in different CLH processes.

Oxygen Carrier			Fuel in Reduction Process	Reactor type	References
Metal oxide	Support material	Preparation method			
Fe_2O_3	–	MM	CO	PB	[186]
Fe_2O_3	–	MM	Syngas produced form in *situ* coal/coal char gasification	PB	[197]
Fe_2O_3	–	WG	H_2, CO	bFB	[198]
Fe_2O_3	–	MM	Char, K–char, Ca–char	bFB	[199]
Fe_2O_3	–	MM	H_2, CO	PB	[200]
Fe_2O_3	–	MM	CO	TGA	[201]
(i) Fe_2O_3 (ii) $NiFe_2O_4$ (iii) $CuFe_2O_4$	–	CAM	H_2, CH_4	ETB	[202]
(i) Fe_2O_3 (ii) Fe_2O_3–M(M= CeO_2, La_2O_3, $Ce_{0.5}Zr_{0.5}O_2$) (iii) M–(Fe_2O_3–$Ce_{0.5}Zr_{0.5}O_2$), M=Cu, Mg, Cr, Mo, M/(Fe_2O_3–$Ce_{0.5}Zr_{0.5}O_2$+M)=0.02, 0.05 as the weight ratio	–	(i)–(ii) UH (iii) UH+IMP	H_2+CO	CT	[203]
(i) Fe_2O_3 (ii) Fe_2O_3(x = 60, 80, 90 wt%)	(i) None (ii) Al_2O_3	(i) MM (ii) SG	CO	PB	[204]
(i) Fe_2O_3 (ii) 98 wt% Fe_2O_3–1.90 wt% Al_2O_3–0.10 wt% MoO_3 (iii) 98 wt% Fe_2O_3–1.75 wt% Al_2O_3–0.25 wt% MoO_3 (iv) 98 wt% Fe_2O_3–1.50 wt% Al_2O_3–0.50 wt% MoO_3 (v) 98 wt% Fe_2O_3–1.75 wt% Al_2O_3–0.25 wt% CeO_2 (vi)97.79 wt% Fe_2O_3–1.75 wt% Al_2O_3–0.20 wt% MoO_3–0.25 wt% CeO_2	–	(i) PUR (ii)–(v) SG (vi) WIMP	H_2,H_2+CH_4	TGA, FxB	[205]
(i) Fe_2O_3 (ii) 60 wt% Fe_2O_3 (iii) xFe_2O_3–5 wt% CeO_2(x = 45, 55, 65 wt%)	(i)None (ii)–(iii)Al_2O_3	SG	CO+H_2	TGA, FxB	[206]
(i) Fe_2O_3 (ii) $La_{0.7}Sr_{0.3}FeO_{3-\delta}$(LSF731) (iii) LSF731–x$Fe_2O_3$ (x = 11, 30 wt%)	–	(i)–(ii) MM (iii)–(iv) MM +PEC	CO	TGA, MR	[207]
(i) Fe_2O_3, (ii) xCaO–Fe_2O_3, n_{Fe2O3}/n_{CaO}=50, 57.3% and 66.7%	–	(i) WG (ii) WG+MM	H_2, CO	TGA, bFB	[208]
$(Fe_2O_3)_{1-x}$–$(Ce_{0.5}Zr_{0.5}O_2)_x$ (x = 0, 0.5, 0.7, 1.0)	–	COP	Syngas produced form in *situ* methane partial oxidation	two-layer reactor	[209]
(i) 15 wt% Fe_2O_3 (ii) 15 wt% Fe_2O_3–5 wt% CeO_2	$LaNiO_3$	CAM, IMP	CH_4	FxB	[210]
20 wt%Fe_2O_3	ZrO_2	COP	CH_4	MB	[211]
20 wt% Fe_2O_3	ZrO_2	COP	CH_4	cFB	[212]
30 wt% Fe_2O_3	$Al_{1.42}Mg_{0.58}O_{2.7}$	MM	CH_4	TGA	[213]
(i) 40 wt% Fe_2O_3 (ii) $Ca_2Fe_2O_5$	(i) ZrO_2 (ii) None	PEC	CO	PB	[214]
xFe_2O_3 (x = 50, 60, 75, 80, 90, 100 wt%)	α-Al_2O_3	COP	H_2, CO	TGA	[215]
50 wt% Fe_2O_3	$MgAl_2O_4$	SG	CH_4, CO	FxB	[216]
xFe_2O_3 (x = 60, 70, 80, 90 wt%)	α-Al_2O_3	COP	H_2	TGA	[217]
60 wt% Fe_2O_3	Al_2O_3	MM	CO	PB	[218]
60 wt% Fe_2O_3	Al_2O_3	MM	CO	TGA	[219]
60 wt% Fe_2O_3	(i)TiO_2 (ii)$La_{0.8}Sr_{0.2}FeO_3$	(i)–(ii) SSM	H_2, CH_4, CO	TGA	[220]
60 wt% Fe_2O_3	(i)Al_2O_3 (ii)13 wt% CuO–Al_2O_3	SSM	char	TGA	[221]
(i) 60 wt% Fe_2O_3 (ii) 60 wt% NiO (iii) 30 wt% NiO–30 wt% Fe_2O_3	Bentonite	MM	H_2, CO	bFB	[222]
(i) xFe_2O_3 (x = 60, 90 wt%) (ii) 60 wt% Fe_2O_3	(i) Al_2O_3 (ii) TiO_2	MM	CO	TGA, bFB	[223]
70 wt% Fe_2O_3	Al_2O_3	SG	H_2, Syngas, CH_4	TGA, FxB, cFB	[193,224,225]
85 wt% Fe_2O_3	xSiO_2+ yCaO +5 wt% Al_2O_3 (x+y = 10 wt%, x=0, 2.5, 5, 6.5, 7.5, 8.5, 10 wt%)	MM	H_2	CT	[226]
90 wt% Fe_2O_3	Al_2O_3	MM	H_2, syngas	TGA, pFxB	[227]
90 wt% Fe_2O_3	Al_2O_3	MM	H_2	pFxB	[228]
90 wt% Fe_2O_3	Al_2O_3	PUR	CO	bFB	[229]
90 wt% Fe_2O_3–5 wt% Al_2O_3–5 wt% CeO_2	–	COP	H_2+CO	pFxB	[230]
98 wt% Fe_2O_3–1.75 wt% Al_2O_3–0.25 wt% CeO_2	–	SG	Bio-fuels	FxB	[231]
Mo–(80 wt% Fe_2O_3–20 wt% $Ce_{0.5}Zr_{0.5}O_2$), x = 1–5 wt%	–	UH+IMP	H_2	TGA, MR	[232]
Mo–(80 wt% Fe_2O_3–20 wt% $Ce_{0.5}Zr_{0.5}O_2$), x = 1–5 wt%	–	UH+IMP	H_2	MR	[233]
98 wt%Fe_2O_3+1.75 wt%Al_2O_3+0.25 wt% CeO_2	–	SG	Methanol	FxB	[234]
N–M, N= Fe_2O_3, Fe, M = Al, Cr, Ni, Co, Zr, Mo, M/(Fe+ M) = 0.05 as mole ratio	–	IMP	H_2	FxB	[235]

(continued on next page)

Table 4 *(continued)*

Oxygen Carrier			Fuel in Reduction Process	Reactor type	References
Metal oxide	Support material	Preparation method			
Fe_2O_3–Mo, Mo/(Mo + Fe) = 0.00, 0.05, 0.08, 0.10 as mole ratio	–	HS	H_2	FxB	[236]
Fe_3O_4[b]	M=Al_2O_3, Cr_2O_3, MgO, SiO_2, $n_M/(n_M+n_{Fe})$=0.01, 0.1, 0.3	WIMP	CO	PB	[237]
(i) Fe_3O_4[b] (ii)M– Fe_3O_4[b](M= Al, Cr, Zn, Ga, V, Ti, Zr, Mg, Ca, Mn, Co, Ni, Cu, Y, Nb, Mo, Ce), molar ratio: M/(M+Fe) =0.03	–	(i) P (ii) COP	H_2	FxB	[184]
(i) Fe_3O_4[b] (ii)M– Fe_3O_4[b](M= Al, Sc, Ti, V, Cr, Y, Zr, Mo, Ce, Mn, Co, Ni, Cu、Zn, Ru, Rh, Pd, Ag, Ir, Re, Ta, W, Pt, Ga, Nb), molar ratio: M/(M+Fe) =0.03	–	(i) P (ii) COP	H_2	FxB	[183]
(i) Fe_3O_4 (ii) 60 wt% Fe_3O_4 –10 wt% CeO_2 (iii) 1 wt% Rh – 59 wt% Fe_3O_4 –10 wt%CeO_2 (iv) 1 wt% Cu – 59 wt% Fe_3O_4 –10 wt%CeO_2 (v) 3 wt% Cu – 57 wt% Fe_3O_4 –10 wt%CeO_2 (vi) 5 wt% Cu – 55 wt% Fe_3O_4 –10 wt%CeO_2 (vii) 3 wt% Cu – 57 wt% Fe_3O_4 –20 wt%CeO_2 (viii) 3 wt% Cu – 57 wt% Fe_3O_4 –30 wt%CeO_2 (ix) 10 wt% Cu – 50 wt% Fe_3O_4 –10 wt%CeO_2	(i)None (ii)–(ix)ZrO_2	COP	H_2	FxB	[238]
(i) 37 wt% Fe_3O_4[b] (ii) 37 wt% $Co_xFe_{3-x}O_4$	ZrO_2	ALD	Synthesis gas	SFR	[239]
40 wt% Fe_3O_4[b] (40 wt% Fe–BHA)	Barium hexaaluminate(BHA)	SG	Synthesis Gas	FxB	[240]
60 wt% Fe_3O_4[b]	$MgAl_2O_4$	FG	CO, Synthesis gas	cFB	[241]
(i) (0.045–0.45 mol%)Pd– Fe_3O_4[b] (ii) (0.0065–0.38 mol%)Zr– Fe_3O_4[b]	–	IMP	H_2	TEOM	[242]
(ii) Pd–Zr –Fe_3O_4[b] (content of (Pd+Zr) is 0.23 mol%).)					
(i) FeOx (ii) 5 mol% M–FeOx(M= Cr, Ni) (iii)5 mol%M–5 mol% Cr–FeOx(M=Co, Ni, Cu, Rh, Pd, Ir, Pt) (iv) 5 mol% Ni–5 mol% M–FeOx(M=Al, Ti, V, Cr, Zr)	–	(i) P (ii)–(iv) COP	CH_4	FxB	[185]
(i) M–FeOx (M= Rh, Mo), M/(M+Fe) =0.05 as mole ratio (ii) Rh–Mo–FeOx, Rh/(Rh+Mo+Fe)=Mo/(Rh+Mo+Fe) =0.05 as mole ratio	–	COP	H_2	FxB	[243]
(i) M–FeO_x(M=Cr, Cu), (M/(M+Fe) =0.05 as mole ratio) (ii) M–Cr–FeO_x(M=Co, Ni, Rh, Cu), M/(M+Cr+Fe) =0.05 as mole ratio (iii) Ni–M–FeO_x(M=Al, Cr, Zr, Mo) M/(M+Ni+Fe) =0.05 as mole ratio	–	COP	H_2, synthesis gas, methane	PB	[244]
$NiFeAlO_4$	–	SSM	CO, H_2	TGA, FxB	[245]
$NiFe_2O_4$	–	(i) SC (ii) COP (iii) HS (iv) SG	CO, H_2+CO	TGA, FxB	[246]
Laboratory iron ore	–	MM	H_2, CO	TGA	[247]
Ilmenite and three iron ores	–	–	Heavy fraction of bio-oil	TGA, FxB	[248]
Austrian MAC iron ore	–	–	Bio-oil	cFB	[249]
xKNO_3–iron ore(x = 0, 3, 6, and 10 wt%)	–	IMP	CO	bFB	[250]

[a] Key for preparation method: ALD: atomic layer deposition; CAM: citric acid method, COP: coprecipitation, DP: deposition-precipitation, DIS: dissolution, FG: freeze granulation, HIMP: hot impregnation, HS: hydrothermal synthesis, IMP: impregnation, MM: mechanical mixing, P: precipitation, PE: pelletizing by extrusion, PEC: Pechini, SC: solution combustion, SD: spray drying, SF: spin flash, SG: sol-gel, SP: spray pyrolysis, SSM: solid state method; WG: wet granulation, WIMP: wet impregnation, UH: urea hydeolysis.

[c] The initial state was Fe_2O_3 in the fresh iron oxide samples, but the second and subsequent redox reactions were performed between Fe_3O_4 and iron metal.

[b] Key for reactor type: FxB: fixed bed, pFxB: pressurized fixed bed, TGA: thermogravimetric analyzer, bFB: batch fluidized bed, cFB: continuous fluidized bed, TEOM: Tapered element oscillating microbalance, ETB: Electronics thermobalance, PB: packed bed, MR: microreactor, CT: ceramic-tube, MB: moving bed reactor. SFR: stagnation flow reactor.

reduction performance of the iron oxide with H_2 and also the reoxidation performance of the reduced iron oxide with water at low temperatures (< 400 °C). The additives moderated the sintering of iron oxide markedly with repeated redox cycles. After that, they [183] examined the effects of 26 metal additives in the iron-steam process at a temperature range of 373–873 K. Among the 26 metal elements examined as additives, Al, Mo and Ce could effectively enhance the stability and reactivity of Fe/Fe_3O_4 material during the repeated cycles. Co-addition of Mn, Co, Ni, Cu, and Zn worsen the reoxidation performance from the first cycle, while the addition of Ru, Rh, Pd, Ag, Ir, and Rt could enhanced the rate of reoxidation at the first cycle but unable to prevent the deactivation after that. Galvita et al. [209,252] also found that when Ce was added to the iron oxide, it could suppress the sintering, and increase the reactivity of the materials during the redox reactions, and the property of inhibiting the carbon deposition has also been confirmed [206]. Liang et al.[210] found that the addition of CeO_2 in Fe_2O_3/$LaNiO_3$ promoted the stability of the oxygen carrier for H_2 production during the 100 successive cycles.

The inclusion of 7.5 wt% SiO_2, 5 wt% Al_2O_3 and less than 2.5 wt% CaO was found to hinder the sintering to a large extent [226]. Rihko-Struckmann et al. [203,232,233] found the Mo species improved the stability of Fe_2O_3–$Ce_{0.5}Zr_{0.5}O_2$ during the redox cycles. The materials showed superior stability compared to those doped with Cu or Mg

additives [203]. The positive effect of Mo has been confirmed by Wang et al. [235,236]. They found the addition of Mo not only decreased the temperature of water decomposition significantly, but also improved the stability of the samples during repeated redox cycles. A clear decrease in the activation energy was also concluded for the steam oxidation process when using iron oxide samples containing Mo. Romero et al. [205] also found out, that for a mixed oxide with the composition of 98 wt% Fe_2O_3–1.75 wt% Al_2O_3–0.25 wt% MoO_3 maintained a slightly better hydrogen production rates than that of the cerium sample.

The temperature of the reaction needs to be higher than 1023 K when methane is used as reducing agent. To increase the reactivity of the oxygen carrier with methane at relatively lower temperatures and increase the stability of the material during the cyclic processes, Takenaka et al. [185] modified iron oxide with both Ni and Cr species. Addition of Ni to iron oxides enhanced the reduction with methane and the subsequent oxidation with water vapor at low temperatures, but Ni species promoted the sintering of iron species. Addition of Cr cations to iron oxides prevented the sintering of iron species. In contrast, the iron oxides containing both Ni and Cr species (denoted as Ni–Cr–FeO_x) with the amount of each metal adjusted to 5 mol%, they found that pure hydrogen could be generated repeatedly and the modified material maintained the reactivity during the redox cycles at temperatures < 923 K. Urasaki et al. [242] tested the performance of the iron oxide modified with very small amounts of Pd and/or Zr in the steam-iron reaction at the temperature of 723 K. Results showed that the addition of Pd or Zr with only 0.23 mol% in the iron oxide suppressed the sintering of iron oxide during the cyclic process. Palladium accelerated both the reduction and oxidation rates of partially reduced iron oxide, while zirconia increased only the oxidation rate. Addition of both palladium and zirconia together to the iron oxide resulted in marked enhancement of both reduction and oxidation.

Takenaka et al. [243] modified the iron oxide using Mo and/or Rh species. It was found that the addition of Rh species to iron oxides decreased the apparent activation energy of the hydrogen production process and enhanced the formation of hydrogen at low temperatures through the oxidation of iron metal with water vapor. However, Rh species in iron oxides promoted sintering of iron species during the redox. The addition of Mo cations to Rh–FeO_x prevented the sintering of iron species during the redox. The Rh–Mo–FeO_x achieved high stability and could produce hydrogen repeatedly through the redox. They [244] also modified the iron oxides containing Cr cations. Addition of Cu, Ni or Rh to iron oxides containing Cr cations enhanced the formation rate of hydrogen through the oxidation with water vapor at 573 K. Ni–Cr–FeO_x and Cu–Cr–FeO_x as well as Rh–Cr–FeO_x are promising oxygen carriers for pure hydrogen repeatedly through the redox.

Peña et al. [202] conducted the kinetic study of different metallic oxides, either alone (Fe_2O_3) or as mixed oxides ($NiFe_2O_4$, $CuFe_2O_4$) in a TGA system. The experimental results showed that the addition of a second metal to form double oxides exhibit greater reaction rates. Liu et al. [246] and Kuo et al. [245] also found the self-supported $NiFe_2O_4$ oxygen carrier showed a good hydrogen production capacity and a high recovery degree of lattice oxygen. Jin et al. [222] found that when NiO was added into the Fe_2O_3/Bentonite particles, the (NiO: Fe_2O_3)/bentonite particle represented better reduction reactivity and stable water splitting reactivity up to 7th cycle. He et al. [221] also found that adding a small amount of CuO to an iron-based oxygen carrier improved the reactivity of the oxygen carrier for solid fuel conversion. Other bi-metallic systems have also been studied where cobalt, manganese or zinc were mixed together with iron [253,254]. These systems were found to be active at high temperature (> 2000 °C) and consequently, but they present little interest when dealing with classic process conditions.

Besides the stability and the reactivity of the CLH process, the hydrogen generation capacity of the material can also be improved by adding small amount of promoters. As mentioned above, it is advantageous to improve the hydrogen production capacity if the iron-based oxygen carrier is reduced to $Fe_{0.947}O$ or Fe, therefore, achieving deep reduction of the oxygen carrier is a challenge for the CLH process. Liu et al. [250] modified the iron ore using KNO_3 and found that the K-decorated iron ore not only could promote the reduction rate and hydrogen production, but could weak the carbon deposition when using CO as fuel. Mixed oxides can also be used to increase the fraction of steam to hydrogen and promote the corresponding hydrogen yield, such as Ca–Fe–O system [214,255] and the perovskite $La_{0.8}Sr_{0.2}FeO_{3-\delta}$ (LSF) [127]. It was found that the equilibrium conversion of steam to hydrogen reached to 75% when using $Ca_2Fe_2O_5$ at 1123 K, which is higher than the theoretically achievable value of 62% when using iron oxide [214]. LSF–promoted iron oxide is shown to be capable of converting over 77.2% steam into H_2 during redox processes [127].

3.2.1.3. Iron ore with iron oxide contained. Most of the work in the literature on oxygen carrier development of CLH process has focused on finding synthetically produced particles. Compared to synthetic oxygen carrier particles, the use of natural minerals can decrease the cost of the operation. Kindermann et al. [247] investigated the feasibility of the industrial iron ore in the reformer sponge iron cycle (RESC) process. They found that the porosity of the particles decreased with the operation of the process, but the porosity would keep stable during 5 redox cycles when the amount of SiO_2 was high. Xiao et al. [248] compared the reactivity and the ability to inhibit or minimize carbon deposition of four iron-based oxygen carriers including an ilmenite and three iron ores in TGA and fixed bed reactor. Results showed that the ilmenite had superior reactivity to minimize the carbon deposition or Fe_3C formation in the reduction process. However, the reactivity and H_2 production capacity of ilmenite also decreased during 15 cycles. Recently, the Australian MAC iron ore was used as an oxygen carrier for hydrogen generation from nonaqueous bio-oil in a dual circulated fluidized bed [249]. It was found that the hydrogen yield and purity declined with the cycling time, but adding some steam in FR was a promising approach to mitigate the oxygen carrier deactivation.

3.2.2. Chemical looping hydrogen production using solid and liquid fuels

As shown in Table 3, CO, H_2, syngas or natural gas (mainly CH_4) is commonly used as a reducing agent in CLH process, and only few investigations use solid fuels. Because the gas fuel supply cannot fully support the energy needs of the electricity demand of the country for the long-term, it would be highly advantageous if the CLH process could be adapted for solid fuels. There are basically two approaches to the application of the CLH technology with solid fuel. The first one is to gasify the solid fuel firstly in a gasifier unit with pure O_2 to produce syngas, and then it can be used in a CLH process with gaseous fuel. The second one is to add the solid fuel directly to the FR with the gasification agents, where the gasification and the combustion processes occur simultaneously.

Müller et al. [197] conducted the experiments to produce hydrogen from three representative coals - a Russian bituminous, a German lignite and a UK sub-bituminous coal. When German lignite was used, pure H_2 with CO < 50 ppm could be obtained from the proposed process. Stable quantities of H_2 were produced over five cycles for all three coals investigated. Independent of the fuel, the produced H_2 was not contaminated with SO_2. It was demonstrated that the CLH process may be an attractive approach to upgrade crude syngas produced by the gasification of low-rank coals to pure H_2 while simultaneous capturing CO_2.

Yang et al. [199] confirmed the feasibility of the hydrogen production using direct CLH process with coal char as fuel in a fluidized-bed

reactor. The reduction of Fe_2O_3 by K–10–char at 1073 K was desirable from the perspective of the carbon conversion rate and high concentration of CO_2. The carbon in char was completely converted to CO_2 when the mass ratio of Fe_2O_3/K–10–char was increased to 10/0.3. The oxidation rate of K–10–char by Fe_2O_3 without a gasifying agent was comparable to the K–10–char steam gasification rate. The H_2 yield equaled to 1000 mL/g K–10–char could be obtained when 3 g of Fe_2O_3 and 0.5 g of K–10–char was added.

The development of solid fuel direct CLH process may be limited. This is because the lower reactivity between the oxygen carrier and the solid fuel due to the low solid-solid contact efficiency. In the FR of CLC, steam or CO_2 cannot added as the gasifying agent to promote the reaction rate and inhibit the carbon deposition. However, in the CLH process, this is not recommended. The reduced oxygen carrier may be partially oxidized by the gasifying agent, therefore the capacity of producing H_2 will be diminished. The conversion of the reducing agents will also be affected, which has been verified by Yang et al. [199] and Zeng et al.[249].

Up to now, there is few report on CLH process using liquid fuel. The biofuels with the advantage of being renewable feedstock are evaluated as possible candidates. The light [231] or heavy [248] fraction of bio-oil has been used as fuels for hydrogen production in CLH process. Hydrogen was also successfully produced from nonaqueous bio-oil in a dual circulated fluidized bed using Australian MAC iron ore as an oxygen carrier [249]. When the steam to oil ratio was set to be 1.5, the hydrogen purity reached to 96% with the yield of 635 mL/mL oil. Other liquid fuels as mentioned in CLR(a) can also be used as reducing agents, which needs to be further investigated.

3.2.3. Continuous operation experience of the circulating reactors

Up to now, only limited amount of studies on the continuous operation of CLH process have been reported. Reed [256] developed a process with interconnected fluidized beds for circulating iron oxides. This enabled continuous production of H_2. Rydén et al. [241] examined the steam-iron reaction in a continuously circulated two-reactor fluidized-bed reactor. The schematic description of the reactor is similar to that shown in Fig. 10**(a).** $Fe_3O_4/MgAl_2O_4$ was used as the oxygen carrier with carbon monoxide or synthesis gas as fuels. The process operated for 12 h with 9 h involved H_2 generation. They demonstrated that the conversion of gaseous fuel was at the range of 60–80% with the H_2 production rate of 0.33–0.58 L/min depending on the fuel added and the reaction temperature. H_2 was produced continuously as is shown in Fig. 13 when syngas was used as reducing fuel. It should be noted that despite reduction of the oxygen carrier to FeO, de-fluidization or stops in the solid circulation were not experienced, which is not as the case in CLC process [257]. Stable operation,

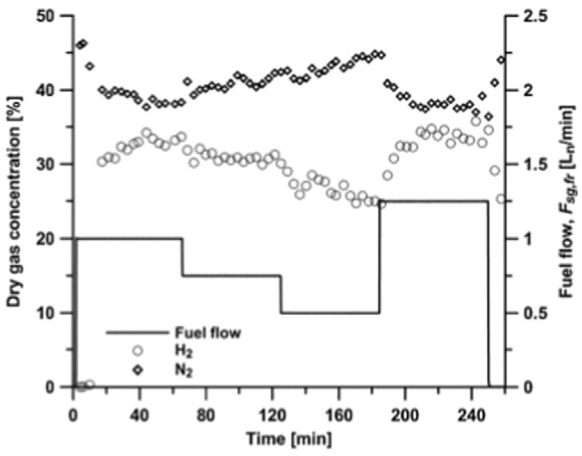

Fig. 13. Dry-gas concentration from the steam reactor with synthesis gas as fuel at 900 °C [241].

low attrition and absence of defluidization were achieved during the operation process, and it is estimated that the process can be successfully obtained in a continuous three-reactor system.

A 25 kWth subpilot CLH unit (see Fig. 14) using syngas as fuel has been constructed and operated in the OSU using synthetic iron-based oxygen carriers [224,225]. The H_2 purity higher than 99.99% with 100% syngas conversion has been achieved in this sub-pilot unit.

A 300 Wth three reactor CLH unit with CH_4 as fuel was constructed and successfully operated for 13 h using 20 wt% Fe_2O_3/ZrO_2 as an oxygen carrier [212]. Both of the FR and SR operated at the moving bed state with the riser operated as an entrained flow reactor. In the FR, the average conversion of CH_4 was 94.15% and the almost pure hydrogen (99.95%) was obtained in the SR.

Recently, hydrogen was also successfully produced from nonaqueous bio-oil in a dual circulated fluidized bed (see Fig. 15) using iron ore as an oxygen carrier in Southeast University [249]. The operation results showed that the hydrogen purity remained not desirable due to the low carbon conversion of the oil. Adding steam in FR could enhance the hydrogen purity by eliminating the solid carbon, but it also suppressed the hydrogen yield simultaneously. When the steam to oil ratio was set to be 1.5 and the temperature of FR was 950 °C, the hydrogen purity reached to 96% with the yield of 635 mL/mL oil.

3.2.4. System integration and economic analysis

The system integration and economic analysis are also the focus of the CLH process. Different systems for hydrogen production or/and power generation has been proposed using the gaseous fuels, such as CH_4 [213], nature gas [272,273], and even the ventilation air methane [270]. Simulation results showed that the cold gas efficiency, the effective thermal efficiency, and the carbon capture efficiency was much higher than that of the conventional SMR process [272]. Considering the three streams of N_2, H_2 and CO_2 produces in chemical looping process, Edrisi et al. [273] recently proposed a novel and green plant configuration for urea production using the CLH process to provide the feedstock of urea synthesis loop. The schematic figure of the proposed plant and conventional process is shown in Fig. 16. In this process, CLH process is used to produce the pure steams of H_2 and N_2 for ammonia production and CO_2 for urea synthesis. The system is simplified and therefore the economic has promising advantage than that of the conventional process. Economic evaluation of the proposed plant showed a considerable rate of return (IRR) and financial interest. The proposed plant had an IRR above 28%, whereas the corresponding value of conventional plants was about 20%.

There are also two ways of system integration with CLH process using solid fuels. One is to couple with fuel gasification process, another way is to direct use solid fuels.

Coal gasification process is a promising technology for clean coal power generation process. The integrated hydrogen and power technology by firstly gasify the coal to syngas not only can increase the power generation efficiency, but also can solve the problem of NO_x and SO_x emission. This technology can also separate the carbon dioxide when combined with CLH process. The basic schematic figure of the CLH process combine the solid fuel gasification is shown in Fig. 17 [259]. The CLH processes in conjunction with solid fuel gasification process using different gasification agents, such as steam [258], O_2 [191], O_2 and CO_2 mixture [262], O_2 and steam mixture [260,261,265], and even the hydrogen produced [266,267] has been proposed and simulated. As shown in Table 5, the system performance including the energy efficiency, the total exergy efficiency, and the carbon capture efficiency compare favorably with to those achieved by hydrogen production via steam reformation of methane.

CLH process also has been integrated with other new technologies for power generation and/or hydrogen generation. Chen et al. [265] proposed a system which integrated the coal gasification, CLH process, and solid oxide fuel cell/gas turbine (SOFC/GT) cycle. The produced hydrogen from the CLH process is fueled to SOFC for power genera-

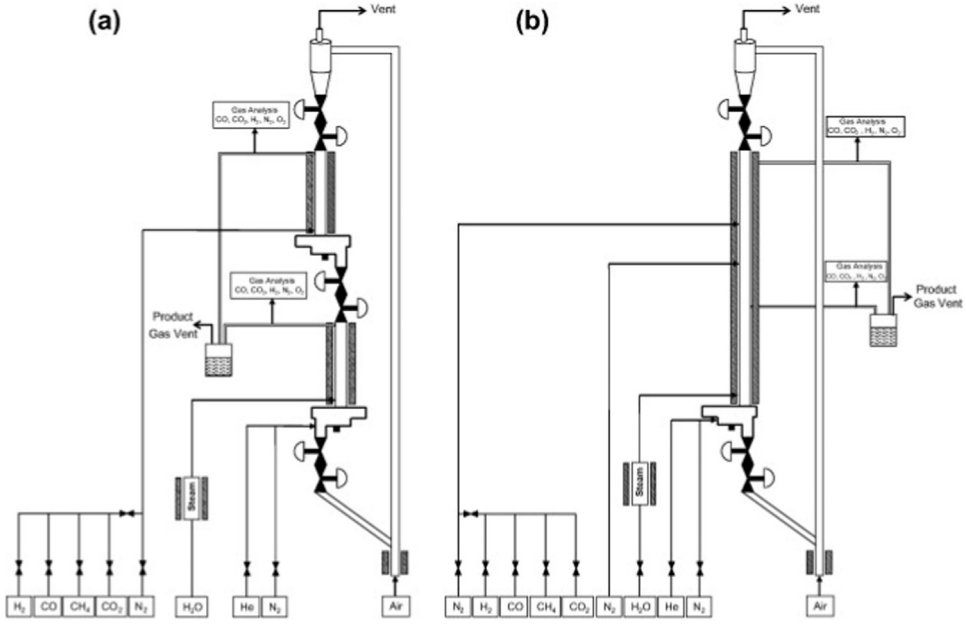

Fig. 14. Schematic diagram of the SCL process in mechanical (a) and non-mechanical (b) valve configuration [225].

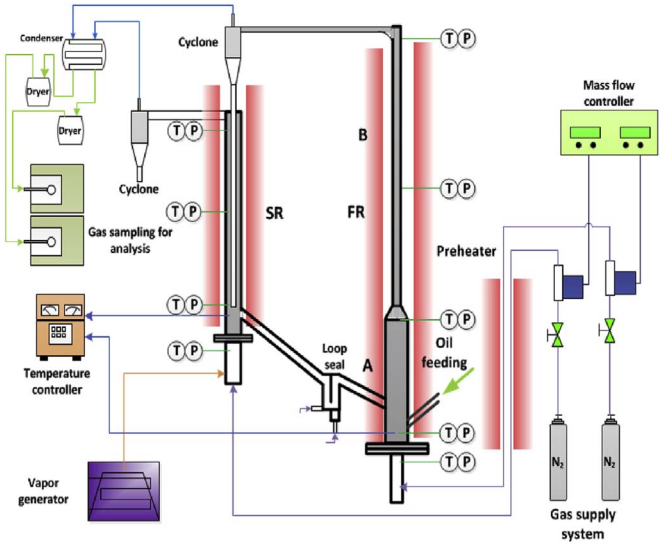

Fig. 15. The schematic of the experimental set-up [249].

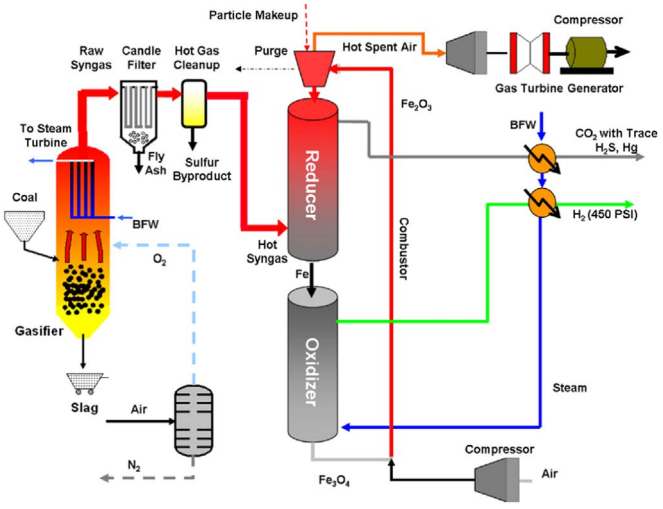

Fig. 17. Simplified schematic of the syngas chemical looping process for hydrogen production from coal [259].

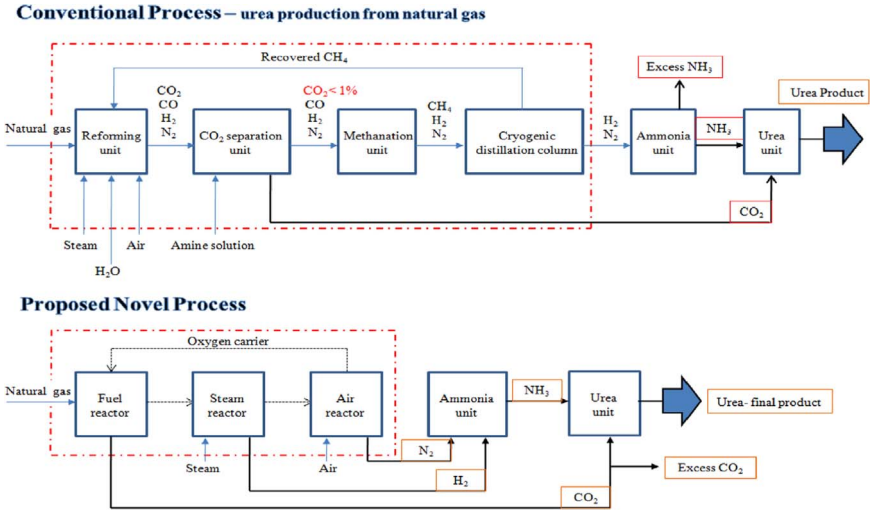

Fig. 16. Scheme of the proposed plant and conventional process for urea production from natural gas [273].

Table 5
Summary of systems integration with CLH process.

System	Fuel	Oxygen Carrier	System Description	Major Remarks	Reference
Chemical-looping and gasification system	Coal	Fe_2O_3	CLH in conjunction with a steam-coal gasification process.	The peak exergetic efficiencies of the fully heat-integrated systems reached to 48.4% and 58.3% at 1 atmosphere and 10 atmospheres respectively, and the values could reach to 53.7% and 59.7% respectively when a bottoming steam turbine cycle was set for waste heat utilization.	[258]
Syngas chemical looping process for hydrogen production from coal	Coal	Fe_2O_3	Integration of the syngas redox (SGR) process into the coal gasification train to produce high purity hydrogen.	The overall efficiency of the process was 64% (HHV) with 100% carbon capture as compared to 57% (HHV) for state-of-the-art coal-to-hydrogen process.	[191,259]
Syngas chemical looping process for hydrogen and electricity coproduction	Coal	Fe_2O_3	The SCL process is used for hydrogen production and electricity generation at various ratios through the utilization of CLG and CLC concepts.	When the hydrogen capacity was 100%, the process efficiency was 67.6% (1.5% in electricity and 66.1% in hydrogen). When electricity was the only product, the process efficiency was 34.9%.	[260]
IGCC scheme for co-generation of hydrogen and electricity with carbon capture and storage using an iron based chemical looping system	Coal	Fe_3O_4	Hydrogen and electricity co-production process based on gasification process with iron oxides chemical looping system used for carbon capture.	When the hydrogen output increased from 0 to 150 MW, the net electrical efficiency decreased from 38.82% to 31.38%, but the cumulative efficiency increased from 38.82% to 44.44%. The carbon capture rate was 99.51%.	[261]
Chemical looping-based hydrogen and electricity plant	Coal	$NiO/NiAl_2O_4$, Fe_2O_3	CLC process (Ni-based oxygen carriers) with the steam-iron process.	The process simulation results showed that at the conditions of Fe-SR 815 °C, Fe-FR 815 °C, Ni-FR 900 °C, Ni-AR 1050 °C, and the supplementary firing temperature of 1350 °C, the net power efficiency, hydrogen efficiency and the equivalent efficiency were 27.47%, 23.39% and 70.75%, respectively; the CO_2 emission was 365.36 g/kWh.	[262]
Syngas-fueled chemical looping systems for H_2 and electricity production	Coal	Fe_2O_3	Two SCL systems with different reactor configurations (moving bed reactor and fluidized bed reactor mode) for H_2 and electricity production.	The H_2 production efficiency of the SCL-MB system (55.1%) was higher than that of the SCL-FB system (44.0%). Both the two systems has a carbon capture efficiency higher than 99.0%.	[263]
O_2/CO_2 blown UCG integrated CLH based PEMFC cycle power plant	Coal	Fe_2O_3	Pure hydrogen is produced by using the CLH process with the underground coal gasification (UCG) gas. Then the pure hydrogen is used to generate electric power in a proton exchange membrane fuel cell (PEMFC) system.	The net efficiency of O_2/CO_2 based UCG integrated with CLH-PEMFC system reaches to 43.6% with carbon capture and storage (CCS), while the corresponding value of the conventional reforming based system is 37.95%.	[264]
CLHG-SOFC/GT hybrid plant	Coal	Fe_2O_3	CLH integrates the SOFC/GT (solid oxide fuel cell/gas turbine) cycle and coal gasification.	The simulation showed that when the system pressure was set to be 20 bar and the cell temperature was 900 °C, the net power efficiency of the CLHG-SOFC/GT plant reached to 43.53% and zero carbon emission achieved.	[265]
Chemical looping zero emission coal (CL-ZEC) system	Coal and biomass (wheat straw)	Fe_2O_3	The system is based on the coal/biomass co-hydrogasification and the CLH technologies.	The energy and exergy of the system operation results were analyzed. The total energy efficiency (η_{te}), the total exergy efficiency (η_{tex}), and the carbon capture efficiency (η_{cc}) of the system were found to be 43.6%, 41.2% and 99.1%, respectively.	[266]
Integrated gasification chemical looping combustion (IGCLC) process	Coal	Fe_2O_3	This process uses a three-step chemical loop for the production of hydrogen, combustion of gaseous fuels, and regeneration of metal oxides.	The proposed system achieved an electricity efficiency of 49.5% at steam/hydrogen to carbon ratio of 2 and feed temperature of 1100 K, which was 80% higher than a conventional coal-fired power station with CCS measures. The carbon capture efficiency was 100%.	[267]
CDCL process	Coal	Fe_2O_3	Coal direct chemical looping hydrogen process.	Simulation showed that the energy conversion efficiency of the CDCL process was higher 80% (HHV) for hydrogen production and over 50% for electricity generation with zero carbon emissions.	[189,259]
Integrated system for energy efficient co-production of H_2 and power	Coal	Fe_2O_3	The system integrates coal drying, coal direct chemical looping, combined cycle and hydrogenation for H_2 production and power generation.	The H_2 production efficiency and the power generation efficiency could reach to 71.4% and 19.9%, respectively at the given conditions.	[268]
BDCL process	Biomass(hybrid poplar)	Fe_2O_3	Biomass direct chemical looping process.	The BDCL process could coproduce hydrogen and electricity with a combined efficiency ($\eta_{H2} + \eta_E$) as high as	[269]

(continued on next page)

Table 5 *(continued)*

System	Fuel	Oxygen Carrier	System Description	Major Remarks	Reference
				67.15%. The concentrated CO_2 produced made this process carbon negative.	
One-Step Hydrogen (OSH) process	CH_4	30% Fe_2O_3 supported on an Mg-Al_2O_3 spinel	Using CLH as an OSH process with CH_4 as fuel for hydrogen generation.	The hydrogen efficiency η_{H2} was related to the excess oxygen in the loop. The maximum value of η_{H2} reached to 83.75% with the corresponding global efficiency η_{H2} of 78.96% and the CO_2 capture rate of 100%.	[213]
Dual-loop CLC process for reforming VAM	Ventilation Air Methane(VAM)	Cu_2O/CuO = 1:4, $Fe_2O_3/Fe_3O_4/Fe_{0.947}O$ supported by 70 wt% Al_2O_3	A Cu-based CLAS unit is used to remove the oxygen content in the VAM stream, and an Fe-based three-reactor CLHG process is incorporated to oxidize the methane content in oxygen-depleted VAM as well as to produce high purity hydrogen.	It was found that the proposed system was able to produce high-purity hydrogen from VAM. If O_2 was not set as a product, 0.021 kWh of energy can be produced per cubic meter of VAM with a hydrogen efficiency of 40.4%. With pure O_2 as a final product, the energy demand from external was 0.32 kWh/m^3 O_2.	[270]
BDCL process	Biomass (sawdust)	Ilmenite	Biomass direct chemical looping for hydrogen and power co-generation	The overall energy efficiency of BDCL concept (~42% net efficiency) was significantly higher compared to the benchmark cases (5.7% higher than the physical gas-liquid absorption design and 4.5% higher than syngas-based chemical looping design). The carbon capture rate of BDCL concept was almost total (> 99%) in comparison with gas-liquid absorption option (90%). The carbon capture energy penalty for BDCL system was significantly lower (about 3.5 net electricity percentage points) than that for the benchmark options: Selexol®-based gas-liquid absorption (about 9.2 points) and syngas-based chemical looping (about 8 points).	[271]
Full-scale chemical looping system for hydrogen generation	Nature gas	Fe_2O_3	The hydrogen production process from nature gas using an iron-based chemical looping process technology.	The cold gas efficiency of the chemical looping process reached to 77.6% (HHV basis) which was 5% higher than the conventional SMR case. For the same amount of H_2 production the effective thermal efficiency was about 75%, which was 6% higher than the baseline case. Moreover, the carbon capture efficiency of the system was greater than 90%.	[272]
Urea production plant	Nature gas	Fe_2O_3	CLH process is used to produce the pure steams of H_2 and N_2 for ammonia production and CO_2 for urea synthesis.	Economic evaluation of the proposed plant showed a considerable rate of return and financial interest. In the different production rate, the proposed plant had a rate of return (IRR) above 28%, while the IRR of conventional plants was almost near 20%.	[273]
Three reactor chemical looping hydrogen production (TRCLH) plant	Nature gas	$Fe_2O_3/MgAl_2O_4$ (30/70 wt%)	A chemical looping hydrogen plant for hydrogen and power co-generation.	When CO_2 is captured, the cost of H_2 production is 1.679 $/kg, which is much lower than the conventional SMR method (~ 2.39 $/kg), while if CO_2 is not captured, the cost of H_2 production is 1.404 $/kg, which is comparable with the SMR technology.	[274]

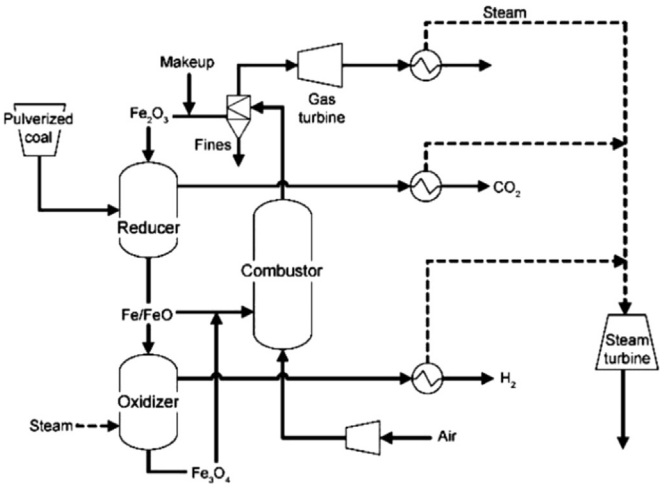

Fig. 18. Schematic diagram of the coal-direct chemical looping process [189].

tion. The simulation showed that at a system pressure of 20 bar and a cell temperature of 900 °C, the CLHG-SOFC/GT plant had a net power efficiency of 43.53% with no CO_2 emissions. Yan et al. [266] developed a CL-ZEC (chemical looping zero emission coal) system based on the coal/biomass co-hydrogasification, the SOFC technology, and the CLH process. Results showed that the energy and exergy efficiencies of this system was high while the carbon discharge was very low and could even be negative.

The coal gasification process in the system will cause the decrease of the exergy efficiency, therefore coal direct chemical looping hydrogen (CDCL) process was proposed by Fan et al [189,259]. The schematic diagram of the CDCL process is shown in Fig. 18. In this process, composite Fe_2O_3 particles are introduced into the reducer to react with pulverized coal, where coal is gasified in situ and reacted with Fe_2O_3 particles. Thus, a mixture of Fe and FeO is produced along with a flue gas stream composed of CO_2 and H_2O. A portion of the reduced Fe/FeO particle from the reducer will enter the oxidizer to react with steam to form hydrogen. The resulting Fe_3O_4 exiting the oxidizer along with the remaining portion of the reduced Fe/FeO particle will be combusted with air in the entrained flow combustor. The combustor conveys the particle back to the reducer pneumatically while regenerating the particle to its original oxidized form. Part of the heat released in the combustor will be carried to the reducer by the oxygen carriers to compensate the endothermic heat required in the reducer. The remaining heat released in the combustor heats up the exhaust gas, which can be used for steam or electricity generation.

The researchers in the OSU found that the counter-current moving bed reactor was the optimal choice for the CLH process from nature gas using iron-based materials [272,275]. They also conducted the CDCL process tests in a 2.5 kW bench scale moving bed unit. Different feedstock such as coal volatiles (simulated), lignite coal char, bituminous coal char, and anthracite coal have been tested. The conversion of coal/coal char can reach to 95.5%, and the CO_2 concentration in the exhaust stream was higher than 97% (dry basis) in all cases. Moreover, the reactivity of the particles was maintained after three redox cycles in which coal was used as the reducing agent. ASPEN Plus® simulation showed that the energy conversion efficiency of the CDCL process was higher 80% (HHV) for hydrogen production and over 50% for electricity generation with zero carbon emissions. Li et al. [269] performed the simulation based on this process using biomass as fuel. It was found that the biomass direct chemical looping (BDCL) process can coproduce hydrogen and electricity with a combined efficiency ($\eta_{H2} + \eta_E$) as high as 67.15%. The concentrated CO_2 produced was readily sequesterable, making this process carbon negative.

Recently, Cormos et al. [271] assessed the techno-economic evaluation of the BDCL concept for hydrogen and power co-production. The concept is illustrated using an ilmenite-based system to produce 400–500 MW net power with flexible hydrogen output (up to 200 MWth). The system showed the superiority not only at the energy efficiencies but also at the carbon capture efficiency. The overall energy efficiency of BDCL concept (~42% net efficiency) was significantly higher compared to the benchmark cases (5.7% higher than the physical gas-liquid absorption design and 4.5% higher than syngas-based chemical looping design). The carbon capture rate of BDCL concept was almost total (> 99%) in comparison with gas-liquid absorption option (90%). The carbon capture energy penalty for BDCL system was significantly lower (about 3.5 net electricity percentage points) than that for the benchmark options: Selexol®-based gas-liquid absorption (about 9.2 points) and syngas-based chemical looping (about 8 points).

4. Conclusions

Hydrogen production using chemical looping technology can achieve high energy conversion efficiency and/or separate CO_2 inherently. The advantageous and the disadvantageous of CLR and CLH are analyzed and the advances of those two categories are summarized.

CLR(s) process combines the chemical looping process and the steam reforming process. It has good prospects for industrial applications but there are still many challenges to be solved. For example, the potential erosion of the reformer tubes by the oxygen carriers and the heat balance between the FR and AR need to be considered. In addition, the gaseous from the fuel reactor contains CH_4, CO and H_2. Compared to CO and H_2, the conversion of CH_4 is much more difficult. The development of the oxygen carrier with high selectivity, high stability and high reactivity with methane and high resistance of carbon deposition is the key aspect for the successful operation of CLR(a) and CLRM processes.

CLH process has aroused great attention because it can produce ultra-pure hydrogen without further purification steps. The CLH process should be developed for use under high temperature and high pressurized conditions. The hydrogen production will increase with the increase of the temperature, but Fe_2O_3 may sinter at high temperature. High pressure also promotes the carbon deposition reactions, which has negative effect on the hydrogen purity. Therefore, increasing the stability of the oxygen carriers at high temperature and high pressure and the ability of resistance against carbon deposition are the key factors in the industrial operation process. Only a very limited number of papers have presented investigations concerning naturally occurring minerals, ores or industrial by-products with the active composition of Fe_2O_3 in CLH process. Comparison to synthetic materials, these kinds of materials have the advantageous of lower cost and lower environmental impact. Because solid coal is considerably more abundant than natural gas, it would be highly advantageous if the CLH process could be adapted for solid fuels. Therefore, the design of proper reactor and the coupled system, and the development of oxygen carriers with low price and excellent property under high temperature and pressure will be the main focus of the study.

Acknowledgements

This work was supported by the Supported by National Natural Science Foundation of China (51606087), Start-Up Foundation of Jiangsu University (15JDG157), National Science and Technology Supporting Program of China (2011BAK06B04) and the Program for New Century Excellent Talents in University of Chinese Education Ministry (NCET-07-0678).

References

[1] van der Hoeven M. CO_2 emissions from fuel combustion highlights. France: International Energy Agency; 2016.

[2] He K, Huo H, Zhang Q. Urban air pollution in China: current status, characteristics, and progress. Annu Rev Energy Environ 2002;27:397–431.
[3] Fu L, Hao J, He D, He K, Li P. Assessment of vehicular pollution in china. J Air Waste Manag Assoc 2001;51:658–68.
[4] Birol F. World energy outlook 2010. Paris: International Energy Agency; 2010.
[5] Kothari R, Buddhi D, Sawhney RL. Comparison of environmental and economic aspects of various hydrogen production methods. Renew Sustain Energy Rev 2008;12:553–63.
[6] Fan L-S. Chemical looping systems for fossil energy conversions. Hoboken, New Jersey, USA: John Wiley & Sons, Inc; 2010.
[7] Fan L-S, Zeng L, Wang W, Luo S. Chemical looping processes for CO_2 capture and carbonaceous fuel conversion - prospect and opportunity. Energy Environ Sci 2012;5:7254–80.
[8] Moghtaderi B. Review of the Recent Chemical looping process developments for novel energy and fuel applications. Energy Fuels 2011;26:15–40.
[9] Adanez J, Abad A, Garcia-Labiano F, Gayan P, de Diego LF. Progress in chemical-looping combustion and reforming technologies. Prog Energy Combust Sci 2012;38:215–82.
[10] Voitic G, Hacker V. Recent advancements in chemical looping water splitting for the production of hydrogen. RSC Adv 2016;6:98267–96.
[11] Tang M, Xu L, Fan M. Progress in oxygen carrier development of methane-based chemical-looping reforming: a review. Appl Energy 2015;151:143–56.
[12] Li K, Wang H, Wei Y. Syngas generation from methane using a chemical-looping concept: a review of oxygen carriers. J Chem 2013;2013:1–8.
[13] Thursfield A, Murugan A, Franca R, Metcalfe IS. Chemical looping and oxygen permeable ceramic membranes for hydrogen production - A review. Energy Environ Sci 2012;5:7421–59.
[14] Protasova L, Snijkers F. Recent developments in oxygen carrier materials for hydrogen production via chemical looping processes. Fuel 2016;181:75–93.
[15] Norskov JK, Christensen CH. Toward efficient hydrogen production at surfaces. Science 2006;312:1322–3.
[16] Rhodes C, Hutchings GJ, Ward AM. Water-gas shift reaction: finding the mechanistic boundary. Catal Today 1995;23:43–58.
[17] Keiski RL, Desponds O, Chang YF, Somorjai GA. Kinetics of the water-gas shift reaction over several alkane activation and water-gas shift catalysts. Appl Catal A: Gen 1993;101:317–38.
[18] Keiski RL, Salmi T, Niemistö P, Ainassaari J, Pohjola VJ. Stationary and transient kinetics of the high temperature water-gas shift reaction. Appl Catal A: Gen 1996;137:349–70.
[19] Anderson JR, Boudart M. Catalysis, science and technology, 5. Berlin: Springer; 1984.
[20] Trimm DL. The formation and removal of coke from Nickel catalyst. Catal Rev 1977;16:155–89.
[21] Trimm DL. Coke formation and minimisation during steam reforming reactions. Catal Today 1997;37:233–8.
[22] Damen K, Troost Mv, Faaij A, Turkenburg W. A comparison of electricity and hydrogen production systems with CO_2 capture and storage. Part A: review and selection of promising conversion and capture technologies. Prog Energy Combust Sci 2006;32:215–46.
[23] Gielen D, Simbolotti G. Prospects for hydrogen and fuel cells. IEA Report; 2005.
[24] Go KS, Son SR, Kim SD, Kang KS, Park CS. Hydrogen production from two-step steam methane reforming in a fluidized bed reactor. Int J Hydrog Energy 2009;34:1301–9.
[25] Richter Horst J, Knoche Karl F. Reversibility of combustion processes. Efficiency and costing. American Chemical Society; 1983. p. 71–85.
[26] Jin H, Okamoto T, Ishida M. Development of a novel chemical-looping combustion: synthesis of a looping material with a double metal oxide of CoO-NiO. Energy Fuels 1998;12:1272–7.
[27] Ishida M, Jin HG. A novel chemical-looping combustor without NO_x formation. Ind Eng Chem Res 1996;35:2469–72.
[28] Ho-Jung Ryu G-TJ, Chang-Keun Yi. Demonstration of inherent CO2 separation and no NOx emission in a 50 kW chemical looping combustor continuous reduction and oxidization experiment. In: Proceedings of 7th International Greenhouse Gas Control Technologies. Vancouver, Canada; 2004.
[29] Gu H, Shen L, Zhong Z, Niu X, Ge H, Zhou Y, et al. NO release during chemical looping combustion with iron ore as an oxygen carrier. Chem Eng J 2015;264:211–20.
[30] Wang SZ, Wang GX, Jiang F, Luo M, Li HY. Chemical looping combustion of coke oven gas by using Fe_2O_3/CuO with $MgAl_2O_4$ as oxygen carrier. Energy Environ Sci 2010;3:1353–60.
[31] Wang Z, Fan W, Zhang G, Dong S. Exergy analysis of methane cracking thermally coupled with chemical looping combustion for hydrogen production. Appl Energy 2016;168:1–12.
[32] Liu F, Chen L, Yang L, Fan Z, Nikolic H, Richburg L, et al. Application of chemical looping process for continuous high purity hydrogen production by methane thermocatalytic decomposition. Int J Hydrog Energy 2016;41:4592–602.
[33] Tobias Mattisson AL. Applications of chemical-looping combustion with capture of CO_2. Second nordic minisymposium on carbon dioxide capture and storage. Sweden: Göteborg; 2001.
[34] Ryden M, Lyngfelt A. Using steam reforming to produce hydrogen with carbon dioxide capture by chemical-looping combustion. Int J Hydrog Energy 2006;31:1271–83.
[35] Rahimpour MR, Hesami M, Saidi M, Jahanmiri A, Farniaei M, Abbasi M. Methane steam reforming thermally coupled with fuel combustion: application of chemical looping concept as a novel technology. Energy Fuels 2013;27:2351–62.
[36] Pans MA, Abad A, de Diego LF, García-Labiano F, Gayán P, Adánez J. Optimization of H_2 production with CO_2 capture by steam reforming of methane integrated with a chemical-looping combustion system. Int J Hydrog Energy 2013;38:11878–92.
[37] Ortiz M, Abad A, de Diego LF, García-Labiano F, Gayán P, Adánez J. Optimization of hydrogen production by chemical-looping auto-thermal reforming working with ni-based oxygen-carriers. Int J Hydrog Energy 2011;36:9663–72.
[38] Pröll T, Bolhàr-Nordenkampf J, Kolbitsch P, Hofbauer H. Syngas and a separate nitrogen/argon stream via chemical looping reforming – A 140 kW pilot plant study. Fuel 2010;89:1249–56.
[39] Ryden M, Lyngfelt A, Mattisson T. Synthesis gas generation by chemical-looping reforming in a continuously operating laboratory reactor. Fuel 2006;85:1631–41.
[40] Garcia-Labiano F, de Diego LF, Gayan P, Adanez J, Abad A, Dueso C. Effect of fuel gas composition in chemical-looping combustion with Ni-based oxygen carriers. 1. Fate of sulfur. Ind Eng Chem Res 2009;48:2499–508.
[41] Steinfeld A. Solar thermochemical production of hydrogen––a review. Sol Energy 2005;78:603–15.
[42] Kodama T, Ohtake H, Matsumoto S, Aoki A, Shimizu T, Kitayama Y. Thermochemical methane reforming using a reactive WO_3/W redox system. Energy 2000;25:411–25.
[43] Sim A, Cant NW, Trimm DL. Ceria–zirconia stabilised tungsten oxides for the production of hydrogen by the methane–water redox cycle. Int J Hydrog Energy 2010;35:8953–61.
[44] Forster M. Theoretical investigation of the system SnO_x/Sn for the thermochemical storage of solar energy. Energy 2004;29:789–99.
[45] Kodama T, Shimizu T, Satoh T, Nakata M, Shimizu KI. Stepwise production of CO-rich syngas and hydrogen via solar methane reforming by using a Ni(II)–ferrite redox system. Sol Energy 2002;73:363–74.
[46] Go KS, Son SR, Kim SD. Reaction kinetics of reduction and oxidation of metal oxides for hydrogen production. Int J Hydrog Energy 2008;33:5986–95.
[47] Kang K-S, Kim C-H, Cho W-C, Bae K-K, Woo S-W, Park C-S. Reduction characteristics of $CuFe_2O_4$ and Fe_3O_4 by methane; $CuFe_2O_4$ as an oxidant for two-step thermochemical methane reforming. Int J Hydrog Energy 2008;33:4560–8.
[48] Cha K-S, Kim H-S, Yoo B-K, Lee Y-S, Kang K-S, Park C-S, et al. Reaction characteristics of two-step methane reforming over a Cu-ferrite/Ce–ZrO_2 medium. Int J Hydrog Energy 2009;34:1801–8.
[49] Kang K-S, Kim C-H, Bae K-K, Cho W-C, Kim W-J, Kim Y-H, et al. Redox cycling of $CuFe_2O_4$ supported on ZrO_2 and CeO_2 for two-step methane reforming/water splitting. Int J Hydrog Energy 2010;35:568–76.
[50] Otsuka K, Wang Y, Nakamura M. Direct conversion of methane to synthesis gas through gas–solid reaction using CeO_2–ZrO_2 solid solution at moderate temperature. Appl Catal A: Gen 1999;183:317–24.
[51] Otsuka K, Wang Y, Sunada E, Yamanaka I. Direct partial oxidation of methane to synthesis gas by cerium oxide. J Catal 1998;175:152–60.
[52] Zhu X, Wang H, Wei Y, Li K, Cheng X. Hydrogen and syngas production from two-step steam reforming of methane over CeO_2–Fe_2O_3 oxygen carrier. J Rare Earths 2010;28:907–13.
[53] Zhu X, Wang H, Wei Y, Li K, Cheng X. Hydrogen and syngas production from two-step steam reforming of methane using CeO_2 as oxygen carrier. J Nat Gas Chem 2011;20:281–6.
[54] Zhu X, Wang H, Wei Y, Li K, Cheng X. Reaction characteristics of chemical-looping steam methane reforming over a Ce–ZrO_2 solid solution oxygen carrier. Mendeleev Commun 2011;21:221–3.
[55] Jeong HH, Kwak JH, Han GY, Yoon KJ. Stepwise production of syngas and hydrogen through methane reforming and water splitting by using a cerium oxide redox system. Int J Hydrog Energy 2011;36:15221–30.
[56] de Diego LF, Ortiz M, Adanez J, Garcia-Labiano F, Abad A, Gayan P. Synthesis gas generation by chemical-looping reforming in a batch fluidized bed reactor using Ni-based oxygen carriers. Chem Eng J 2008;144:289–98.
[57] Spallina V, Marinello B, Gallucci F, Romano MC, Van Sint Annaland M. Chemical looping reforming in packed-bed reactors: modelling, experimental validation and large-scale reactor design. Fuel Process Technol 2017;156:156–70.
[58] Dou B, Dupont V, Rickett G, Blakeman N, Williams PT, Chen H, et al. Hydrogen production by sorption-enhanced steam reforming of glycerol. Bioresour Technol 2009;100:3540–7.
[59] Pimenidou P, Rickett G, Dupont V, Twigg MV. Chemical looping reforming of waste cooking oil in packed bed reactor. Bioresour Technol 2010;101:6389–97.
[60] Pimenidou P, Rickett G, Dupont V, Twigg MV. High purity H_2 by sorption-enhanced chemical looping reforming of waste cooking oil in a packed bed reactor. Bioresour Technol 2010;101:9279–86.
[61] Lea-Langton A, Zin RM, Dupont V, Twigg MV. Biomass pyrolysis oils for hydrogen production using chemical looping reforming. Int J Hydrog Energy 2012;37:2037–43.
[62] Cheng F, Dupont V. Nickel catalyst auto-reduction during steam reforming of bio-oil model compound acetic acid. Int J Hydrog Energy 2013;38:15160–72.
[63] Ryden M, Lyngfelt A, Mattisson T. Chemical-looping combustion and chemical-looping reforming in a circulating fluidized-bed reactor using Ni-based oxygen carriers. Energy Fuels 2008;22:2585–97.
[64] de Diego LF, Ortiz M, Garcia-Labiano F, Adanez J, Abad A, Gayan P. Hydrogen production by chemical-looping reforming in a circulating fluidized bed reactor using Ni-based oxygen carriers. J Power Sources 2009;192:27–34.
[65] Ortiz M, de Diego LF, Abad A, García-Labiano F, Gayán P, Adánez J. Catalytic activity of Ni-based oxygen-carriers for steam methane reforming in chemical-looping processes. Energy Fuels 2012;26:791–800.
[66] Ortiz M, de Diego LF, Abad A, Garcia-Labiano F, Gayan P, Adanez J. Hydrogen production by auto-thermal chemical-looping reforming in a pressurized fluidized bed reactor using Ni-based oxygen carriers. Int J Hydrog Energy 2010;35:151–60.

[67] Dueso C, Ortiz M, Abad A, García-Labiano F, de Diego LF, Gayán P, et al. Reduction and oxidation kinetics of nickel-based oxygen-carriers for chemical-looping combustion and chemical-looping reforming. Chem Eng J 2012;188:142–54.

[68] García-Labiano F, García-Díez E, de Diego LF, Serrano A, Abad A, Gayán P, et al. Syngas/H_2 production from bioethanol in a continuous chemical-looping reforming prototype. Fuel Process Technol 2015;137:24–30.

[69] Md Zin R, Ross AB, Jones JM, Dupont V. Hydrogen from ethanol reforming with aqueous fraction of pine pyrolysis oil with and without chemical looping. Bioresour Technol 2015;176:257–66.

[70] Nakayama O, Ikenaga N, Miyake T, Yagasaki E, Suzuki T. Production of synthesis gas from methane using lattice oxygen of NiO–Cr_2O_3–MgO complex oxide. Ind Eng Chem Res 2009;49:526–34.

[71] Medrano JA, Hamers HP, Williams G, van Sint Annaland M, Gallucci F. NiO/$CaAl_2O_4$ as active oxygen carrier for low temperature chemical looping applications. Appl Energy 2015;158:86–96.

[72] Jiang B, Dou B, Song Y, Zhang C, Du B, Chen H, et al. Hydrogen production from chemical looping steam reforming of glycerol by Ni-based oxygen carrier in a fixed-bed reactor. Chem Eng J 2015;280:459–67.

[73] Zafar Q, Mattisson T, Gevert B. Integrated hydrogen and power production with CO_2 capture using chemical-looping reforming-redox reactivity of particles of CuO, Mn_2O_3, NiO, and Fe_2O_3 using SiO_2 as a support. Ind Eng Chem Res 2005;44:3485–96.

[74] Bolhar-Nordenkampf J, Proll T, Kolbitsch P, Hofbauer H. Performance of a NiO-based oxygen carrier for chemical looping combustion and reforming in a 120 kW unit. Greenh Gas Control Technol 2009;9(1):19–25, [4984].

[75] Ryden M, Johansson M, Lyngfelt A, Mattisson T. NiO supported on Mg-ZrO_2 as oxygen carrier for chemical-looping combustion and chemical-looping reforming. Energy Environ Sci 2009;2:970–81.

[76] Silvester L, Antzara A, Boskovic G, Heracleous E, Lemonidou AA, Bukur DB. NiO supported on Al_2O_3 and ZrO_2 oxygen carriers for chemical looping steam methane reforming. Int J Hydrog Energy 2015;40:7490–501.

[77] Berguerand N, Lind F, Israelsson M, Seemann M, Biollaz S, Thunman H. Use of nickel oxide as a catalyst for tar elimination in a chemical-looping reforming reactor operated with biomass producer gas. Ind Eng Chem Res 2012;51:16610–6.

[78] Moldenhauer P, Ryden M, Mattisson T, Lyngfelt A. Chemical-looping combustion and chemical-looping reforming of kerosene in a circulating fluidized-bed 300W laboratory reactor. Int J Greenh Gas Control 2012;9:1–9.

[79] Mendiara T, Johansen JM, Utrilla R, Geraldo P, Jensen AD, Glarborg P. Evaluation of different oxygen carriers for biomass tar reforming (I): carbon deposition in experiments with toluene. Fuel 2011;90:1049–60.

[80] Mendiara T, Johansen JM, Utrilla R, Jensen AD, Glarborg P. Evaluation of different oxygen carriers for biomass tar reforming (II): carbon deposition in experiments with methane and other gases. Fuel 2011;90:1370–82.

[81] Johansson M, Mattisson T, Lyngfelt A, Abad A. Using continuous and pulse experiments to compare two promising nickel-based oxygen carriers for use in chemical-looping technologies. Fuel 2008;87:988–1001.

[82] Dou B, Song Y, Wang C, Chen H, Yang M, Xu Y. Hydrogen production by enhanced-sorption chemical looping steam reforming of glycerol in moving-bed reactors. Appl Energy 2014;130:342–9.

[83] Antzara A, Heracleous E, Silvester L, Bukur DB, Lemonidou AA. Activity study of NiO-based oxygen carriers in chemical looping steam methane reforming. Catal Today 2016;272:32–41.

[84] Jiang B, Dou B, Wang K, Zhang C, Song Y, Chen H, et al. Hydrogen production by chemical looping steam reforming of ethanol using NiO/montmorillonite oxygen carriers in a fixed-bed reactor. Chem Eng J 2016;298:96–106.

[85] He F, Wei YG, Li HB, Wang H. Synthesis Gas Generation by chemical-looping reforming using Ce-based oxygen carriers modified with Fe, Cu, and Mn Oxides. Energy Fuels 2009;23:2095–102.

[86] Pojanavaraphan C, Satitthai U, Luengnaruemitchai A, Gulari E. Activity and stability of Au/CeO_2–Fe_2O_3 catalysts for the hydrogen production via oxidative steam reforming of methanol. J Ind Eng Chem 2015;22:41–52.

[87] Fathi M, Bjorgum E, Viig T, Rokstad OA. Partial oxidation of methane to synthesis gas: elimination of gas phase oxygen. Catal Today 2000;63:489–97.

[88] Fathi M, Bjorgum E, Viig T, Rokstad OA. Partial oxidation of methane to synthesis gas: elimination of gas phase oxygen. Catal Today 2000;63:489–97.

[89] Wei Y, Wang H, He F, Ao X, Zhang C. CeO_2 as the oxygen carrier for partial oxidation of methane to synthesis gas in molten salts: thermodynamic analysis and experimental investigation. J Nat Gas Chem 2007;16:6–11.

[90] Zheng Y, Li K, Wang H, Tian D, Wang Y, Zhu X, et al. Designed oxygen carriers from macroporous $LaFeO_3$ supported CeO_2 for chemical-looping reforming of methane. Applied. Catal B: Environ 2017;202:51–63.

[91] Wei Y, Wang H, Li K. Ce-Fe-O mixed oxide as oxygen carrier for the direct partial oxidation of methane to syngas. J Rare Earths 2010;28:560–5.

[92] Li K, Wang H, Wei Y, Yan D. Transformation of methane into synthesis gas using the redox property of Ce–Fe mixed oxides: effect of calcination temperature. Int J Hydrog Energy 2011;36:3471–82.

[93] Yaremchenko AA, Kharton VV, Veniaminov SA, Belyaev VD, Sobyanin VA, Marques FMB. Methane oxidation by lattice oxygen of $CeNbO_{4+\delta}$. Catal Commun 2007;8:335–9.

[94] Zheng Y, Li K, Wang H, Zhu X, Wei Y, Zheng M, et al. Enhanced activity of CeO_2–ZrO_2 solid solutions for chemical-looping reforming of methane via tuning the macroporous structure. Energy Fuels 2016;30:638–47.

[95] Wei Yonggang WH, Kongzhai Li, Mingchun Liu. Ao Xianquan. Preparation and performance of Ce/Zr mixed oxides for direct conversion of methane to syngas. J Rare Earths 2007;25:110.

[96] Zhu X, Du Y, Wang H, Wei Y, Li K, Sun L. Chemical interaction of Ce-Fe mixed oxides for methane selective oxidation. J Rare Earths 2014;32:824–30.

[97] Li K, Wang H, Wei Y, Yan D. Syngas production from methane and air via a redox process using Ce–Fe mixed oxides as oxygen carriers. Appl Catal B: Environ 2010;97:361–72.

[98] Zhu X, Wei Y, Wang H, Li K. Ce–Fe oxygen carriers for chemical-looping steam methane reforming. Int J Hydrog Energy 2013;38:4492–501.

[99] Cheng X, Wang H, Wei Y, Li K, Zhu X. Preparation and characterization of Ce-Fe-Zr-O(x)/MgO complex oxides for selective oxidation of methane to synthesize gas. J Rare Earths 2010;28:316–21.

[100] Bhavsar S, Veser G. Chemical looping beyond combustion: production of synthesis gas via chemical looping partial oxidation of methane. RSC Adv 2014;4:47254–67.

[101] Pantu P, Kim K, Gavalas GR. Methane partial oxidation on Pt/CeO_2–ZrO_2 in the absence of gaseous oxygen. Appl Catal A: Gen 2000;193:203–14.

[102] Dai XP, Li RJ, Yu CC, Hao ZP. Unsteady-state direct partial oxidation of methane to synthesis gas in a fixed-bed reactor using $AFeO_3$ (A = La, Nd, Eu) perovskite-type oxides as oxygen storage. J Phys Chem B 2006;110:22525–31.

[103] Zhao K, He F, Huang Z, Zheng A, Li H, Zhao Z. Three-dimensionally ordered macroporous $LaFeO_3$ perovskites for chemical-looping steam reforming of methane. Int J Hydrog Energy 2014;39:3243–52.

[104] Mihai O, Chen D, Holmen A. Catalytic consequence of oxygen of lanthanum ferrite perovskite in chemical looping reforming of methane. Ind Eng Chem Res 2011;50:2613–21.

[105] Dai XP, Wu Q, Li RJ, Yu CC, Hao ZP. Hydrogen production from a combination of the water–gas shift and redox cycle process of methane partial oxidation via lattice oxygen over $LaFeO_3$ perovskite catalyst. J Phys Chem B 2006;110:25856–62.

[106] He F, Zhao K, Huang Z, Li Xa, Wei G, Li H. Synthesis of three-dimensionally ordered macroporous $LaFeO_3$ perovskites and their performance for chemical-looping reforming of methane. Chin J Catal 2013;34:1242–9.

[107] Zhao K, He F, Huang Z, Wei G, Zheng A, Li H, et al. Perovskite-type oxides $LaFe_{1-x}Co_xO_3$ for chemical looping steam methane reforming to syngas and hydrogen co-production. Appl Energy 2016;168:193–203.

[108] Zhao Kun HF, Huang Zhen, Li HaiBin, Zhao ZengLi. $LaFe_{1-x}Ni_xO_3$ perovskites as oxygen carriers for chemical-looping steam methane reforming. J Eng Thermophys 2014;35:2546–50.

[109] Wei HJ, Cao Y, Ji WJ, Au CT. Lattice oxygen of $La_{1-x}Sr_xMO_3$ (M=Mn, Ni) and $LaMnO_{3-\alpha}F_\beta$ perovskite oxides for the partial oxidation of methane to synthesis gas. Catal Commun 2008;9:2509–14.

[110] Li R, Yu C, Shen S. Partial oxidation of methane to syngas using lattice oxygen of $La_{1-x}Sr_xFeO_3$ perovskite oxide catalysts instead of molecular oxygen. J Nat Gas Chem 2002;11:8.

[111] He F, Li X, Zhao K, Huang Z, Wei G, Li H. The use of $La_{1-x}Sr_xFeO_3$ perovskite-type oxides as oxygen carriers in chemical-looping reforming of methane. Fuel 2013;108:465–73.

[112] Zeng Y, Tamhankar S, Ramprasad N, Fitch F, Acharya D, Wolf R. A novel cyclic process for synthesis gas production. Chem Eng Sci 2003;58:577–82.

[113] Zhao K, He F, Huang Z, Zheng A, Li H, Zhao Z. $La_{1-x}Sr_xFeO_3$ perovskites as oxygen carriers for the partial oxidation of methane to syngas. Chin J Catal 2014;35:1196–205.

[114] Rydén M, Lyngfelt A, Mattisson T, Chen D, Holmen A, Bjørgum E. Novel oxygen-carrier materials for chemical-looping combustion and chemical-looping reforming; $LaxSr_{1-x}Fe_yCo_{1-y}O_{3-\delta}$ perovskites and mixed-metal oxides of NiO, Fe_2O_3 and Mn_3O_4. Int J Greenh Gas Control 2008;2:21–36.

[115] Keller M, Leion H, Mattisson T. Chemical looping tar reforming using La/Sr/Fe-containing mixed oxides supported on ZrO_2. Applied. Catal B: Environ 2016;183:298–307.

[116] Galvita V, Sundmacher K. Redox behavior and reduction mechanism of Fe_2O_3–$CeZrO_2$ as oxygen storage material. J Mater Sci 2007;42:9300–7.

[117] Ochoa JV, Trevisanut C, Millet J-MM, Busca G, Cavani F. In situ DRIFTS-MS study of the anaerobic oxidation of ethanol over spinel mixed oxides. J Phys Chem C 2013;117:23908–18.

[118] Trevisanut C, Mari M, Millet J-MM, Cavani F. Chemical-loop reforming of ethanol over metal ferrites: an analysis of structural features affecting reactivity. Int J Hydrog Energy 2015;40:5264–71.

[119] Cocchi S, Mari M, Cavani F, Millet J-MM. Chemical and physical behavior of $CoFe_2O_4$ in steam–iron process with methanol. Appl Catal B: Environ 2014;152–153:250–61.

[120] Crocellà V, Cavani F, Cerrato G, Cocchi S, Comito M, Magnacca G, et al. On the role of morphology of $CoFeO_4$ spinel in methanol anaerobic oxidation. J Phys Chem C 2012;116:14998–5009.

[121] Trevisanut C, Bosselet F, Cavani F, Millet JMM. A study of surface and structural changes of magnetite cycling material during chemical looping for hydrogen production from bio-ethanol. Catal Sci Technol 2015;5:1280–9.

[122] Guo Q, Cheng Y, Liu Y, Jia W, Ryu H-J. Coal chemical looping gasification for syngas generation using an iron-based oxygen carrier. Ind Eng Chem Res 2014;53:78–86.

[123] De Vos Y, Jacobs M, Van Der Voort P, Van Driessche I, Snijkers F, Verberckmoes A. Optimization of spray dried attrition-resistant iron based oxygen carriers for chemical looping reforming. Chem Eng J 2017;309:824–39.

[124] Neal L, Shafiefarhood A, Li F. Effect of core and shell compositions on MeO_x@$La_ySr_{1-y}FeO_3$ core–shell redox catalysts for chemical looping reforming of methane. Appl Energy 2015;157:391–8.

[125] Shafiefarhood A, Galinsky N, Huang Y, Chen Y, Li F. Fe_2O_3@$La_xSr_{1-x}FeO_3$ core–shell redox catalyst for methane partial oxidation. ChemCatChem 2014;6:790–9.

[126] Suzuki T, Nakayama O, Okamoto N. Partial oxidation of methane to nitrogen free synthesis gas using air as oxidant. Catal Surv Asia 2012;16:75–90.
[127] He F, Li F. Perovskite promoted iron oxide for hybrid water-splitting and syngas generation with exceptional conversion. Energy Environ Sci 2015;8:535–9.
[128] He F, Trainham J, Parsons G, Newman JS, Li F. A hybrid solar-redox scheme for liquid fuel and hydrogen coproduction. Energy Environ Sci 2014;7:2033–42.
[129] Hafizi A, Rahimpour MR, Hassanajili S. Calcium promoted Fe/Al_2O_3 oxygen carrier for hydrogen production via cyclic chemical looping steam methane reforming process. Int J Hydrog Energy 2015;40:16159–68.
[130] Hafizi A, Rahimpour MR, Hassanajili S. Hydrogen production by chemical looping steam reforming of methane over Mg promoted iron oxygen carrier: optimization using design of experiments. J Taiwan Inst Chem Eng 2016;62:140–9.
[131] Hafizi A, Rahimpour MR, Hassanajili S. Hydrogen production via chemical looping steam methane reforming process: effect of cerium and calcium promoters on the performance of Fe_2O_3/Al_2O_3 oxygen carrier. Appl Energy 2016;165:685–94.
[132] Hafizi A, Rahimpour MR, Hassanajili S. High purity hydrogen production via sorption enhanced chemical looping reforming: application of $22Fe_2O_3/MgAl_2O_4$ and $22Fe_2O_3/Al_2O_3$ as oxygen carriers and cerium promoted CaO as CO_2 sorbent. Appl Energy 2016;169:629–41.
[133] Hsuan-Chih WuYK. Chemical looping gasification of charcoal with iron-based oxygen carriers in an annular dual-tube moving bed reactor. Aerosol and Air Quality. Research 2016;16:1093–103.
[134] Wei G, He F, Huang Z, Zhao K, Zheng A, Li H. Chemical-looping reforming of methane using iron based oxygen carrier modified with low content nickel. Chin J Chem 2014;32:1271–80.
[135] Siriwardane R, Riley J, Tian H, Richards G. Chemical looping coal gasification with calcium ferrite and barium ferrite via solid–solid reactions. Appl Energy 2016;165:952–66.
[136] Cha K-S, Yoo B-K, Kim H-S, Ryu T-G, Kang K-S, Park C-S, et al. A study on improving reactivity of Cu-ferrite/ZrO_2 medium for syngas and hydrogen production from two-step thermochemical methane reforming. Int J Energy Res 2010;34:422–30.
[137] Wei G, He F, Zhao Z, Huang Z, Zheng A, Zhao K, et al. Performance of Fe–Ni bimetallic oxygen carriers for chemical looping gasification of biomass in a 10 kWth interconnected circulating fluidized bed reactor. Int J Hydrog Energy 2015;40:16021–32.
[138] Karimi E, Forutan HR, Saidi M, Rahimpour MR, Shariati A. Experimental study of chemical-looping reforming in a fixed-bed reactor: performance investigation of different oxygen carriers on Al_2O_3 and TiO_2 support. Energy Fuels 2014;28:2811–20.
[139] Forutan HR, Karimi E, Hafizi A, Rahimpour MR, Keshavarz P. Expert representation chemical looping reforming: a comparative study of Fe, Mn, Co and Cu as oxygen carriers supported on Al_2O_3. J Ind Eng Chem 2015;21:900–11.
[140] Neal LM, Shafiefarhood A, Li F. Dynamic methane partial oxidation using a $Fe_2O_3@La_{0.8}Sr_{0.2}FeO_{3-\delta}$ core–shell redox catalyst in the absence of gaseous oxygen. ACS Catalysis, 4 2014; 2014. p. 3560–9.
[141] Chen L, Yang L, Liu F, Nikolic HS, Fan Z, Liu K. Evaluation of multi-functional iron-based carrier from bauxite residual for H2-rich syngas production via chemical-looping gasification. Fuel Process Technol 2017;156:185–94.
[142] Ge H, Guo W, Shen L, Song T, Xiao J. Biomass gasification using chemical looping in a 25 kWth reactor with natural hematite as oxygen carrier. Chem Eng J 2016;286:174–83.
[143] Lind F, Seemann M, Thunman H. Continuous Catalytic Tar Reforming of biomass derived raw gas with simultaneous catalyst regeneration. Ind Eng Chem Res 2011;50:11553–62.
[144] Lind F, Berguerand N, Seemann M, Thunman H. Ilmenite and nickel as catalysts for upgrading of raw gas derived from biomass gasification. Energy Fuels 2013;27:997–1007.
[145] Huang Z, He F, Feng Y, Liu R, Zhao K, Zheng A, et al. Characteristics of biomass gasification using chemical looping with iron ore as an oxygen carrier. Int J Hydrog Energy 2013;38:14568–75.
[146] Huang Z, He F, Feng Y, Zhao K, Zheng A, Chang S, et al. Synthesis gas production through biomass direct chemical looping conversion with natural hematite as an oxygen carrier. Bioresour Technol 2013;140:138–45.
[147] Huang Z, He F, Zheng A, Zhao K, Chang S, Zhao Z, et al. Synthesis gas production from biomass gasification using steam coupling with natural hematite as oxygen carrier. Energy 2013;53:244–51.
[148] Ge H, Guo W, Shen L, Song T, Xiao J. Experimental investigation on biomass gasification using chemical looping in a batch reactor and a continuous dual reactor. Chem Eng J 2016;286:689–700.
[149] Lancee RJ, Dugulan AI, Thüne PC, Veringa HJ, Niemantsverdriet JW, Fredriksson HOA. Chemical looping capabilities of olivine, used as a catalyst in indirect biomass gasification. Appl Catal B: Environ 2014;145:216–22.
[150] Luo M, Wang S, Wang L, Lv M. Reduction kinetics of iron-based oxygen carriers using methane for chemical-looping combustion. J Power Sources 2014;270:434–40.
[151] Zeng J, Xiao R, Zeng D, Zhao Y, Zhang H, Shen D. High H_2/CO ratio syngas production from chemical looping gasification of sawdust in a dual fluidized bed gasifier. Energy Fuels 2016;30:1764–70.
[152] Huang Z, He F, Feng Y, Zhao K, Zheng A, Chang S, et al. Biomass char direct chemical looping gasification using NiO-modified iron ore as an oxygen carrier. Energy Fuels 2014;28:183–91.
[153] Ding H, Xu Y, Luo C, Zheng Y, Shen Q, Liu Z, et al. Synthesis and characteristics of BaSrCoFe-based perovskite as a functional material for chemical looping gasification of coal. Int J Hydrog Energy 2016;41:22846–55.
[154] Keller M, Fung J, Leion H, Mattisson T. Cu-impregnated alumina/silica bed materials for chemical looping reforming of biomass gasification gas. Fuel 2016;180:448–56.
[155] Alirezaei I, Hafizi A, Rahimpour MR, Raeissi S. Application of zirconium modified Cu-based oxygen carrier in chemical looping reforming. J CO_2 Util 2016;14:112–21.
[156] Keller M, Leion H, Mattisson T. Use of $CuO/MgAl_2O_4$ and $La_{0.8}Sr_{0.2}FeO_3/\gamma\text{-}Al_2O_3$ in chemical looping reforming system for tar removal from gasification gas. AIChE J 2016;62:38–45.
[157] Lind F, Israelsson M, Seemann M, Thunman H. Manganese oxide as catalyst for tar cleaning of biomass-derived gas. Biomass- Convers Biorefin 2012;2:133–40.
[158] Keller M, Leion H, Mattisson T, Thunman H. Investigation of natural and synthetic bed materials for their utilization in chemical looping reforming for tar elimination in biomass-derived gasification gas. Energy Fuels 2014;28:3833–40.
[159] Liu Y, Guo Q. Investigation into syngas generation from solid fuel using $CaSO_4$-based chemical looping gasification process. Chin J Chem Eng 2013;21:127–34.
[160] Liu Y, Guo Q, Cheng Y, Ryu H-J. Reaction mechanism of coal chemical looping process for syngas production with $CaSO_4$ oxygen carrier in the CO_2 atmosphere. Ind Eng Chem Res 2012;51:10364–73.
[161] Yang J, Ma L, Dong S, Liu H, Zhao S, Cui X, et al. Theoretical and experimental demonstration of lignite chemical looping gasification of phosphogypsum oxygen carrier for syngas generation. Fuel 2017;194:448–59.
[162] Du Y, Zhu X, Wang H, Wei Y, Li K. Synthesis gas generation by chemical-looping selective oxidation of methane using $Pr_{1-x}Zr_xO_{2-\delta}$ oxygen carriers. J Energy Inst 2016;89:745–54.
[163] Mattisson T, Johansson M, Jernda E, Lyngfelt A. The reaction of $NiO/NiAl_2O_4$ particles with alternating methane and oxygen. Can J Chem Eng 2008;86:756–67.
[164] Vizcaíno AJ, Arena P, Baronetti G, Carrero A, Calles JA, Laborde MA, et al. Ethanol steam reforming on Ni/Al_2O_3 catalysts: effect of Mg addition. Int J Hydrog Energy 2008;33:3489–92.
[165] Elias KFM, Lucrédio AF, Assaf EM. Effect of CaO addition on acid properties of $Ni–Ca/Al_2O_3$ catalysts applied to ethanol steam reforming. Int J Hydrog Energy 2013;38:4407–17.
[166] Otsuka K, Ushiyama T, Yamanaka I. Partial oxidation of methane using the redox of cerium oxide. Chem Lett 1993;22:1517–20.
[167] O'Connell M, Norman AK, Hüttermann CF, Morris MA. Catalytic oxidation over lanthanum-transition metal perovskite materials. Catal Today 1999;47:123–32.
[168] López Ortiz A, Meléndez Zaragoza M, Collins-Martínez V. Thermodynamic analysis of the ethanol chemical looping autothermal reforming with CO_2 capture. Int J Hydrog Energy 2015;40:17180–91.
[169] Dupont V, Ross AB, Hanley I, Twigg MV. Unmixed steam reforming of methane and sunflower oil: a single-reactor process for H_2 - rich gas. Int J Hydrog Energy 2007;32:67–79.
[170] Jiang B, Dou B, Wang K, Song Y, Chen H, Zhang C, et al. Hydrogen production from chemical looping steam reforming of glycerol by Ni based Al-MCM-41 oxygen carriers in a fixed-bed reactor. Fuel 2016;183:170–6.
[171] Udomsirichakorn J, Salam PA. Review of hydrogen-enriched gas production from steam gasification of biomass: the prospect of CaO-based chemical looping gasification. Renew Sustain Energy Rev 2014;30:565–79.
[172] Wang K, Yu Q, Qin Q, Hou L, Duan W. Thermodynamic analysis of syngas generation from biomass using chemical looping gasification method. Int J Hydrog Energy 2016;41:10346–53.
[173] García-Díez E, García-Labiano F, de Diego LF, Abad A, Gayán P, Adánez J, et al. Optimization of hydrogen production with CO_2 capture by autothermal chemical-looping reforming using different bioethanol purities. Appl Energy 2016;169:491–8.
[174] Rydén M, Lyngfelt A. Hydrogen and power production with integrated carbon dioxide capture by chemical-looping reforming. Proceedings of the seventh international conference on greenhouse gas control technologies. Vancouver, Canada; 2004.
[175] Magnus Rydén, Anders Lyngfelt, Mattisson T. Two novel approaches for hydrogen production, chemical-looping reforming and steam reforming with carbon dioxide capture by chemical-looping combustion. Proceedings of the 16th World Hydrogen Energy Conference. Lyon, France; 2006.
[176] Rydén M. Hydrogen production from fossil fuels with carbon dioxide capture, using chemical-looping technologies [PhD Thesis]. Chalmers University of Technology; 2008.
[177] Lima da Silva A, Dick LFP, Lourdes Müller I. Performance of a PEMFC system integrated with a biogas chemical looping reforming processor: a theoretical analysis and comparison with other fuel processors (steam reforming, partial oxidation and auto-thermal reforming). Int J Hydrog Energy 2012;37:6580–600.
[178] Spallina V, Pandolfo D, Battistella A, Romano MC, Van Sint Annaland M, Gallucci F. Techno-economic assessment of membrane assisted fluidized bed reactors for pure H_2 production with CO_2 capture. Energy Convers Manag 2016;120:257–73.
[179] He F, Li F. Hydrogen production from methane and solar energy – Process evaluations and comparison studies. Int J Hydrog Energy 2014;39:18092–102.
[180] Song C. Fuel processing for low-temperature and high-temperature fuel cells: challenges, and opportunities for sustainable development in the 21st century. Catal Today 2002;77:17–49.
[181] Trimm DL. Minimisation of carbon monoxide in a hydrogen stream for fuel cell application. Appl Catal A: Gen 2005;296:1–11.
[182] Armor JN. The multiple roles for catalysis in the production of H_2. Appl Catal A: Gen 1999;176:159–76.
[183] Otsuka K, Kaburagi T, Yamada C, Takenaka S. Chemical storage of hydrogen by modified iron oxides. J Power Sources 2003;122:111–21.
[184] Otsuka K, Yamada C, Kaburagi T, Takenaka S. Hydrogen storage and production

by redox of iron oxide for polymer electrolyte fuel cell vehicles. Int J Hydrog Energy 2003;28:335–42.
[185] Takenaka S, Hanaizumi N, Son V, Otsuka K. Production of pure hydrogen from methane mediated by the redox of Ni- and Cr-added iron oxides. J Catal 2004;228:405–16.
[186] Bohn CD, Muller CR, Cleeton JP, Hayhurst AN, Davidson JF, Scott SA, et al. Production of very pure hydrogen with simultaneous capture of carbon dioxide using the redox reactions of iron oxides in packed beds. Ind Eng Chem Res 2008;47:7623–30.
[187] Messerschmitt A. Process of producing hydrogen. Germany: Wasserstoff aktien-gesellschaft; 1910.
[188] Chiesa P, Lozza G, Malandrino A, Romano M, Piccolo V. Three-reactors chemical looping process for hydrogen production. Int J Hydrog Energy 2008;33:2233–45.
[189] Fan L-S, Li FX. Chemical looping technology and its fossil energy conversion applications. Ind Eng Chem Res 2010;49:10200–11.
[190] Lane H. Process for the production of hydrogen. Germany; 1913.
[191] Gupta P, Velazquez-Vargas LG, Fan L-S. Syngas redox (SGR) process to produce hydrogen from coal derived syngas. Energy Fuels 2007;21:2900–8.
[192] Steinfeld A, Frei A, Kuhn P. Thermoanalysis of the combined Fe_3O_4-reduction and CH_4-reforming processes. Metall Mater Trans B 1995;26:509–15.
[193] Fan L-S, Li FX, Kim HR, Sridhar D, Wang F, Zeng L, et al. Syngas chemical looping gasification process: oxygen carrier particle selection and performance. Energy Fuels 2009;23:4182–9.
[194] Svoboda K, Siewiorek A, Baxter D, Rogut J, Puncochar M. Thermodynamic possibilities and constraints of pure hydrogen production by a chromium, nickel, and manganese-based chemical looping process at lower temperatures. Chem Pap 2007;61:110–20.
[195] Kang KS, Kim CH, Bae KK, Cho WC, Kim SH, Park CS. Oxygen-carrier selection and thermal analysis of the chemical-looping process for hydrogen production. Int J Hydrog Energy 2010;35:12246–54.
[196] Solunke RD, Veser Gt. Hydrogen production via chemical looping steam reforming in a periodically operated fixed-bed reactor. Ind Eng Chem Res 2010;49:11037–44.
[197] Muller CR, Bohn CD, Song Q, Scott SA, Dennis JS. The production of separate streams of pure hydrogen and carbon dioxide from coal via an iron-oxide redox cycle. Chem Eng J 2011;166:1052–60.
[198] Liu W, Lim JY, Saucedo MA, Hayhurst AN, Scott SA, Dennis JS. Kinetics of the reduction of wüstite by hydrogen and carbon monoxide for the chemical looping production of hydrogen. Chem Eng Sci 2014;120:149–66.
[199] Yang JB, Cai NS, Li ZS. Hydrogen production from the steam-iron process with direct reduction of iron oxide by chemical looping combustion of coal char. Energy Fuels 2008;22:2570–9.
[200] Hua X, Fan Y, Wang Y, Fu T, Fowler GD, Zhao D, et al. The behaviour of multiple reaction fronts during iron (III) oxide reduction in a non-steady state packed bed for chemical looping water splitting. Appl Energy 2017;193:96–111.
[201] Wang YD, Hua XN, Zhao CC, Fu TT, Li W, Wang W. Step-wise reduction kinetics of Fe2O3 by CO/CO_2 mixtures for chemical looping hydrogen generation. Int J Hydrog Energy 2017;42:5667–75.
[202] Peña JA, Lorente E, Romero E, Herguido J. Kinetic study of the redox process for storing hydrogen: reduction stage. Catal Today 2006;116:439–44.
[203] Galvita V, Hempel T, Lorenz H, Rihko-Struckmann LK, Sundmacher K. Deactivation of modified iron oxide materials in the cyclic water gas shift process for CO-free hydrogen production. Ind Eng Chem Res 2008;47:303–10.
[204] Kierzkowska AM, Bohn CD, Scott SA, Cleeton JP, Dennis JS, Muller CR. Development of iron oxide carriers for chemical looping combustion using sol-gel. Ind Eng Chem Res 2010;49:5383–91.
[205] Romero E, Soto R, Durán P, Herguido J, Peña JA. Molybdenum addition to modified iron oxides for improving hydrogen separation in fixed bed by redox processes. Int J Hydrog Energy 2012;37:6978–84.
[206] Sun S, Zhao M, Cai L, Zhang S, Zeng D, Xiao R. Performance of CeO_2-modified iron-based oxygen carrier in the chemical looping hydrogen generation process. Energy Fuels 2015;29:7612–21.
[207] Dueso C, Thompson C, Metcalfe I. High-stability, high-capacity oxygen carriers: iron oxide-perovskite composite materials for hydrogen production by chemical looping. Appl Energy 2015;157:382–90.
[208] Ismail M, Liu W, Dunstan MT, Scott SA. Development and performance of iron based oxygen carriers containing calcium ferrites for chemical looping combustion and production of hydrogen. Int J Hydrog Energy 2016;41:4073–84.
[209] Galvita V, Sundmacher K. Hydrogen production from methane by steam reforming in a periodically operated two-layer catalytic reactor. Appl Catal A: Gen 2005;289:121–7.
[210] Liang H. Study on the effect of CeO_2 on $Fe_2O_3/LaNiO_3$ as the oxygen carrier applied in chemical-looping hydrogen generation. Int J Hydrog Energy 2015;40:13338–43.
[211] Cho WC, Seo MW, Kim SD, Kang KS, Bae KK, Kim CH, et al. Reactivity of iron oxide as an oxygen carrier for chemical-looping hydrogen production. Int J Hydrog Energy 2012;37:16852–63.
[212] Cho WC, Lee DY, Seo MW, Kim SD, Kang K, Bae KK, et al. Continuous operation characteristics of chemical looping hydrogen production system. Appl Energy 2014;113:1667–74.
[213] Sanfilippo D. One-step hydrogen through water splitting with intrinsic CO_2 capture in chemical looping. Catal Today 2016;272:58–68.
[214] Chan MSC, Liu W, Ismail M, Yang Y, Scott SA, Dennis JS. Improving hydrogen yields, and hydrogen: steam ratio in the chemical looping production of hydrogen using $Ca_2Fe_2O_5$. Chem Eng J 2016;296:406–11.
[215] Kidambi PR, Cleeton JPE, Scott SA, Dennis JS, Bohn CD. Interaction of iron oxide with alumina in a composite oxygen carrier during the production of hydrogen by chemical looping. Energy Fuels 2012;26:603–17.
[216] Zeng D-W, Peng S, Chen C, Zeng J-M, Zhang S, Zhang H-Y, et al. Nanostructured $Fe_2O_3/MgAl_2O_4$ material prepared by colloidal crystal templated sol–gel method for chemical looping with hydrogen storage. Int J Hydrog Energy 2016;41:22711–21.
[217] Rihko-Struckmann LK, Datta P, Wenzel M, Sundmacher K, Dharanipragada NVRA, Poelman H, et al. Hydrogen and carbon monoxide production by chemical looping over iron-aluminium oxides. Energy Technol 2016;4:304–13.
[218] Zhu J, Wang W, Hua XN, Wang F, Xia Z, Deng Z. Phase distribution and stepwise kinetics of iron oxides reduction during chemical looping hydrogen generation in a packed bed reactor. Int J Hydrog Energy 2015;40:12097–107.
[219] Zhu J, Wang W, Lian S, Hua X, Xia Z. Stepwise reduction kinetics of iron-based oxygen carriers by CO/CO_2 mixture gases for chemical looping hydrogen generation. J Mater Cycles Waste Manag 2017;19:453–62.
[220] Galinsky NL, Huang Y, Shafiefarhood A, Li F. Iron oxide with facilitated O_2–transport for facile fuel oxidation and CO_2 capture in a chemical looping scheme. ACS Sustain Chem Eng 2013;1:364–73.
[221] He F, Galinsky N, Li F. Chemical looping gasification of solid fuels using bimetallic oxygen carrier particles – Feasibility assessment and process simulations. Int J Hydrog Energy 2013;38:7839–54.
[222] Jin GT, Ryu HJ, Jo SH, Lee SY, Son SR, Kim SD. Hydrogen production in fluidized bed by chemical-looping cycle. Korean J Chem Eng 2007;24:542–6.
[223] Shiyi C, Qiliang S, Zhipeng X, Xiaoyan S, Wenguo X. Experimental investigation of chemical-looping hydrogen generation using Al_2O_3 or TiO_2-supported iron oxides in a batch fluidized bed. Int J Hydrog Energy 2011;36:8915–89268926.
[224] Sridhar D, Tong A, Kim H, Zeng L, Li F, Fan L-S. Syngas chemical looping process: design and construction of a 25 kWth subpilot unit. Energy Fuels 2012;26:2292–302.
[225] Tong A, Sridhar D, Sun Z, Kim HR, Zeng L, Wang F, et al. Continuous high purity hydrogen generation from a syngas chemical looping 25 kWth sub-pilot unit with 100% carbon capture. Fuel 2013;103:495–505.
[226] Thaler M, Hacker V, Anilkumar M, Albering J, Besenhard JO, Schröttner H, et al. Investigations of cycle behaviour of the contact mass in the RESC process for hydrogen production. Int J Hydrog Energy 2006;31:2025–31.
[227] Nestl S, Voitic G, Lammer M, Marius B, Wagner J, Hacker V. The production of pure pressurised hydrogen by the reformer-steam iron process in a fixed bed reactor system. J Power Sources 2015;280:57–65.
[228] Voitic G, Nestl S, Lammer M, Wagner J, Hacker V. Pressurized hydrogen production by fixed-bed chemical looping. Appl Energy 2015;157:399–407.
[229] Chen SY, Xiang WG, Xue ZP, Sun XY. Experimental investigation of chemical looping hydrogen generation using iron oxides in a batch fluidized bed. Proc Combust Inst 2011;33:2691–9.
[230] Voitic G, Nestl S, Malli K, Wagner J, Bitschnau B, Mautner F-A, et al. High purity pressurised hydrogen production from syngas by the steam-iron process. RSC Adv 2016;6:53533–41.
[231] Plou J, Durán P, Herguido J, Peña JA. Hydrogen from bio-fuels by “steam-iron” process: modelling and kinetics. Int J Hydrog Energy 2016;41:19349–56.
[232] Datta P, Rihko-Struckmann LK, Sundmacher K. Quantification of produced hydrogen in a cyclic water gas shift process with Mo stabilized iron oxide. Fuel Process Technol 2014;128:36–42.
[233] Datta P, Rihko-Struckmann LK, Sundmacher K. Influence of molybdenum on the stability of iron oxide materials for hydrogen production with cyclic water gas shift process. Mater Chem Phys 2011;129:1089–95.
[234] Campo R, Durán P, Plou J, Herguido J, Peña JA. Combined production and purification of hydrogen from methanol using steam iron process in fixed bed reactor. J Power Sources 2013;242:520–6.
[235] Wang H, Wang G, Wang X, Bai J. Hydrogen production by redox of cation-modified iron oxide. J Phys Chem C 2008;112:5679–88.
[236] Wang H, Zhang J, Wen F, Bai J. Effect of Mo dopants on improving hydrogen production by redox of iron oxide: catalytic role of Mo cation and kinetic study. RSC Adv 2013;3:10341–8.
[237] Bohn JPC CD, Müller CR, Chuang SY, Scott SA, Dennis JS. Stabilizing iron oxide used in cycles of reduction and oxidation for hydrogen production. Energy Fuels 2010;24:4025–33.
[238] Kim H-S, Cha K-S, Yoo B-K, Ryu T-G, Lee Y-S, Park C-S, et al. Chemical hydrogen storage and release properties using redox reaction over the Cu-added Fe/Ce/Zr mixed oxide medium. J Ind Eng Chem 2010;16:81–6.
[239] Scheffe JR, Allendorf MD, Coker EN, Jacobs BW, McDaniel AH, Weimer AW. Hydrogen production via chemical looping redox cycles using atomic layer deposition-synthesized iron oxide and cobalt ferrites. Chem Mater 2011;23:2030–8.
[240] Solunke RD, Veser G. Hydrogen production via chemical looping steam reforming in a periodically operated fixed-bed reactor. Ind Eng Chem Res 2010;49:11037–44.
[241] Rydén M, Arjmand M. Continuous hydrogen production via the steam–iron reaction by chemical looping in a circulating fluidized-bed reactor. Int J Hydrog Energy 2012;37:4843–54.
[242] Urasaki K, Tanimoto N, Hayashi T, Sekine Y, Kikuchi E, Matsukata M. Hydrogen production via steam–iron reaction using iron oxide modified with very small amounts of palladium and zirconia. Appl Catal A: Gen 2005;288:143–8.
[243] Takenaka S, Kaburagi T, Yamada C, Nomura K, Otsuka K. Storage and supply of hydrogen by means of the redox of the iron oxides modified with Mo and Rh species. J Catal 2004;228:66–74.
[244] Takenaka S, Nomura K, Hanaizumi N, Otsuka K. Storage and formation of pure hydrogen mediated by the redox of modified iron oxides. Appl Catal A: Gen

2005;282:333–41.
[245] Yu-Lin Kuo W-CH, Wei-Mau Hsu, Yao-Hsuan Tseng, Young Ku. Use of spinel nickel aluminium ferrite as self-supported oxygen carrier for chemical looping hydrogen generation process. Aerosol Air Qual Res 2015;15:2700–8.
[246] Liu S, He F, Huang Z, Zheng A, Feng Y, Shen Y, et al. Screening of $NiFe_2O_4$ nanoparticles as oxygen carrier in chemical looping hydrogen production. Energy Fuels 2016;30:4251–62.
[247] Kindermann H, Kornberger M, Hierzer J, Besenhard JO, Hacker V. First investigations of structural changes of the contact mass in the RESC process for hydrogen production. J Power Sources 2005;145:697–701.
[248] Xiao R, Zhang S, Peng S, Shen D, Liu K. Use of heavy fraction of bio-oil as fuel for hydrogen production in iron-based chemical looping process. Int J Hydrog Energy 2014;39:19955–69.
[249] Zeng D-W, Xiao R, Huang Z-c, Zeng J-M, Zhang H-Y. Continuous hydrogen production from non-aqueous phase bio-oil via chemical looping redox cycles. Int J Hydrog Energy 2016;41:6676–84.
[250] Liu W, Shen L, Gu H, Wu L. Chemical looping hydrogen generation using potassium-modified iron ore as an oxygen carrier. Energy Fuels 2016;30:1756–63.
[251] Bleeker MF, Veringa HJ, Kersten SRA. Deactivation of iron oxide used in the steam-iron process to produce hydrogen. Appl Catal A: Gen 2009;357:5–17.
[252] Galvita VV, Poelman H, Bliznuk V, Detavernier C, Marin GB. CeO_2-modified Fe_2O_3 for CO_2 utilization via chemical looping. Ind Eng Chem Res 2013;52:8416–26.
[253] Ehrensberger K, Frei A, Kuhn P, Oswald HR, Hug P. Comparative experimental investigations of the water-splitting reaction with iron oxide $Fe_{1-y}O$ and iron manganese oxides $(Fe_{1-x}Mn_x)_{1-y}O$. Solid State Ion 1995;78:151–60.
[254] Inoue M, Hasegawa N, Uehara R, Gokon N, Kaneko H, Tamaura Y. Solar hydrogen generation with $H_2O/ZnO/MnFe_2O_4$ system. Sol Energy 2004;76:309–15.
[255] Ismail M, Liu W, Scott SA. The performance of Fe_2O_3-CaO oxygen carriers and the interaction of iron oxides with CaO during chemical looping combustion and H_2 production. Energy Procedia 2014;63:87–97.
[256] Homer C Reed G, Clyde H Berg O. Hydrogen Process. America; 1953.
[257] Cho P, Mattisson T, Lyngfelt A. Defluidization conditions for a fluidized bed of iron oxide-, nickel oxide-, and manganese oxide-containing oxygen carriers for chemical-looping combustion. Ind Eng Chem Res 2006;45:968–77.
[258] Cleeton JPE, Bohn CD, Muller CR, Dennis JS, Scott SA. Clean hydrogen production and electricity from coal via chemical looping: identifying a suitable operating regime. Int J Hydrog Energy 2009;34:1–12.
[259] Fan LS, Li FX, Ramkumar S. Utilization of chemical looping strategy in coal gasification processes. Particuology 2008;6:131–42.
[260] Li F, Zeng L, Fan L-S. Techno-economic analysis of coal-based hydrogen and electricity cogeneration processes with CO_2 capture. Ind Eng Chem Res 2010;49:11018–28.
[261] Cormos CC. Evaluation of iron based chemical looping for hydrogen and electricity co-production by gasification process with carbon capture and storage. Int J Hydrog Energy 2010;35:2278–89.
[262] Chen S, Xue Z, Wang D, Xiang W. Hydrogen and electricity co-production plant integrating steam-iron process and chemical looping combustion. Int J Hydrog Energy 2012;37:8204–16.
[263] Cebrucean D, Cebrucean V, Ionel I, Spliethoff H. Performance of two iron-based syngas-fueled chemical looping systems for hydrogen and/or electricity generation combined with carbon capture. Clean Technol Environ Policy 2017;19:451–70.
[264] Vairakannu P, Kumari G. CO_2-Oxy underground coal gasification integrated proton exchange membrane fuel cell operating in a chemical looping mode of reforming. Int J Hydrog Energy 2016;41:20063–77.
[265] Chen S, Xue Z, Wang D, Xiang W. An integrated system combining chemical looping hydrogen generation process and solid oxide fuel cell/gas turbine cycle for power production with CO_2 capture. J Power Sour 2012;215:89–98.
[266] Yan L, Yue G, He B. Exergy analysis of a coal/biomass co-hydrogasification based chemical looping power generation system. Energy 2015;93:1778–87.
[267] Zhang YX, Doroodchi E, Moghtaderi B. Thermodynamic assessment of a novel concept for integrated gasification chemical looping combustion of solid fuels. Energy Fuels 2012;26:287–95.
[268] Aziz M, Zaini IN, Oda T, Morihara A, Kashiwagi T. Energy conservative brown coal conversion to hydrogen and power based on enhanced process integration: integrated drying, coal direct chemical looping, combined cycle and hydrogenation. Int J Hydrog Energy 2017;42:2904–13.
[269] Li FX, Zeng LA, Fan LS. Biomass direct chemical looping process: process simulation. Fuel 2010;89:3773–84.
[270] Zhang Y, Doroodchi E, Moghtaderi B, Han X, Liu Y. Hydrogen production from ventilation air methane in a dual-loop chemical looping process. Energy Fuels 2016;30:4372–80.
[271] Cormos C-C. Biomass direct chemical looping for hydrogen and power co-production: process configuration, simulation, thermal integration and techno-economic assessment. Fuel Process Technol 2015;137:16–23.
[272] Kathe MV, Empfield A, Na J, Blair E, Fan L-S. Hydrogen production from natural gas using an iron-based chemical looping technology: thermodynamic simulations and process system analysis. Appl Energy 2016;165:183–201.
[273] Edrisi A, Mansoori Z, Dabir B. Urea synthesis using chemical looping process – Techno-economic evaluation of a novel plant configuration for a green production. Int J Greenh Gas Control 2016;44:42–51.
[274] Khan MN, Shamim T. Techno-economic assessment of a plant based on a three reactor chemical looping reforming system. Int J Hydrog Energy 2016;41:22677–88.
[275] Zeng L, Tong A, Kathe M, Bayham S, Fan L-S. Iron oxide looping for natural gas conversion in a countercurrent moving bed reactor. Appl Energy 2015;157:338–47.